Università degli Studi di Ferrara

DOTTORATO DI RICERCA IN

"Biochimica, Biologia Molecolare e Biotecnologie"

CICLO XXV

COORDINATORE Prof. Francesco Bernardi

Mitochondrial dysfunctions in cancer and neurodegenerative disease

Settore Scientifico Disciplinare **MED/04**

Dottorando:

Dott. Simone Patergnani

Tutore:

Prof. Paolo Pinton

Anni 2010/2012

TABLE OF CONTENTS

ABBREVIATIONS

$[Ca^{2+}]_c$	Cytoplasmic calcium concentration
$[Ca^{2+}]_{er}$	Endoplsmic reticulum calcium concentration
$[Ca^{2+}]_m$	Mitochondrial calcium concentration
ADP	Adenosine diphosphate
ANT	Adenine nucleotide translocator
Apaf-1	Apoptotic protease activating factor
ATP	Adenosine triphosphate
ATP5A	ATP synthase, H+ transporting, mitochondrial F1 complex, alpha subunit
Bcl-2/Xl	B cell leukemia/lymphoma 2/Extra large
BH1-4	Bcl-2 homology domain 1-4
BiP	Endoplasmic reticulum HSC70-cognate binding protein
CCH	Carbachol
CNS	Central nervous system
DBD	DNA binding domain
DCF	Dicloro-fluoroscein
DHE	Dihydroethidium
DOA	Dominant optic atrophy
DRP1	Dynamin related protein 1
EAE	Experimental autoimmune encephalomyelitis
EM	Electron microscopy
ER	Endoplasmic reticulum
ETC	Electron transport chain
FAD	Flavin adenine dinucleotide
FCCP	Carbonylcyanide-p-trifluoromethoxyphenylhydrazone

FIS1	Mitochondrial fission 1 protein
FRET	Fluorescence resonant energy transfert
GFAP	Glial fibrillary acid protein
GFP	Green fluorescent protein
GTP	Guanosine triphosphate
HA	Hemagglutinin
HIF1α	Hypoxia-inducible factors 1 alpha
HSP60	Heat shock protein 60
IAP	Inhibitor of apoptosis protein
INFγ	Interferon gamma
IP3R	Inositol phosphate 3 receptor
MAP-LC3	Microtubule associated protein 1 light chain 3
LETM1	leucine zipper-EF-hand containing transmembrane protein 1
MAM	Mitochondria associated membrane
MAPK	Mitogen activated protein kinase
MBP	Myelin basic protein
MCU	Mitochondrial Calcium Uniporter
MCUR1	Mitochondrial Calcium Uniporter Regulator 1
MEF	Mouse embryonic fibroblast
MFN1/2	Mitofusin 1/2
MICU1	Mitochondrial Calcium Uptake 1
Ψ_m	Mitochondrial membrane potential
MS	Multiple sclerosis
MTCO1	Mitochondrially encoded cytochrome c oxidase I
NADH	Nicotinamide adenine dinucleotide

NCX	Sodium Calcium exchanger
NDUF8B	NADH dehydrogenase [ubiquinone] 1 beta subcomplex subunit 8
NG2	Chondroitin sulfate proteoglycan NG2
OMM	Outer mitochondrial membrane
OPA1	Optic atrophy 1
OSP	Oligodendrocyte specific protein
OXPHOS	Oxidative phosphorylation
$p66^{Shc}$	66 kD isoform of Shc
PACS-2	Phosphofurin acidic cluster sorting protein 2
PINK1	PTEN-putative kinase 1
PML	Promyelocytic leukemia protein
PTP	Permeability Transition Pore
RNS	Reactive nitrogen species

ABSTRACT

Mitochondria are dynamic, semi-autonomous organelles surrounded by a double membrane that have their own genome and protein synthesis machinery. In addition to being the major source of ATP in eukaryotes, they are the site of many important metabolic reactions such as the urea cycle, lipid metabolism, steroid hormone and porphyrin synthesis and interconversion of amino acids. Moreover, mitochondria play a central role in complex physiological processes including cellular proliferation, differentiation, apoptosis and in cellular processes like glucose sensing/insulin regulation and cellular Ca^{2+} homeostasis. It is therefore not surprising that mitochondrial dysfunctions have been found to be associated with several diseases such as neurodegenerative diseases, aging and cancer.

In this work, we investigate on the relationship between mitochondrial dynamics and two of the main research priorities in the world: cancer and neurodegenerative disease. In particular, we have addressed:

- i) The role of the PKCβ and mitochondrial physiology in the modulation of autophagy, a major phenomenon of cell biology, which acts as a pro-survival or pro-death mechanism and takes part in different biological events.
- ii) The identification of a microRNA (miR-25), highly expressed in cancer cells, that by targeting the newly discovered calcium channel of mitochondria (Mitochondrial Calcium Uniporter) reduces the sensitivity of cancer cells to apoptotic agents.
- iii) How, one of the most important cytokines for the aetiology of Multiple Sclerosis, TNFα, lead to alteration of the mitochondrial bioenergetics, with a consequent impairment of oligodendrocytes differentiation

In conclusion, these findings reveal new relations between mitochondria, calcium signalling and cell physiology, shedding new light on the role for this fascinating organelle.

RIASSUNTO

I mitocondri, considerati come le centrali energetiche delle nostre cellule, sono organelli dinamici e "semi-autonomi" che possiedono un proprio genoma e un proprio macchinario adibito alla sintesi proteica. In aggiunta ad essere la principale fonte di ATP negli organismi eucarioti, sono sede di una considerevole serie di importanti reazioni metaboliche come il ciclo dell'urea, il metabolismo dei lipidi ed ormoni e la produzione di aminoacidi.

Inoltre, i mitocondri ricoprono un ruolo fondamentale in diversi processi fisiologici, tra cui la proliferazione cellulare, il differenziamento, l'apoptosi e la regolazione dell'omeostasi del Ca^{2+} cellulare. Non ci si sorprende, quindi, che disfunzioni a livello dell'omeostasi mitocondriale sono state profondamente associate a una serie di patologie, come il cancro, l'invecchiamento e le malattie neurodegenerative.

In questo lavoro abbiamo studiato il rapporto tra la fisiologia mitocondriale e due tra le principali priorità di ricerca scientifica del mondo: cancro e malattie neurodegenerative. In particolare, abbiamo focalizzato la nostra attenzione principalmente su:

- i) il ruolo della Protein kinase C β (PKCβ) e della fisiologia mitocondriale nella regolazione dell'autofagia, uno dei principali processi biologici cellulari, in grado di modulare meccanismi di morte e sopravvivenza e allo stesso tempo capace di regolare diverse cascate molecolari di altrettanti differenti eventi biologici.
- ii) l'identificazione di un microRNA (miR-25), altamente espresso nelle cellule tumorali, il quale, agendo sulla funzionalità del canale del calcio dei mitocondri (uniporto mitocondriale del calcio), determina una riduzione della sensitività delle cellule tumorali agli stimoli apoptotici.
- iii) come, una delle principali citochine coinvolte nella patogenesi della Sclerosi Multipla, il TNFα, induca una forte alterazione della bioenergetica mitocondriale, con una conseguente blocco del differenziamento delle cellule oligodendrocitarie.

Concludendo, queste nuove scoperte permettono di identificare relazioni completamente nuove tra mitocondri, il segnale calcio e la fisiologia cellulare, sottolineando il ruolo cruciale di questo organello nella fisiopatologia cellulare.

Mitochondrial structure

Mitochondria are organelles with extremely complex structures and functions. They are derived from an α-proteobacterium-like ancestor, due to an ancient "invasion" that occurred more than a billion years ago [1]. The acquisition of mitochondria (and plastids) was a key event in the evolution of the eukaryotic cell, supplying it with bioenergetic and biosynthetic factors.

At subcellular resolution mitochondria appear as composed of an outer membrane (OMM), mostly permeable to ions and metabolites up to 10 kDa, and a highly selective inner mitochondrial membrane (IMM), characterized by invaginations called cristae. The space between these two structures is traditionally called the intermembrane space (IMS). Together, the OMM and IMM enclose the mitochondrial matrix. The IMM is further subdivided into two distinct compartments: the peripheral inner boundary membrane and the cristae [2]. Cristae are not simply random folds, but rather internal compartments formed by profound invaginations originating from very tiny "point-like structures" in the inner membrane. These narrow tubular structures, called cristae junctions, can limit the diffusion of molecules from the intra-cristae space towards the IMS, thus creating a microenvironment where mitochondrial electron transport chain (ETC) complexes (as well as other proteins) are hosted and protected from random diffusion. The inner boundary membrane is enriched with structural proteins and components of the import machinery of mitochondria [3].

Mitochondrial morphology in living cells is heterogeneous and can range from small spheres to interconnected tubules. This heterogeneity results from the balance between fusion and fission processes, and represents a phenomenon termed mitochondrial dynamics [4]. A growing body of evidence indicates that mitochondrial morphology is critical for the physiology of the cell and changes in mitochondrial shape have been related to many different processes such as development, neurodegeneration, calcium (Ca^{2+}) signalling, reactive oxygen species (ROS) production, cell division, and apoptotic cell death [5].

Mitochondrial shape is controlled by the recently identified "mitochondria-shaping proteins", which regulate the fusion-fission equilibrium of the organelle. In mammals, key components of the fusion machinery include the homologues MFN1 and MFN2 [6]. The only dynamin-like GTPase currently identified in the IMM is OPA1, a fusion protein that is mutated in dominant optic atrophy (DOA), the most common cause of inherited optic neuropathy. Post-transcriptional mechanisms, including proteolytic processing, tightly regulate OPA1 activity. In mammalian cells, mitochondrial division is regulated by DRP1 and FIS1 [7, 8]. The large GTPase DRP1 is a cytosolic dynamin-related protein, whose inhibition or downregulation results in a highly interconnected mitochondrial network. The

same phenotype is caused by the downregulation of FIS1, a protein of the OMM, proposed to act as a mitochondrial receptor for DRP1 [9]. For example, mitochondrial
dynamics seem to influence production of ROS and cellular longevity. DRP1-dependent fragmentation of the mitochondrial reticulum is a crucial component for accumulation of ROS in pathological conditions [10]. How mitochondrial fission is required for ROS production and lifespan remains unclear, although a link between the two processes seems plausible. Hence, factors other than mitochondrial metabolism *per se* could have a role in the pathogenesis of ROS-related diseases. Interestingly, many ROS (as well as Reactive Nitrogen Species, RNS) sources and targets are localized in the mitochondria and ER with are relevant consequences for different pathways [11].

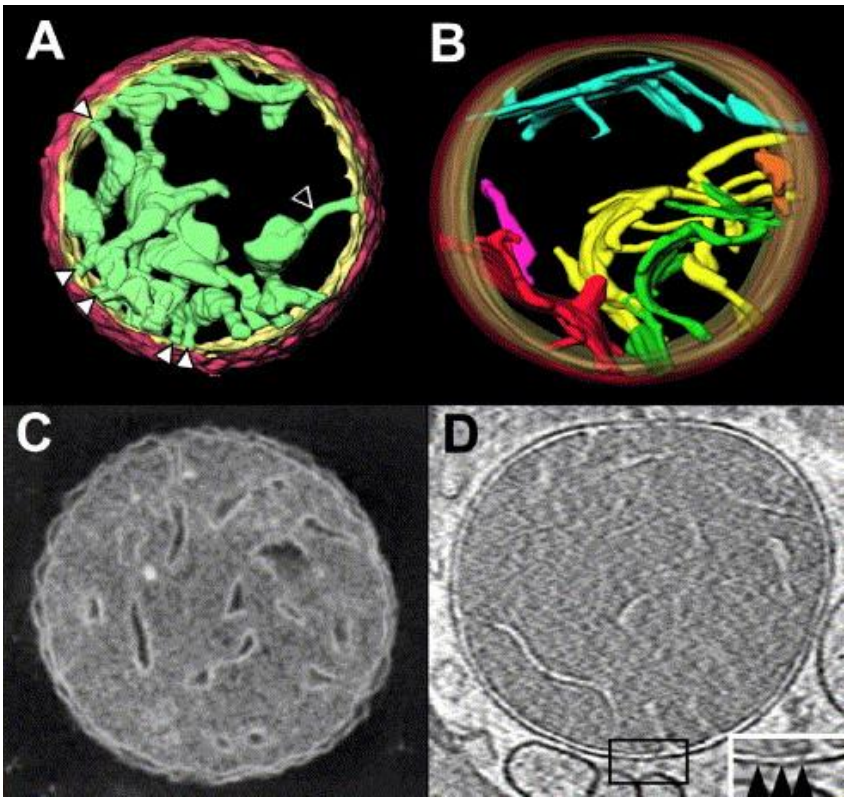

Figure 1 - Tomographic reconstructions of rat liver mitochondria. (A) Surface-rendering of the membranes in a condensed mitochondrion. (B) Surface-rendering of the membranes in a mitochondrion suspended in 300mM sucrose, plunge-frozen at liquid nitrogen temperature and imaged in a cryo-electron microscope. (C, D) 2-nm-thick slices from the tomograms in A and B, respectively. Arrows in 2X inset of (D) point to 10–15 nm particles in intermembrane space. Adapted from (Frey and Mannella, 2000).

Mitochondria are the site for major energy production

Within cells, energy is provided by oxidation of "metabolic fuels" such as carbohydrates, lipids and

proteins. It is then used to sustain energy-dependent processes, such as the synthesis of macromolecules, muscle contraction, active ion transport or thermogenesis. The oxidation process results in free energy production that can be stored in phosphoanhydrine "high-energy bonds" within molecules such as nucleoside diphosphate and nucleoside triphosphate (*i.e.*, adenosine 5' diphosphate and adenosine 5' trisphosphate, ADP and ATP, respectively), phosphoenolpyruvate, carbamoyl phosphate, 2,3-bisphosphoglycerate, and other phosphates like phosphoarginine or phosphocreatine. Among them, ATP is the effective central link—the exchange coin—between energy producing and the energy demanding processes that effectively involve formation, hydrolysis or transfer of the terminal phosphate group.

In general, the main energy source for cellular metabolism is glucose, which is catabolized in the three subsequent processes: glycolysis, tricarboxylic acid cycle (TCA or Krebs cycle), and finally oxidative phosphorylation to produce ATP. In the first process, when glucose is converted into pyruvate the amount of ATP produced is low. Subsequently, pyruvate is converted to acetyl coenzyme A (acetyl-CoA) which enters the TCA cycle, enabling the production of NADH. Finally, NADH is used by the respiratory chain complexes to generate a proton gradient across the inner mitochondrial membrane, necessary for the production of large amounts of ATP by mitochondrial ATP synthase. In addition, it should be mentioned that acetyl-CoA could be generated also by lipid and protein catabolism.

Citric Acid Cycle

The TCA, also known as the citric acid cycle, was elucidated by Sir Hans Krebs in 1940 when he concluded, "*the oxidation of a triose equivalent involves one complete citric acid cycle*" [12]. The "*triose*" deriving from glycolysis is completely oxidized into three molecules of CO_2 during a sequence of reactions that allow the reduction of cofactors NAD and flavin adenine nucleotide (FAD), providing energy for the respiratory chain in the form of electrons. In 1949 it was demonstrated by Kennedy and Lehningher that the entire cycle occurs inside mitochondria [13]. The starting material for the citric acid cycle is directly provided by the pyruvate coming from glycolysis through the activity of the pyruvate dehydrogenase complex. This enzymatic complex, composed of multiple copies of the three enzymes pyruvate dehydrogenase (E1), dihydrolipoyl transacetylase, (E2) and dihydrolipoyl dehydrogenase (E3), oxidizes pyruvate to acetyl-CoA and CO_2 in an irreversible reaction in which the carboxyl group is removed from pyruvate as a molecule of CO_2. This reaction is strictly related to the cycle, even if is not comprised in it. The acetyl group introduces two carbons in each turn of the cycle; these carbons will then leave the cycle as CO_2.

The first reaction of the citric acid cycle is the condensation of one Acetyl-CoA and a molecule of citrate to generate oxaloacetate and is catalysed by citrate synthase. Citrate is then transformed into isocitrate by aconitase through the formation of cis-aconitate. This step is reversible and could lead to the formation of both citrate and isocitrate. Only the fast consumption of isocitrate by its dehydrogenase can force the reaction to the proper direction. Isocitrate dehydrogenase catalyses the first irreversible oxidation leading to the decarboxylation of isocitrate, generating CO_2 and α-ketoglutarate. The second carbon leaves the cycle in the following step, when the newly generated α-ketoglutarate is immediately decarboxylated by the α-ketoglutarate dehydrogenase complex in a reaction similar to the pyruvate decarboxylation. In fact, both these complexes share high similarities in enzyme amino acid composition and in the organization of the different subunits. Energy released from both oxidations is used to generate NADH from NAD that directly feeds into the respiratory chain.

The following step is catalysed by succinyl-Coa synthetase and utilizes the energy derived from the CoA removal to phosphorylate GDP (or ADP) to GTP (or ATP). Selectivity for the nucleotide is determined by the isozyme involved. It has been well established that at least two isozymes of succinyl-CoA synthetase are expressed in animal tissues [14] and the proportion between them seems to be tissue specific.

The succinate generated in the previous step is the 4 carbon compound that is then converted, by three sequential reactions, to oxaloacetate to conclude the cycle. The first of these steps is the oxidation of succinate to fumarate by succinate dehydrogenase. This enzyme, tightly bound to the inner mitochondrial membrane (IMM), catalyses FAD reduction to $FADH_2$ that provides electrons for the respiratory chain. Fumarate is then hydrated by fumarate hydratase to L-malate. It is particularly interesting that both succinate dehydrogenase and fumarate hydratase are oncosuppressor genes. It has been demonstrated that inactivation of these oncosuppressors leads to the accumulation of succinate and fumarate that spread in the cytosol and promote hypoxiainducible factor 1α (HIF1α) accumulation by inactivating prolyl hydroxilase enzymes (promoter of HIF1α degradation); HIF1α, promotes a pseudo-hypoxic condition that favours tumour development[15]. The last event that completes the citric acid cycle is the oxidation of L-malate to oxaloacetate. This reaction is performed by L-malate dehydrogenase, which induces the reduction of another molecule of NAD to NADH. The resulting molecule of oxaloacetate is suitable for starting another cycle through condensation with an acetyl group.

During all these processes, only one molecule of ATP (or GTP) is produced, but three molecules of NADH and one of $FADH_2$ (plus one molecule of NADH from pyruvate dehydrogenase), which

provide electrons for respiratory chain, are also generated and subsequently result in the production of large amounts of ATP (discussed later).

Respiratory chain and Oxidative Phosphorylation

Respiratory chain comprises a series of components (complexes) conducting electron transfer across the membrane and involved in oxidative phosphorylation (OXPHOS), a process that occurs in aerobic conditions. In eukaryotic cells, electron transport occurs in mitochondria and chloroplasts, whereas in bacteria it is carried out across the plasma membrane. As mentioned, the electron transfer is considered a part OXPHOS, the process through which ADP is phosphorylated into ATP by dint of energy derived from the oxidation of nutrients. Four protein complexes and ATP synthase, all bound to the IMM, as well as two shuttles are the known players of one of the trickiest mechanisms resolved in biochemistry. The first of these complexes is the NADH:ubiquinone oxidoreductase (complex I) which removes electrons from NADH (produced in the citric acid cycle) and passes them on to the first shuttle, ubiquinone, a liposoluble cofactor located within the phospholipid bilayer of the IMM. Succinate dehydrogenase (or complex II) is another entrance site for electrons into the respiratory chain. In this case, electrons derived from the oxidation of succinate are passed through FAD to ubiquinone.

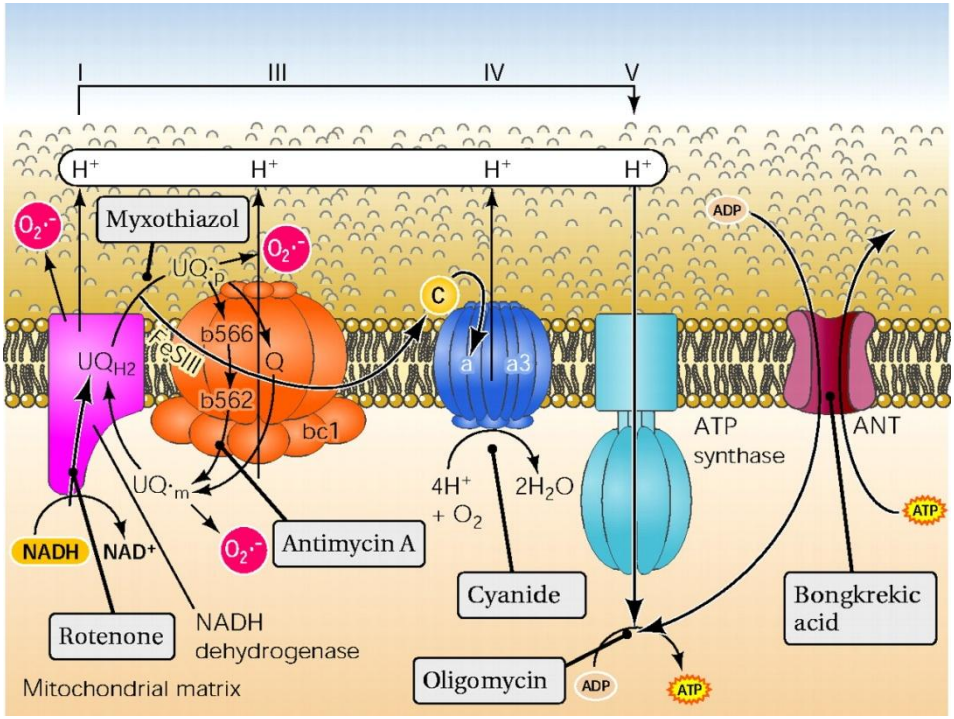

Figure 2 - Schematic representation of mitochondrial electron transport chain (adapted from *Physiology* 20:303-315, 2005)

Once ubiquinone is reduced to ubiquinol, it is able to pass electrons to the third complex, ubiquinone: cytochrome *c* oxidoreductase. Here, electrons are moved through several heme groups from the liposoluble shuttle ubiquinone to the water soluble shuttle cytochrome *c*. Cytochrome *c* is a small protein (about 12.5 kDa), located in the intermembrane space (IMS), which can accommodate one electron in its heme group. Despite its water solubility, cytochrome *c* is usually bound to the external surface of the IMM due to the interaction with the cardiolipin [16]. This interaction (crucial in the determination of the cell fate) helps the shuttle to reach its electron acceptor, complex IV. Cytochrome *c* oxidase is the last complex of the electron transport. Electrons from cytochrome *c* are accumulated in copper centres and passed to oxygen through heme groups. Oxygen is then reduced to water. This constitutes the bulk of oxygen consumption in all aerobic life.

Electron transport through complexes I, III and IV induces the pumping of protons from the matrix to the IMS. Specifically, for every two electrons coming from one molecule of NADH, four H+ are moved by complex I, four by complex III, and two by complex IV. The second respiratory complex does not generate any proton movement [17]. The respiratory chain in active mitochondria generates a large difference in $[H^+]$ across the IMM, resulting in the generation of an electrical potential (about -180 to -200 mV) and variation in the pH of about 0.75. A constant proton motive force drives the ATP synthesis trough the last step of OXPHOS, the ATP synthase. Understanding the activity and organization of this enzyme won researchers more than one Nobel Prize. First, Peter Mitchell in 1978 received his prize for the formulation of the chemiosmotic theory. Initially he hypothesized how an enzymatic activity could at the same time involve ion transport (proton transport through the IMM) and a chemical reaction (ATP phosphorylation). Almost two decades later, in 1997, the Nobel Prize was awarded to Paul Boyer and John Walker who elucidated the mechanism of action of ATP synthase, here briefly reviewed. ATP synthase could be divided in two main components: F0 that allows the channelling of protons, and F1 that catalyses ATP phosphorylation. The F0 is embedded in the IMM, while the F1 resides in the mitochondrial matrix and is bound to the F0 through a γ subunit (which drives conformational changes) and a b2δ dimer (that holds F0 and F1 together). The protons flow from the intermembrane space to the matrix through the F0 inducing its rotation; the movement is transmitted from the γ subunit to the F1 causing conformational rearrangements. The F1 has a trimeric structure consisting of αβ dimers. The sequential changes are linked to the binding of substrates, phosphorylation and release of ATP.

The three available dimers are never in the same conformational state and, what is more, the conformational changes in one dimer drive rearrangements in the other (for a more detailed explanation refer to [18]). It has been calculated that for the synthesis of one ATP molecule, 4 protons

are required (3 for the ATP synthase rearrangements and 1 for ATP, ADP and Pi transport). Once synthetized, ATP can locate inside mitochondrial matrix or be transported into the IMS by the nucleotide exchanger adenine nucleotide translocase (ANT) that passively exchanges ATP with ADP. Once in the IMS, ATP can freely pass the OMM through the voltage dependent anion channel (VDAC).

Modulation of cell calcium signals by mitochondria

The intracellular Ca^{2+}-signalling network

Intracellular Ca^{2+} signalling is versatile and fundamental for the regulation of multiple cellular processes, including development, proliferation, secretion, gene activation and cell death. The universality of Ca^{2+} as an intracellular messenger depends on its enormous versatility in terms of speed, amplitude, and spatio-temporal patterning. The Ca^{2+}-signalling network can be divided into four functional units:

• signalling is triggered by a stimulus that generates various Ca^{2+} -mobilizing signals;

• the latter activate the ON mechanisms that feed Ca^{2+} into the cytoplasm;

• Ca^{2+} functions as a messenger to stimulate numerous Ca^{2+}-sensitive processes; and finally,

• the OFF mechanisms, composed of pumps and exchangers, remove Ca^{2+} from the cytoplasm to restore the resting state [19].

Inside cells, Ca^{2+} concentration ($[Ca^{2+}]$) is controlled by the simultaneous interplay of multiple counteracting processes, which can be split into “ON mechanisms” and “OFF mechanisms”. With these, cells maintain a rigid control over the cytosolic level of Ca^{2+}. In resting conditions, cells maintain a low Ca^{2+} concentration in the cytoplasm (around 100 nM). Ca^{2+} influx from the extracellular space (that posses a concentration around 1-2 mM), or Ca^{2+} release from intracellular Ca^{2+} stores, such as the ER (with concentrations of 250–600 μM) generate the intracellular calcium signals ([20]).

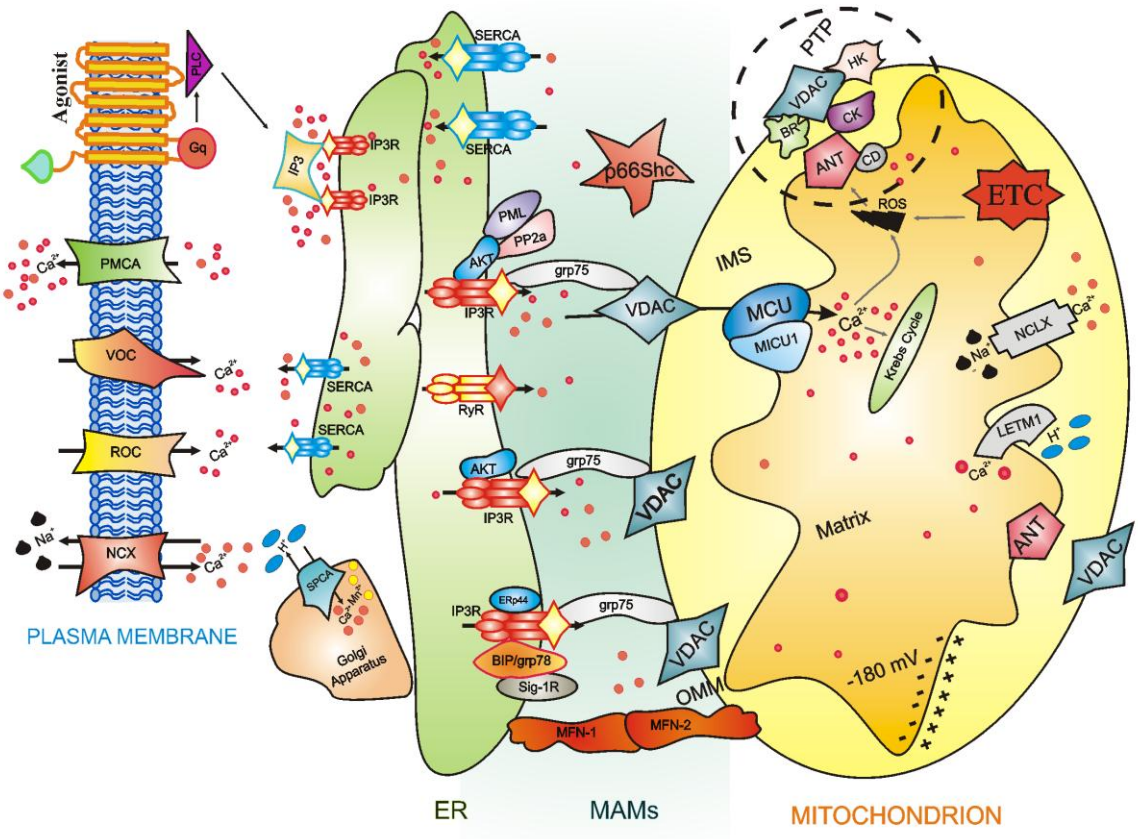

Figure 3 – The Intracellular Ca^{2+} signalling

Mitochondria in calcium signalling

Mitochondria are important components of the "OFF" reaction since they modulate both the amplitude and the spatio-temporal patterns of Ca^{2+} signal ([21]).

That mitochondria can accumulate certain ions from the suspending medium was first observed in the early 1960s, when was discovered that isolated mitochondria from rat liver, kidney, brain and heart can accumulate large net amounts of Ca^{2+} from the suspending medium during electron transport, up to several hundred times the initial Ca^{2+} content [22].

In these studies, initial velocities of energy-dependent Ca^{2+} uptake were measured by stopped-flow and dual-wavelength techniques in mitochondria isolated from hearts of rats. The first rate of Ca^{2+} uptake shows that the initial velocity of Ca^{2+} uptake was slow at low concentrations of Ca^{2+} and increased sigmoidally to 10 nM Ca^{2+}/s/ mg protein at 300 μM Ca^{2+}. Similar results were obtained by the employment of mitochondria subjected of a wide range of mitochondrial protein in the medium (0.5-10 mg/ml), when these organelles were oxidizing glutamate-malate and when acetate was replacing phosphate as a permanent anion [23].

Comparable rates of Ca^{2+} uptake and sigmoidal plots were obtained with mitochondria from other mammalian hearts, as like guinea pigs, squirrels, pigeons, and frogs where the rate of Ca^{2+} uptake was 0.05 nM/mg/s at 5 μM Ca^{2+} and increased sigmoidally to 8 nM/mg/s at 200 μM Ca^{2+} [24].

Mitochondrial Ca^{2+} uptake plays a key role in the regulation of many cells functions, ranging from ATP production to cell death. Increases in mitochondrial calcium activates several dehydrogenases and carriers, inducing an increase in the respiratory rate, H^+ extrusion, and ATP production necessary for the correct energy state of the cell. However, prolonged increase in $[Ca^{2+}]_m$ leads to the opening of the mitochondrial permeability transition pore (PTP), a critical event driving to cell death by apoptosis [25].

Although it is generally accepted that cellular energy metabolism, survival and death are controlled by mitochondrial calcium signals, the underlying molecular mechanisms have been completely elucidated yet. Several studies have identified three essential proteins mediating the processes of calcium influx and efflux:

Mitochondrial Calcium Uniporter (MCU)

The main transporters involved in the uptake of Ca^{2+} into mitochondria is the MCU, characterized by a low affinity for Ca^{2+}; in fact, MCU takes up Ca^{2+} in the micromolar range and experiments in permeabilized cells report a K_d of the uniporter of 10 μM [26]. In addition, a biphasic effect of calcium on the MCU has been reported: beyond a certain level, cytosolic Ca^{2+} inactivates the uniporter, preventing further Ca^{2+} uptake and this process might avoid an excessive accumulation of the cation in mitochondria [27].

In spite of repeated efforts by different researchers, the molecular identity of the MCU has remained elusive. Among the early candidates proposed for the MCU were the uncoupling proteins UCP2/3 [28], but experiments in different tissues of mice lacking UCP2 and UCP3 showed a normal Ca^{2+} uptake [29]. Recently, Perocchi and colleagues [30] demonstrated that MICU1 (mitochondrial calcium uptake 1), also known as FLJ12684 or CBARA1, has a key role in regulating the classically defined uniporter. MICU1 is associated with the IMM and has two canonical EF hands that are essential for its activity and it caused a significant suppression of the $[Ca^{2+}]_m$ signal evoked by an IP3-linked agonist. Silencing MICU1 does not impair mitochondrial respiration or membrane potential but abolishes Ca^{2+} entry in intact and permeabilized cells, and attenuates the metabolic coupling between cytosolic Ca^{2+} transients and activation of matrix dehydrogenases.

More recently, in 2011, two distinct laboratories have been identified a transmembrane protein (CCDC109A) that fulfilling the criteria for being the MCU [31, 32]. Indeed, in planar lipid bilayers CCDC109A showed channel activity with electrophysiological properties as those previously

reported for the MCU [33]. The over-expression of CCDC109A (that now is called "MCU"), increases mitochondrial Ca^{2+} uptake and sensitizes cells to apoptotic stimuli, and the employment of short interfering RNA (siRNA) silencing of MCU strongly reduced mitochondrial Ca^{2+} uptake. This reduction is specific for mitochondria (Ca^{2+} cytosolic levels remain almost unaffected), does not induce impairment of the electrochemical gradient or change in mitochondrial morphology and the induction of specific mutations at the level of the putative pore-forming region reduce the mitochondrial calcium uptake and blocks the channel activity of the protein [31, 32].

Finally, in 2012, it has been identified CCDC90A, referred to as MCUR1 (mitochondrial calcium uniporter regulator 1), as an integral membrane protein required for MCU-dependent mitochondrial Ca^{2+} uptake [34]. MCUR1 binds to MCU and regulates ruthenium-red-sensitive MCU-dependent Ca^{2+} uptake. MCUR1 knockdown does not alter MCU localization, but abrogates Ca^{2+} uptake by energized mitochondria in intact and permeabilized cells. Ablation of MCUR1 disrupts oxidative phosphorylation, lowers cellular ATP and activates AMP kinase-dependent pro-survival autophagy. Thus, MCUR1 is a critical component of a mitochondrial uniporter channel complex required for mitochondrial Ca^{2+} uptake and maintenance of normal cellular bioenergetics.

LETM1:

As described above, MCU only takes up Ca^{2+} in the micromolar range, but evidence has shown that mitochondria are able to take up Ca^{2+} also at much lower concentrations, as recently reported by Jang and colleagues who identified a high-affinity mitochondrial Ca^{2+}/H^{+} exchanger capable of importing calcium in the nanomolar range [35]. This group conducted a genome-wide RNAi screen in *Drosophila* cells stably expressing a mitochondria-targeted ratiometric Pericam and identified the gene CG4589 (*Drosophila* homolog of the human gene LETM1, leucine zipper-EF-hand containing transmembrane protein 1) as a regulator of mitochondrial Ca^{2+} and H^{+} concentrations, supporting electrogenic import of Ca^{2+} (one Ca^{2+} in for one H^{+} out).

However, the effective role of LETM1 as Ca^{2+}/H^{+} exchanger still remains a subject of discussion, since its activity is blocked by treatment with CGP37157 (channel inhibitor that mediates mitochondrial calcium efflux) and red/Ru360 (inhibitor of MCU). Furthermore, LETM1 is associated with K^{+} homeostasis, and the loss of LETM1 lowers mitochondrial membrane potential, and the mitochondrial H^{+}/Ca^{2+} exchanger turned out to be non-electrogenic (one Ca^{2+} in for two H^{+} out) [35, 36].

NCLX/NCKX6:

A Na^{+}-dependent mechanism that mediates mitochondrial Ca^{2+} efflux has been demonstrated, but the molecular identity of this transporter has also remained elusive. In a recent study, Palty and co-

workers showed that the Na^+/Ca^{2+} exchanger NCLX is enriched in mitochondria, where it is localized to the cristae [37]. This protein was identified as a member of the Na^+/Ca^{2+} exchanger situated in the ER or plasma membrane, but Palty et al., shown that in several tissues endogenous NCLX is enriched primarily in mitochondria, but not in ER and plasma membrane. The same observation is achieved overexpressing the protein in different cell lines, and the results show that expression of NCLX enhances mitochondrial Ca^{2+} efflux; this is blocked by CGP37157 and by mutations in the catalytic site of NCLX. Besides, the role of NCLX as a mitochondrial Na^+/Ca^{2+} exchanger is supported by evidence that NCLX mediates Li^+/Ca^{2+} exchange, a functional property that, among NCX proteins, is shared exclusively with the mitochondrial exchanger [37].

MAMs, a functional link between ER and mitochondria

As described above, mitochondria and endoplasmic reticulum networks are fundamental for the maintenance of calcium homeostasis. Recently, different studies have documented the crucial role that MAMs play in intracellular Ca^{2+} signalling. The physical proximity of the ER to mitochondria enables a direct, selective transmission of physiological and pathological Ca^{2+} signals [38] , an aspect highly variable between cell types. In fact, mitochondria are not always morphologically continuous, functionally homogenous and associated to ER. At demonstration of this, different works revealed the existence of a largely interconnected mitochondria network akin to ER in HeLa cells, COS-7 cells, cardiac myocytes and rat hepatocytes [39, 40]. Contrary, it has been also reported that mitochondria can exist as two distinct populations, one in perinuclear position and the other one in cell periphery, with different biochemical and respiratory properties [41]. Or, again, mitochondria within individual cells are morphologically heterogeneous and appear as distinct entities [42]. These different aspects could carry out diverse aspect of mitochondrial functions, in particular Ca^{2+} sequestration, fundamental for the regulation of mitochondrial metabolism and regulation of apoptosis [25]. Lately, it has been demonstrated that the juxtaposition between ER and mitochondria is also regulated by cellular status. In fact, a condition of starvation (an autophagic trigger) leads to PKA activation, which in turn phosphorylates the pro-fission dynamin-related protein 1 (DRP1) with consequent mitochondria elongation in a network of highly interconnected organelles. This mitochondrial elongation protects cells from death and is required to sustain ATP levels and viability [43].

The MAMs, these ER-contiguous membranes, contain multiple phospholipid- and glycosphingolipid-synthesizing enzymes, including long-chain fatty acid-CoA ligase type 4 (FACL4) and phosphatidylserine synthase-1 (PSS-1), enzymes required for cholesterol and ceramide biosynthesis, enzymes involved in glucose metabolism and support direct transfer of

lipids between the ER and mitochondria [38, 44]. MAMs also constitute a calcium signaling hub regulating ER chaperone-assisted folding of newly synthesized proteins, the mitochondria-localized dehydrogenases activity, and the activation of Ca^{2+}-dependent enzymes that execute cell death programs [45]. The importance of MAMs began to emerge when it was found that, after cell stimulation, mitochondria were able to uptake Ca^{2+} directly from IP3Rs [33, 46]. It was thus possible to identify specialized signalling microdomains, selectively enriched in critical Ca^{2+} signalling elements, labelled as "hotspots zones", where Ca^{2+} is transferred from the ER into mitochondria (Table 1). The interactions between the two organelles are modulated by mitochondria-shaping proteins and chaperone proteins. MFN-1 and -2 (mitofusin-1 and -2) belong to the first group and stabilize the interaction between adjacent mitochondria, regulate ER morphology and calcium homeostasis, and directly tether ER to mitochondria, thus facilitating efficient Ca^{2+} uptake by mitochondria [20]. The hsp70 homologous cytosolic chaperone grp75 (glucose-regulated protein 75) tethers the N-terminal domain of the type-1 IP3Rs to the isoform 1 of VDAC, generating a molecular bridge that enhances the Ca^{2+} accumulation in mitochondria [47].

Recently identified, the Sigma-1 ER receptor (Sig-1R) selectively resides at the MAMs, forms a Ca^{2+}-sensitive chaperone complex with BiP/GRP78 (78-kDa glucose-regulated protein GRP78, also referred to as the immunoglobulin binding protein BiP) and associates with isoform 3 of IP3R. Upon activation of IP3Rs, which causes the decrease of Ca^{2+} concentration at the MAM, redistribution of Sig-1Rs occurs, from MAMs to the periphery of the ER: here Sig-1Rs dissociates from BiP/GRP78 and the chaperone activity of free Sig-1Rs attenuates the aggregation of IP3R3 [48].

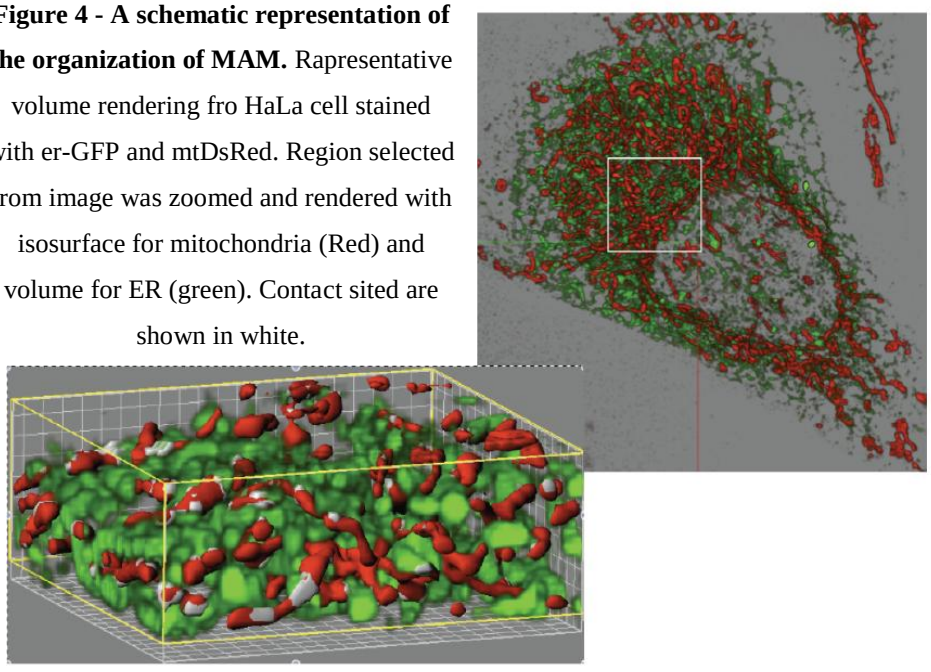

Figure 4 - A schematic representation of the organization of MAM. Rapresentative volume rendering fro HaLa cell stained with er-GFP and mtDsRed. Region selected from image was zoomed and rendered with isosurface for mitochondria (Red) and volume for ER (green). Contact sited are shown in white.

Role of mitochondria in cell survival or cell death - which way to go?

Apoptosis

At the same time, mitochondria are also important checkpoints of the apoptotic process, as they may release caspase cofactors [49]. Indeed, the apoptotic intrinsic pathway is activated by the release of several mitochondrial proteins into the cytosol. The main player in the finely tuned apoptotic activation process is undoubtedly cytochrome c. The majority of cytochrome c is tightly bound to mitochondrial inner membrane, thanks to its electrostatic interactions with acidic phospholipids, but a small fraction probably exists loosely attached to inner mitochondrial membrane and available for mobilization.

This protein is an irreplaceable component of the mitochondrial electron transport chain, shuttling electrons from complexes III to IV, and is thus essential to life: the disruption of its only gene is embryonic lethal [50]. Once released in the cytoplasm, this protein drives the assembly of a caspases activating complex together with Apaf-1 (apoptosis–protease activating factor 1) and caspase 9, the so-called 'apoptosome'. Cytochrome c, once in the cytosol, induces the rearrangement and heptaoligomerization of Apaf-1: each of these complexes can recruit up to seven caspase molecules, leading to their proteolytic self-processing and consequent activation [51].

Mitochondria contain several other proapoptotic, intermembrane space-resident proteins, such as Smac/ DIABLO, HtrA2/Omi, AIF and EndoG. DIABLO (direct inhibitor of apoptosis-binding protein with a low isoelectric point) and HtrA2 (high temperature requirement protein A2) both have an N-terminal domain that can interact and inhibit IAPs (inhibitor of apoptosis proteins). IAPs, such as XIAP, cIAP-1 and cIAP-2, are cytosolic soluble peptides that normally associate and stabilize procaspases, thus preventing their activation. Conversely, apoptosis-inducing factor and EndoG (endonuclease G) translocate from intermembrane space to the nucleus upon treatment with several apoptotic stimuli where they seem to mediate chromatin condensation and DNA fragmentation [52].

In HeLa cells upon ceramide treatment, we observed Ca^{2+} release from the ER and loading into mitochondria. As a consequence, organelle swelling and fragmentation were detected that were paralleled by the release of cytochrome c. These changes were prevented by Bcl-2 expression as well as experimental conditions that lowered $[Ca^{2+}]er$ [53]. Mitochondrial permeability transition pore (PTP: a large conductance channel that opens through a conformational change of its still debated protein components) opening in ceramide-dependent apoptosis was directly demonstrated by Hajnoczky and colleagues [54] who could demonstrate that the lipid mediator facilitates PTP

opening. In this case, ceramide acts as a 'mitochondrial sensitizer' that transforms physiological IP3-mediated Ca^{2+} signals into inducers of apoptosis.

The Bcl-2 protein family controls the above-described intrinsic pathway of apoptosis. Proapoptotic Bax and Bak proteins exist as inactive monomers in viable cells with Bax localizing in the cytosol, loosely attached to membranes, and Bak residing in mitochondrial fraction. Upon apoptosis induction, Bax translocate to mitochondria where it homo-oligomerizes and inserts in the outer membrane; similarly, also Bak undergoes a conformational change, which induces its oligomerization at the outer mitochondrial membrane. Together, these events trigger mitochondrial outer membrane permeabilization, the crucial process mediating the release of intermembrane space-resident caspase cofactors into the cytoplasm [55].

Mitochondria also undergo a more 'macroscopic' remodelling of their shape during the programmed cell death. Indeed, after apoptosis induction, mitochondria become largely fragmented, resulting in small, rounded and numerous organelles. This process occurs quite early in apoptotic cell death, soon after Bax/Bak oligomerization, but before caspase activation. Interestingly, the perturbation of the equilibrium between fusion and fission rates seems to correlate with cell death sensitivity. In particular, conditions in which mitochondrial fission is inhibited, such as DRP1 (dynamin-like protein 1) downregulation or mitofusins overexpression, strongly delay caspase activation and cell death induced by numerous stimuli. Similarly, stimulation of organelle fission (by DRP1 overexpression or Mfn1/2 and OPA1 inhibition) promotes apoptosis by facilitating cytochrome c release and apoptosome assembly [56]. However, the relationship between mitochondrial fusion/fission and apoptosis is complex and mitochondrial fragmentation is not necessarily related to apoptosis. Indeed, mitochondrial fission per se does not increase cell death and DRP1 overexpression has been reported to protect cells from some apoptotic challenges, such those dependent on mitochondrial Ca^{2+} overload.

Another hallmark of apoptosis is the loss of mitochondrial membrane potential, secondary to the opening of mPTP triggered by different pathological conditions (e.g., Ca^{2+} overload, ATP depletion, oxidative stress, high inorganic phosphate or fatty acid). The molecular structure of this pore is currently highly debated, but the main players in mPTP assembly seem to include the adenine nucleotide transporter (ANT) in the inner membrane, the voltage-dependent anion channel (VDAC), the peripheral benzodiazepine receptor in the outer membrane and cyclophilin D, a matrix protein [57]. The availability of chemical mPTP inhibitors such as cyclosporine A and related compounds lacking the cytosolic inhibitory effect on calcineurin, as well as the development of cyclophilin D knockout mouse will help to clarify the role of mPTP in physiological and

pathological condition and identify areas of pharmacological intervention in common disorders such as ischemia-reperfusion injury, liver diseases, neurodegenerative and muscle disorders.

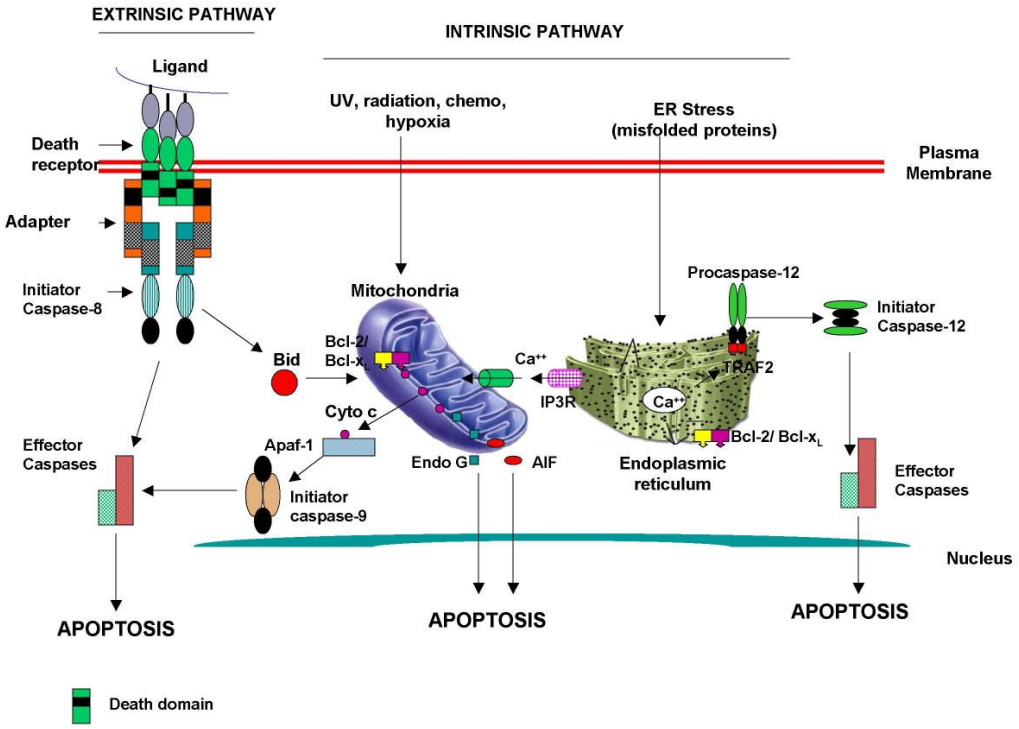

Figure 5 – Molecular mechanism of apoptosis

Interestingly, some of the proposed components of the mPTP participate in Ca^{2+} homeostasis. Indeed, transient expression of VDAC enhanced the amplitude of the agonist-dependent increases in mitochondrial matrix Ca^{2+} concentration by allowing the fast diffusion of Ca^{2+} from ER release sites to the inner mitochondrial membrane. As to the functional consequences, VDAC overexpressing cells are more susceptible to ceramide-induced cell death, thus confirming that mitochondrial Ca^{2+} uptake has a key function in the process of apoptosis [58]. ANT overexpression instead reduced the amplitude of the $[Ca^{2+}]_m$ peak following ER Ca^{2+} release, and this effect was partially reversed by treating the cells with cyclosporine A, suggesting the involvement of mPTP in ER-mitochondria Ca^{2+} transfer [59]. Moreover, mitochondria are quantitatively the most important source of intracellular reactive oxygen species and leak from the electron transfer chain is supposed to be the main route [60]. Recently, a totally new, unexpected pathway has emerged that involves $p66^{Shc}$ in mitochondrial reactive oxygen species production. Intriguingly, upon phosphorylation by PKCβ and peptidyl–prolyl cis/trans isomerase (Pin1) recognition, $p66^{Shc}$ translocates to mitochondria [61] where it exerts its own oxidoreductase activity [62]. As a consequence, $p66^{Shc}$ directly oxidizes cytochrome c (thus allowing electron to escape mitochondrial electron transport chain) and generates H_2O_2, leading to mPTP opening and in turn cell death. The existence of a protein that

'steals' electrons from the mitochondrial electron transport chain and produces reactive oxygen species provides direct evidence for the role of reactive oxygen species in signal transduction, that may represent the biochemical basis of the free radical theory of ageing.

Autophagy

Cell homeostasis is achieved by balancing biosynthesis and turnover of macromolecules and organelles. There are two major systems in eukaryotic cells that degrade cellular components: the ubiquitin proteasome system (UPS) and the lysosome. The UPS only degrades proteins, mainly short-lived proteins, which must be tagged by ubiquitin to be recognized by the proteasome [63]. The lysosomal system is responsible for degrading macromolecules, including proteins, and for the turnover of organelles by autophagy [64]. The term "autophagy" was coined by Christian de Duve soon after his discovery of lysosomes [65, 66].

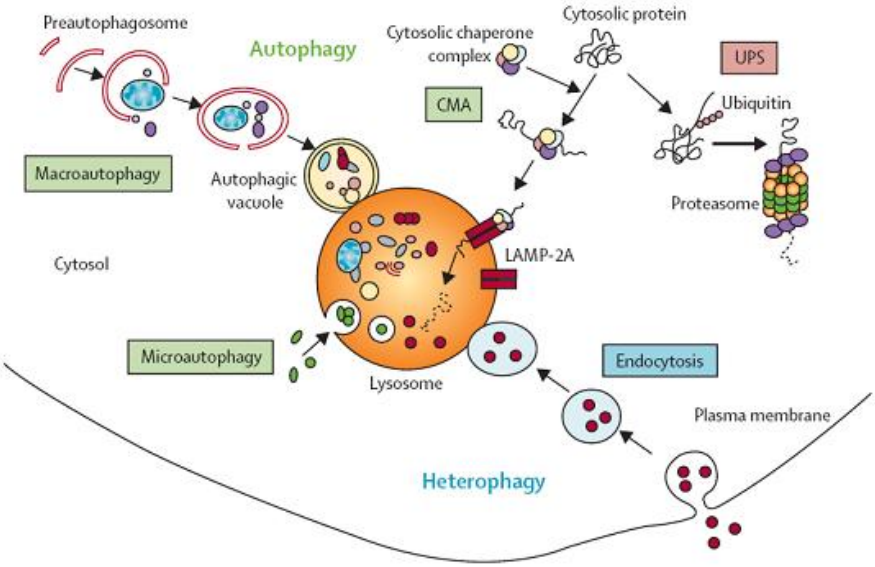

Figure 6 – The mammalian autophagy

The seminal discovery of *ATG* genes, originally in yeast and subsequently in multicellular organisms, has provided an important breakthrough in the understanding of macroautophagy and of its functions in physiology and disease [67, 68]. The term "autophagy" also embraces microautophagy and chaperone-mediated autophagy (CMA). In contrast to macroautophagy, which starts with the formation of a vacuole, known as the autophagosome, which sequesters cytoplasmic components, microautophagy consists of the direct uptake of portions of the cytoplasm by the lysosomal membrane.

Macroautophagy and microautophagy are conserved from yeast to humans. These processes were originally described as mechanisms for bulk degradation. Microautophagy is dependent on GTP hydrolysis and on Ca^{2+} [69]. However, the molecular regulation of microautophagy remains to be unraveled.

CMA is a selective form of autophagy that has only been described in mammalian cells [70] and provides the selective removal of substrates which contain a KFERQ-related motif in their amino acid sequence. This motif is recognized by the cytosolic constitutive chaperone hsc70 (heat shock cognate of the heat shock protein 70 family); this recognition allows for the lysosomal delivery of CMA substrates. The lysosomal membrane protein, LAMP-2A, serves as a receptor in the translocation of unfolded polypeptides across the lysosomal membrane. KFERQ-like motifs are found mainly in cytosolic proteins and are estimated to occur in about 30% of such proteins. CMA performs several general functions, such as the elimination of oxidized proteins and the removal of misfolded proteins, and also provides amino acids during prolonged periods of starvation. It is interesting to note that during starvation, cross talk occurs between macroautophagy and CMA [70]. When CMA is stimulated, macroautophagy is first induced and then declines. The molecular basis for this switch has not been identified. Prevention of the age-related decline of CMA is beneficial for the homeostasis of organs and function . This observation is indicative of the potential importance of CMA and macroautophagy, as we discuss below, as possible antiaging mechanisms. CMA is also involved in more specific functions, such as antigen presentation by major histocompatibility complex (MHC) class II molecules, neuronal survival, and kidney growth [71].

Molecular machinery of autophagy

Under stress conditions such as amino acid starvation, autophagy is induced in cells. Energy levels are primarily sensed by AMP activated protein kinase (AMPK), a key factor for cellular energy homeostasis. In low energy states, AMPK is activated and the activated AMPK then inactivates mammalian Target of rapamycin, MTOR .Depending on nutrient conditions, MTOR regulates the activities of the ULK1 kinase complex [72]. Under growing and high-nutrient conditions, the active MTORC1 interacts with the ULK1 kinase complex and phosphorylates ULK1 and ATG13, and thus inhibits the membrane targeting of the ULK1 kinase complex. During starvation condition, on the other hand, the inactivated MTORC1 dissociates from the ULK1 kinase complex and results in the ULK1 kinase complex free to phosphorylate components, such as ATG13 and FIP200, in the ULK1 kinase complex, leading to autophagy induction [73].

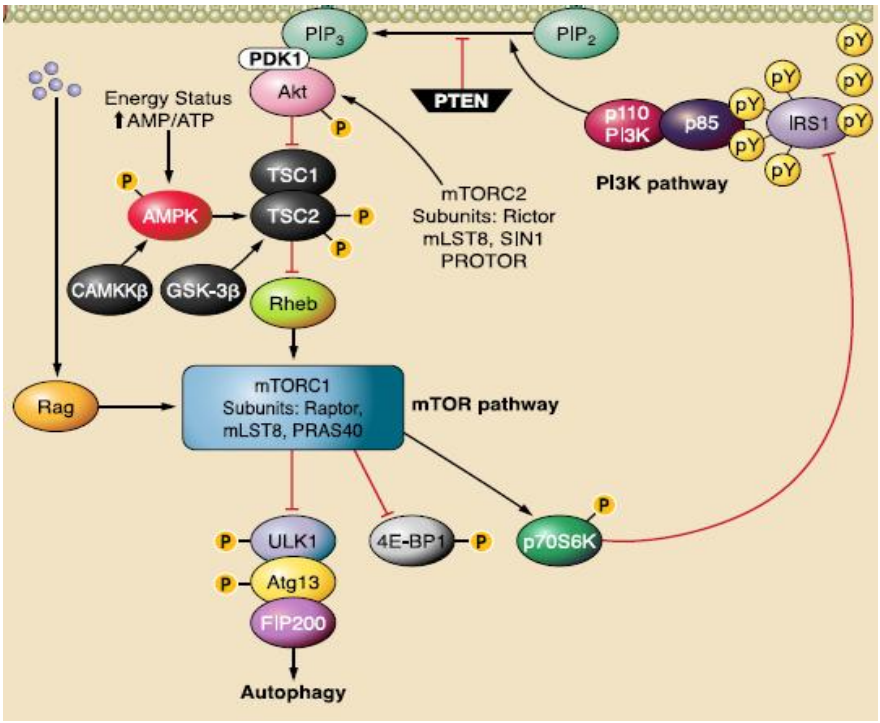

Figure 7 – An overview of the autophagic machinery

Autophagosome formation process is composed of isolation membrane nucleation, elongation and completion steps (**Figure 7**). In mammals, the class III PI3K complex plays an essential role in isolation membrane nucleation during autophagy. The class III PI3K (VPS34) is associated with BECLIN1 (mammalian ATG6 homologue) and VPS15 (phosphoinositide-3- kinase, regulatory subunit 4), the homolog of yeast p150, to form the class III PI3K core complex. The first step of autophagosome formation, autophagosome nucleation requires BECLIN1. The interaction of BECLIN1 with VPS34 is known to promote the catalytic activity of VPS34 and increase levels of PI(3)P, but is dispensable for the normal function of VPS34 in protein trafficking or recruitment of endocytic events.

Depending on the proteins recruited by BECLIN1, class III PI3K complexes differentially regulate the process of autophagosome formation.80 BECLIN1 complex binding partner acting as autophagy positive regulator are: ATG14L, UVRAG, AMBRA1, BIF1, PINK1, VMP1, HMGB1.81 In contrast to these positive regulators, there are negative regulators among Beclin1-interacting partners such as RUBICON, BCL-2 and BCL-XL [74].

The expansion of the isolation membrane is basically the simultaneous elongation and nucleation of the phagophore. Two ubiquitin-like protein conjugation systems are involved in the expansion of autophagosome membranes, the ATG12-ATG5 and the ATG8- phosphatidylethanolamine (PE). ATG12-ATG5-ATG16 is essential for the formation of pre-autophagosomes. ATG12 is a 186-amino acid protein and is conjugated to ATG5 through a carboxy-terminal glycine residue.

The ATG12-ATG5 conjugate further interacts with ATG16 to form a ~350 kDa multimeric ATG12-ATG5-ATG16 protein complex through the homo-oligomerization of Atg16. The second ubiquitin-like protein conjugation system is the modification of ATG8 by PE, an essential process for the formation of autophagosome. ATG8 is cleaved by cysteine protease ATG4 and then conjugated with PE by ATG7 and ATG3, a second E2-like enzyme. This lipidated ATG8-PE then associates with newly forming autophagosome membranes.

The conversion of ATG8 to ATG8-PE is thus well-known as a marker of autophagy induction. While ATG8 in yeast is represented by a single gene, its homologues in humans are represented by at least eight members that can be divided into two subgroups based on their amino acid sequence homology: the microtubule-associated protein 1 light chain 3 (LC3) family (LC3A, LC3B, LC3B2 and LC3C) and the GABA(A) receptor-associated protein (GABARAP) family (GABARAP, GABARAPL1, GABARAPL2 and GABARAPL3). Importantly, apart from GABARAPL3, they are all conjugated to PE and, consequently, incorporated into autophagosomal membranes. The two protein subfamilies are essential for autophagosomes biogenesis and probably have distinct roles in the overall autophagic process. Notably, the functions of ATG8 human orthologs are mostly based on their interaction with a large cohort of proteins, with extensive binding partner overlap between family members [75].

Finally, autophagosome fuses with lysosomes or vacuoles, which is an essential process for completion of the autophagy pathway. Sequestration of cytoplasm into a double-membrane cytosolic vesicle is followed by the fusion of the vesicle with a late endosome or lysosome to form an autophagolysosome (or autolysosome). Then, inner membrane of the autophagosome and autophagosome-containing cytoplasm-derived materials are degraded by lysosomal or vacuolar hydrolases inside the autophagosome. Autophagy is one of the major responses to stress in eukaryotic cells and is implicated in several pathological conditions such as infections, neurodegenerative diseases and cancer [76].

Still, as upstream signaling events leading to stimulation of autophagy are still poorly characterized, possibilities to interfere with this process and, eventually, take advantage of its modulation for therapeutic purposes are limited.

Mitochondria and autophagy

One link between autophagy and mitochondria is the selective elimination of excess or damaged mitochondria, a process called mitophagy. Mitochondria are degraded under a variety of different conditions, including basal mitochondrial quality control, mitochondrial dysfunction, and during

developmental processes, such as during the maturation of immature red blood cells [77]. To date, considerable progress has been made in identifying mitophagic adaptors or the degradation of parental mitochondria after fertilization and understanding the overall importance of mitophagy for aging and neurodegenerative diseases.

Mitochondrial depolarization can occur naturally during mitochondrial fission or can be induced through cellular stress pathways, including apoptosis. Upon extensive damage, mitochondrial membranes can be permeabilized through distinct routes, and mitochondrial membrane permeabilization (MMP) constitutes one of the hallmarks of apoptotic or necrotic cell death [49].

However, if the mitochondrial insult is not too severe and only a fraction of the mitochondrial pool is damaged, mitophagic degradation could rescue the cell and prevent cell death.

Damaged mitochondria can be recognized through the voltage-sensitive kinase PINK1. Under normal circumstances, PINK1 is continuously degraded on mitochondria, but upon loss of $\Delta\psi m$, PINK1 is stabilized on the outer mitochondrial membrane [78]. The rapid accumulation of PINK1 on the mitochondrial surface facilitates recruitment of Parkin, an E3 ligase to mitochondria, where it ubiquitinates multiple mitochondrial proteins, including the fusion proteins Mfn1/2 and the VDAC1 protein. The accumulation of ubiquitin-modifications is thought to facilitate the recruitment of the autophagy adaptor p62, eventually leading to the autophagosomal degradation of the damaged mitochondrion [79]. Mutations in the genes coding for both PINK1 and Parkin were identified in the early-onset forms of Parkinson disease. In cell culture models, disease-associated mutants of PINK1 and Parkin dramatically reduced the recruitment of Parkin to damaged mitochondria and their subsequent degradation [80].

Another protein linked to mitophagy in mammalian cells is NIX. In immature red blood cells, NIX mediates the mitophagic removal of excess mitochondria. But the elimination of damaged mitochondria seems also be NIX-dependent in some cell lines [81]. In addition to mitophagy-mediators, the loss of general autophagy regulators, like ATG5 or ATG7, also leads to significant accumulation of damaged mitochondria, further supporting the idea that autophagy plays an essential role in mitochondrial quality control to ensure the health of the mitochondrial pool [82].

Recent studies demonstrated that mitochondria are not only a downstream substrate of mitophagy, but that they are able to actively influence their own fate during starvation-induced autophagy. Two recent studies showed that during starvation, mitochondria react to the depletion of nutrients (especially nitrogen sources) with rapid and extensive mitochondrial tubulation. The formation of elongated mitochondrial networks appears to be dependent on the PKA-mediated inactivation of the fission protein Drp1, removing the counterbalancing force to fusion. Interestingly, these mitochondrial networks resulted in sustained mitochondrial ATP production, enhanced cellular

survival and, most importantly, prevented the elimination of mitochondria. In contrast to this, fusion-incompetent mitochondria were heavily degraded during starvation. This suggests that mitochondrial morphology actively influences mitophagic responses. The exact mechanism by which mitochondrial fusion prevents mitophagy is still unclear. The mitochondrial size alone could be a determining factor, as the loss of Drp1-activity also decreases mitophagy under basal conditions and upon external mitochondrial damage. Alternatively, changes in mitochondrial activity and/or recruitment of mitophagy-adaptors (like Parkin) could be causative for the decreased degradation of fused mitochondria [43, 83].

Mitochondrial depolarization/fragmentation are two common prerequisites for mitophagy, and mitochondrial fusion can block mitophagy. This intimate link between mitochondrial shape and degradation suggests that both processes could also be coupled on the molecular level. Indeed, two different systems were identified that affect both mitophagy and mitochondrial shape. Parkin has been suggested to regulate mitochondrial fusion in addition to its well-established function as a mitophagy adaptor. A similar connection has been suggested for the autophagy-regulating proteins ATG12 and ATG3. During the induction of autophagy, ATG12 gets covalently linked to ATG5, thus driving the expansion and formation of the autophagosome. A recent study by Debnath and colleagues identified ATG3 as a further acceptor for ATG12. Lack of the covalent ATG12/3 complex led to mitochondrial fragmentation and loss of mitophagy, partially mimicking the effects of Parkin depletion in mammalian cells. Even though mitochondrial dynamics and mitophagy are linked by several means, it will be important to understand which processes/proteins directly affect mitochondrial dynamics and which effects on mitochondrial shape are only secondary to changes in mitophagy and/or the accumulation of dysfunctional mitochondria [84].

Mitochondria and neurodegeneration

The involvement of mitochondria and their dysfunction in the pathogenic context of neurological disorders has been extensively debated and is now generally accepted [85, 86]. While mitochondria have long been known for their role in ATP generation through oxidative phosphorylation (OxPhos), many more diverse (patho)physiological roles for these organelles have been described during the last two decades. The traditional view of mitochondria as powerhouses quietly lingering around/resting in the cytosol of cells is now replaced by the perspective of a dynamic mitochondrial network that not only physically connects remote cellular compartments (such as neuronal

synapses) to the soma but which is also intrinsically involved in major cellular life and death decisions [87].

Beyond ATP generation, mitochondria are also involved in a number of critical pathways, including the buffering of calcium ions, lipid metabolism, the synthesis of iron-sulfur clusters, and the regulation of programmed cell death.

This deep integration of mitochondria into cellular physiology is reflected by the sometimes dramatic consequences linked to mitochondrial dysfunction. Physiological aging as well as age-related diseases are frequently associated with decreased mitochondrial function. Thus, diverse maintenance mechanisms, operating to keep mitochondria in a peak functional state, are of uttermost importance to prevent mitochondrial dysfunction-linked diseases, premature aging and associated cell death.

Multiple Sclerosis

Multiple sclerosis is a complex chronic immune mediated disease of the central nervous system (CNS) [88]. Its etiology is currently unknown and its pathogenesis is only partly understood. Complex genetic traits as well as environmental factors determine the susceptibility to develop the disease and the respective results indicate that immune mechanisms play an essential role in driving the disease process[89]. Major support for an autoimmune hypothesis comes from studies of experimental autoimmune encephalomyelitis (EAE), a disease in animals, which can be induced by sensitization with CNS antigens. EAE shares clinical and pathological features with MS, and in particular by immunologists EAE is generally accepted as the animal model for MS [90]. Thus, when searching medical databases for publications of the last decades related to the pathogenesis of MS, the vast majority of the respective studies describe disease mechanisms in EAE animals. Furthermore, it shed light on different pathways of tissue injury triggered by immune reactions in the CNS. It is now well accepted that these studies form the background, on which modern anti-inflammatory and immunomodulatory treatments, which are effective in MS patients, have been developed. However, there were also major disappointments [91]. Quite a significant number of therapies, which were potential candidates from EAE studies, failed the test of human trials. Prominent examples for divergent results between EAE models and human trials are treatments with tumor necrosis factor alpha (TNF) blockers [92], with gamma-interferon [93] or the blockade of Th1/Th17 pathways [94]. This is even worse for "neuroprotective" therapies, for which so far none has been proven to be effective in MS patients. One potential reason for this disappointing situation may be that the pathogenesis of the disease, in particular in the progressive stage, is more complex than that of current EAE models and seems to involve mechanisms of innate immunity in the process of neurodegeneration. In

addition, chronic inflammation in the MS brain may provoke additional autoimmune responses directed against antigens different from those tested in classical models of EAE. For these reasons, much more effort has to be invested to study the disease process of MS with particular focus on immunological and molecular events, which take place in the brain and spinal cord lesions of the patients themselves, and to reflect these findings on the basis of knowledge, obtained in EAE models before.

Basic features of MS pathology

Multiple sclerosis is a chronic inflammatory disease of the CNS. Its pathology was originally defined by the presence of focal white matter lesions, characterized by primary demyelination with partial preservation of axons and reactive astrocytic scar formation [95]. Although axons are quite well preserved within the lesions in comparison to the complete demyelination, they too are affected and axonal loss has been shown to be a major correlate of permanent neurological deficit in MS patients. In the early stages of the disease, when patients present with clinical relapses and remissions inflammatory demyelination leads to the formation of focal plaques, which are predominantly located in the white matter. In later stages of the disease, dominating in patients with secondary or primary progressive disease, additional pathology is seen, which includes widespread demyelination in the cerebral and cerebellar cortex as well as diffuse degenerative changes throughout the entire white and grey matter [96]. This finally results in patients with longstanding severe disease in profound brain and spinal cord atrophy with extensive tissue loss and dilatation of cerebral ventricles. Thus, while the disease process starts with inflammation driven focal demyelinating lesions, which arise around small drainage veins in the white matter, in time diffuse neurodegeneration ensues which affects the entire CNS [97].

Mitochondrial Injury in MS Lesions

Demyelination is the hallmark of the lesions, and it has been shown more recently that it is preceded by destruction of oligodendrocytes through apoptosis [98]. In addition, axonal loss is present in all lesions and its extent varies between different lesions and patients. Remyelination may occur, but in the majority of the patients it is impaired, even when oligodendrocyte progenitor cells are present. Astrocytes are also affected within the lesions, showing retraction of their cell processes and loss of molecules, which are normally expressed in the most peripheral processes, forming the perivascular and subpial glia limiting membrane. Thus, in essence all cellular components of the CNS are affected in MS lesions, albeit in quantitatively variable extent. To explain such a scenario by a

single mechanism cell type specific vulnerability has to be postulated. Interestingly, the tissue alterations, present in fulminant active MS lesions, are strikingly similar to those seen in fresh lesions of patients with an acute white matter stroke [99]. These data place energy deficiency in the center of interest, when discussing neurodegeneration in MS patients.

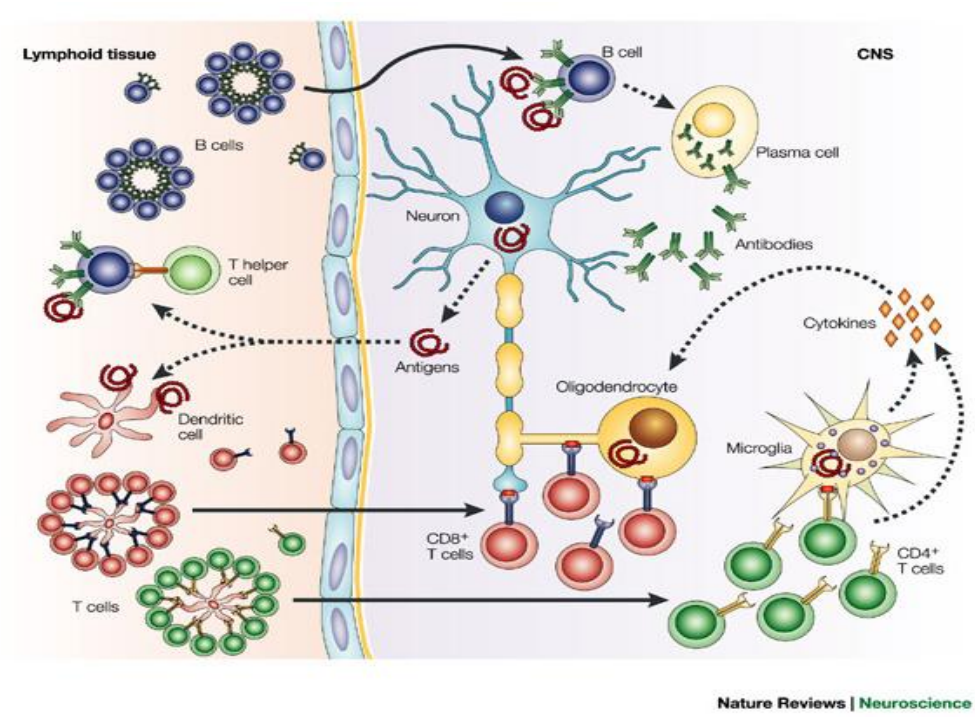

Figura 8 – The mechanism of direct neuron and oligodendrocyte damage in MS

In line with this concept recent data identified mitochondrial injury with subsequent energy deficiency as an important component of MS pathogenesis. Profound mitochondrial disturbances have been found in MS lesions by microarray based gene expression analysis, by immunohistochemistry, biochemical analysis and by electron microscopy [100, 101] . In acute and active lesions first changes in mitochondria are reflected by a dominant loss of immunoreactivity of cytochrome C oxidase (COX1) and loss of the respective complex IV activity of the mitochondrial respiratory chain. In contrast, in chronic inactive lesions mitochondrial numbers and activity are increased, apparently reflecting the higher energy demand of demyelinated compared to myelinated axons. Tissue injury due to mitochondrial dysfunction can be induced in principle by three different mechanisms: energy failure, the induction of apoptosis and enhanced production of reactive oxygen species. Mitochondrial injury can trigger pro-apoptotic events, for instance by the liberation of apoptosis-inducing factor (AIF) or cytochrome C. This apparently represents an important pathway of oligodendrocyte destruction and demyelination. Energy failure provides a good explanation for

other aspects of MS pathology [102]. It explains the preferential destruction of small caliber axons, resulting in disturbed ion clearance from the axoplasm, Ca^{2+} accumulation and axonal demise predominantly in those axons with low mitochondrial content and large axonal surface area [103].

In oligodendrocyte progenitor cells mitochondrial injury results in an impaired maintenance of cell processes and differentiation into myelinating cells resulting in remyelination failure. This is in line with previous studies indicating an important role of inflammatory factors and differentiation block of oligodendrocyte progenitor cells in remyelination failure in MS [104]. A similar mechanism may underlay the disturbance of astrocyte polarity in active MS lesions. Importantly, recent findings demonstrate the occurrence of extensive neuronal mtDNA deletions in MS cortex. The cause of these mtDNA alterations might be ongoing microglial activation, but this has to be proven yet. Nonetheless, it is conceivable that respiratory-deficient mitochondria in affected neurons significantly contribute to neurodegenerative processes underlying MS progression. Thus, taken together the complex pathological alterations, which occur side by side within active MS lesions, can in principle be explained by a single mechanism, which involves mitochondrial injury and dysfunction [97].

The protein kinase C β and the mitochondrial axis as key regulators of autophagy

Introduction

Macroautophagy (herein "autophagy") is a degradation pathway that is primarily regulated by nutrient starvation. A double-membrane vesicle, called autophagosome, encloses a portion of the cytoplasm, long-lived proteins and organelles and then fuses with a lysosome (to form an autolysosome) for the degradation and consequent recycling of its contents.[105] Autophagy is a major phenomenon of cell biology, acts as a pro-survival or pro-death mechanism and takes part in different biological events, such as protein and organelle turnover, development, aging, pathogen infection, neurodegeneration and cancer.[106-108]

Various tumor suppressor proteins (such as BECN1, PTEN, BH3-only proteins, TSC1 and TSC2) induce autophagy, whereas several oncogenes (such as AKT, PI3K and anti-apoptotic proteins from the BCL-2 family) simultaneously inhibit it.[109-113] Although PKCβ is not considered to be a classical oncogene, this PKC family isoform is considered to be a tumor promoter because it enhances certain cellular signaling pathways.[114] For example, it has been demonstrated that the activation of PKCβ promotes phosphorylation of p66-kilodalton isoform of the growth factor adapter Shc ($p66^{Shc}$) and triggers its mitochondrial accumulation and redox response.[115] Recently, it has been demonstrated that different PKC isoforms negatively or positively modulate the rate of autophagy,[116-120] but the exact mechanism remains ambiguous, and no information on PKCβ involvement in the autophagic process has been reported. The PKCs are a family of serine/threonine kinases that are involved in tumor formation and progression and are divided into three major groups based on their activating factors: (i) the classical (or conventional) PKC isoforms, α, βI, βII, and γ; (ii) the novel PKC isoforms, δ, ε, θ, η, and μ; and (iii) the atypical PKC isoforms, ζ and λ.[121] The number of PKC isozymes expressed and their levels vary in different tissues, and the biological significance for this heterogeneity is not known.[122] However, different PKC isoforms phosphorylate different target proteins on serine or threonine residues, mediating distinct biological responses.[123, 124]

PKCβ localization at mitochondrial level has been known for some time, and this kinase is implicated in the regulation of mitochondrial integrity and oxidative phosphorylation.[125, 126]

Mitochondria are the primary energy producers of the cell and are recognized as key participants and transducers of several cell death pathways.[127] Moreover, dysfunctions in mitochondrial physiology contribute to the pathophysiology of several disorders.[128-130]

It has been demonstrated that the energy status of the mitochondria is a fundamental regulator both of autophagy (the nonselective catabolism of cellular components, such as the cytosol, organelles and protein aggregates, which occurs upon nutrient deprivation)[43] and of targeted or specific autophagy (the removal of superfluous or damaged organelles and protein aggregates, which occurs under nutrient-rich conditions).[131] However, the role of mitochondrial homeostasis during autophagy remains unclear. Here, we investigate the existence of a putative relationship between PKCβ, mitochondria and autophagy. In the present study, we report that the activation of PKCβ attenuates mitochondrial energy, which in turn reduces autophagy, both in vitro and in vivo. Moreover, we show that the administration of compounds that positively modulate the mitochondrial membrane potential (Ψ_m) reverses the mitochondrial alterations induced by PKCβ activation and rescues the normal rate of autophagy induction. Finally, we suggest the involvement of $p66^{Shc}$ in PKCβ-mediated regulation of autophagic machinery.

Results

PKCβ overexpression attenuates autophagy

The initial goal of our work was to evaluate whether the β isoform of PKC could affect the autophagy machinery. To unveil this possible interaction, we quantified the levels of autophagy in HEK293 cells transfected with a PKCβ chimera or with a mock plasmid empty vector as a control.

Microtubule-associated protein light chain 3 (LC3) is a mammalian homolog of yeast Atg8, which is used as a specific marker to monitor autophagy.[132] After translation, proLC3 (which is neither LC3-I nor LC3-II) is processed to LC3-I, which is localized to the cytosol. After a short starvation period, LC3-I is modified to a membrane-bound form, LC3-II, which is localized to pre-autophagosomes.

This conversion can be detected by immunoblotting with antibodies against LC3 that recognize the two different forms of LC3: LC3-I possesses a molecular mass of approximately 16 kD, whereas LC3-II (the amount of which is correlated with the number of autophagosomes) is 14 kD in size.[133]

In all of the experiments, the level of autophagy was quantified as the ratio of LC3-II to β-ACTIN (our loading control) and as the ratio of LC3-II/LC3-I, how recommended in different guidelines for the study of autophagy.[134, 135]

The overexpression of PKCβ led to a significant down-regulation of autophagy compared with HEK293 cells transfected with empty vector under resting conditions, as assessed by a decrease in the endogenous LC3-II levels, which is indicative of defective autophagy. Furthermore, PKCβ overexpression also inhibits the formation of autophagosomes after serum starvation (**Fig. 9A**). The negative regulation of the autophagic machinery promoted by PKCβ has been also confirmed in

control and PKCβ-overexpressing HEK293 cells treated with rapamycin (a MTOR inhibitor), which produces a higher flux autophagy response.

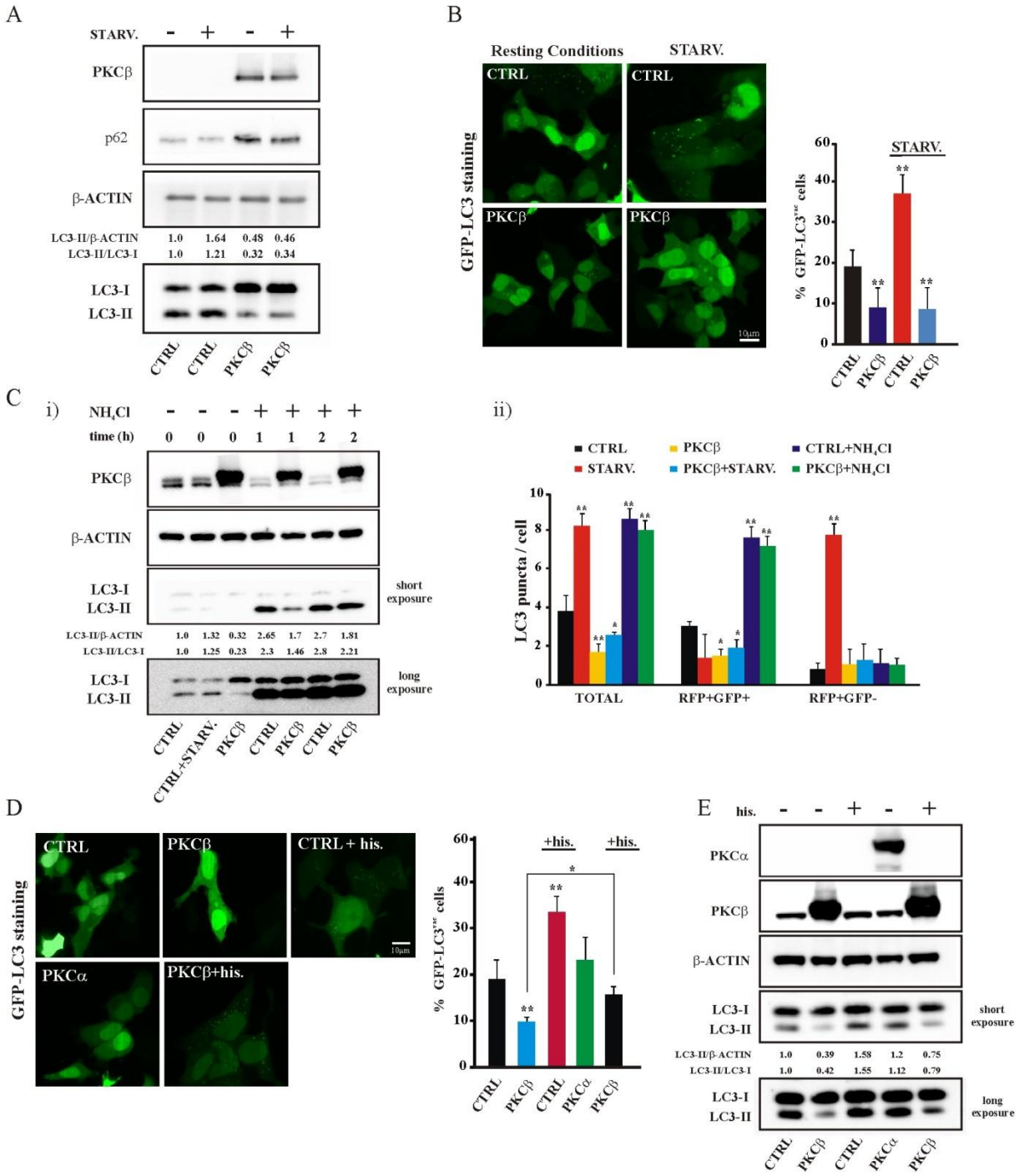

Figure 9 – PKCβ reduces the autophagic levels

In addition to LC3, it is possible to use the protein p62/SQSTM1 as autophagy marker. In this case, p62 is inversely correlated with autophagic activity because it is selectively incorporated into autophagosomes via an interaction with LC3; thus, it is efficiently degraded by autophagy.[136, 137]

The overexpression of PKCβ boosts the abundance of the autophagy substrate p62/SQSTM1, suggesting that this kinase effectively acts as an endogenous inhibitor of autophagy (**Fig. 9A**). To confirm our findings, we performed a live microscopy analysis to monitor the formation of autophagosomes in HEK293 cells that were co-transfected with the PKCβ chimera or empty vector and the GFP-LC3 reporter. As reported above, the amount of LC3-II is closely correlated with the number of autophagosomes; thus, another widely used method of monitoring autophagic activity is the employment of the chimeric protein GFP-LC3. Upon the induction of autophagy, autophagosomes can be visualized as ring-shaped or punctate structures.[138]

In control cells maintained in resting conditions, LC3 staining showed a small amount of autophagosomes. After 1h of serum starvation, many ring-shaped GFP-LC3 structures were observed in control cells, indicating the translocation of LC3-II from the cytosol to autophagic vacuoles (AV).

PKCβ-overexpressing cells showed a cytosolic staining pattern for LC3 both under resting conditions and after nutrient withdrawal, confirming that PKCβ plays a critical role as a negative regulator of autophagy (**Fig. 9B**).

The quantitation of cellular autophagosomes indicates the level of cellular autophagic activity, but the presence of the autophagosomal marker LC3 can be attributed either to an increased initiation of autophagy or to a block in the degradation of autophagosomes. To distinguish between these possibilities, we performed an autophagic flux assay.[132] In particular, we evaluated the induction of autophagy in the presence of the lysosomal activity inhibitor NH_4Cl. As results, we found that after a short treatment (1h) with NH_4Cl 20mM in cells expressing PKCβ, the increase in the LC3-II levels was minor comparing treated mock-transfected cells. This suggest that the autophagic response is not compromised in our experimental condition and it is consistent with the ability of PKCβ to attenuate the autophagic process, which in turn led a minor availability of the lapidated form of LC3 (**Fig. 9Ci**). Contrary, after a longer NH_4Cl treatment (2h) we observed a marked and comparable accumulation of LC3-II either in PKCβ-expressing or control cells, probably due to a saturating level of the lysosomal activity inhibitor (**Fig. 9Ci**).

To confirm this finding, we performed direct fluorescence microscopy to monitor the LC3 turnover in HEK293 cells in the presence of NH_4Cl with the tandem construct mCherry-LC3-eGFP. This assay is based on the concept that the low pH inside the lysosome quenches the signal of GFP, whereas a red fluorescent protein (such as mCherry) is relatively stable in acidic compartments. Thus, most GFP-LC3 puncta do not co-localize with lysosomes. In contrast, mCherry-eGFP-LC3 is detectable in the lysosomal compartment. Thus, it is possible to trace the autophagic flux with the construct mCherry-eGFP-LC3.[139]

LC3 staining under resting conditions showed a small number of autophagosomes and autolysosomes labeled with yellow (RED+GFP+) and red (RED+GFP-), respectively. In starved cells, the number of red puncta (RED+GFP-) was much greater than the number of yellow puncta (RED+GFP+). After treatment with NH_4Cl, the number of yellow puncta (RED+GFP+) was obviously increased without a corresponding increase in red puncta (RED+GFP-), both in control and PKCβ-expressing cells (**Fig. 9Cii**), suggesting that the accumulation of autophagosomal markers is not due to a block in the degradation of autophagosomes.

To exclude a broad effect of the classic PKCs and not a specific effect of the β isoform, we performed autophagy measurements in HEK293 cells transfected with the other two conventional PKC. In agreement with our hypothesis, the overexpression of PKCα or PKCγ-HA did not modulate autophagy, confirming the specific involvement of PKCβ in the attenuation of autophagy (**Fig. 9D, E**).

Finally, to rule out the possibility that we were observing spurious effects of a global perturbation of cellular functions due to the overexpression of PKCβ, we aimed to confirm these observations using the pharmacologic agent hispidin (6-(3,4-dihydroxystyryl)-4-hydroxy-2-pyrone), reported to be a specific blocker of the PKCβ isoform.[140]

To verify the effective selectivity of hispidin for PKCβ, we performed live fluorescence microscopy analysis to monitor the PKCβ localization. In these experiments, HEK293 cells were transfected with PKCβ-GFP or PKCα-GFP chimera, treated for 24h with 5 μM of hispidin and exposed to phorbol-12-myristate-13-acetate (PMA), a strong PKC activator.

Expression of both PKCα–GFP and PKCβ–GFP chimeras reveal a bright fluorescence throughout the cytoplasm, meanwhile after 30 minutes of treatment with PMA 10 nM, they were localized uniformly in the plasma membrane compartment (PKCβ-GFP: 98 ± 10.3 % from control levels, n=12, $p<0.01$; PKCα-GFP: 93 ± 19.5 % from control levels, n=9, $p<0.01$), as previously reported by us and others.[61, 141, 142] Afterwards, we analyzed the behavior of PKCβ and PKCα upon a pre-treatment with hispidin. In this case, it is apparent that treatment with PMA induces no change in the distribution of PKCβ (PKCβ-GFP: 5 ± 3.9 % from control levels, n=11), whereas hispidin treatment does not affect the translocation of part of the PKCα pool to the plasma membrane (PKCα-GFP: 92 ± 24.6 % from control levels, n=8, $p<0.01$). These observations provide evidence that hispidin is a selective inhibitor of the β isoform of PKC and, as expected, HEK293 cells that were treated for 24h with 5 μM of hispidin reveal an increase in the overall levels of autophagy (**Fig. 9D, E**). Moreover, the same treatment with hispidin in PKCβ-overexpressing cells counteract the negative effect of PKCβ on autophagy, inducing increase both in number of autophagosome and in LC3-II levels (**Fig. 9D, E**).

Cells lacking PKCβ exhibit enhanced autophagy levels

To confirm the crucial role of PKCβ in the regulation of the autophagy machinery, we executed an autophagy analysis in MEFs Pkcβ ko and compared them with MEFs WT. The depletion of this kinase induced an accumulation of GFP-LC3 puncta and stimulated the lipidation of endogenous LC3, denoting higher autophagy levels in Pkcβ ko than in WT (**Fig. 10A, C, D, E, F**). To investigate whether the effects on autophagy were effectively dependent on the absence of PKCβ, we have reintroduced the kinase into Pkcβ ko MEFs, monitoring also the expression level of the reintroduced gene. First, we assessed the expression of isoform β in MEFs ko for this kinase by immunocytochemical staining (**Fig. 10B**). Next, we found that a low expression of the reintroduced Pkcβ gene restored the autophagy levels relative to those of the wild-type MEFs. Moreover, higher levels of expression of the kinase into Pkcβ ko MEFs resulted in a strong inhibition of autophagy (**Fig. 10C, D**).

As reported above, the changes in autophagosome number can be also caused by perturbation of the normal autophagic activity. To rule out the possibility of a global alteration in the autophagic flux, we evaluated the accumulation of LC3-II after treatment with NH_4Cl. As result, treatment with 20 mM NH_4Cl for 1h led to a significant increment of the LC3-II band in Pkcβ ko and wild-type MEFs (**Fig. 10E**). Next, we tested whether the modulation of autophagy observed in HEK293 cells, promoted by hispidin, did not occur in Pkcβ ko MEFs. As expected, a treatment with 5 μM hispidin for 24h, induced an increase in LC3-II levels in wild-type MEFs, whereas the same experimental conditions achieved on Pkcβ ko MEFs did not modify the autophagic activity compared to Pkcβ ko MEFs (**Fig. 2F**). Finally, to understand whether the kinasic activity is a fundamental aspect of PKCβ autophagic role, we used a kinase dead Pkcβ HA-tagged construct (Pkcβ-KD)[143] in Pkcβ ko MEFs and investigated their autophagic levels.

As showed in **Figure 10C** by immunoblot technique and in **Figure 10D** by direct fluorescence microscopy, expression of Pkcβ-KD did not influence the accumulation of LC3-II band. Similar results were obtained when we performed analyses of autophagy in different tissues (liver and muscle) derived from WT and Pkcβ ko mice under resting conditions and in response to starvation treatment for 24h (**Fig. 10G**).

Thus, the experiments performed in this more physiological setting show that the knockdown of PKCβ leads to an enhancement of autophagy, confirming that PKCβ plays an essential function in regulation of autophagy, both in vitro (in cultured human and mouse cells) and in vivo (in mice).

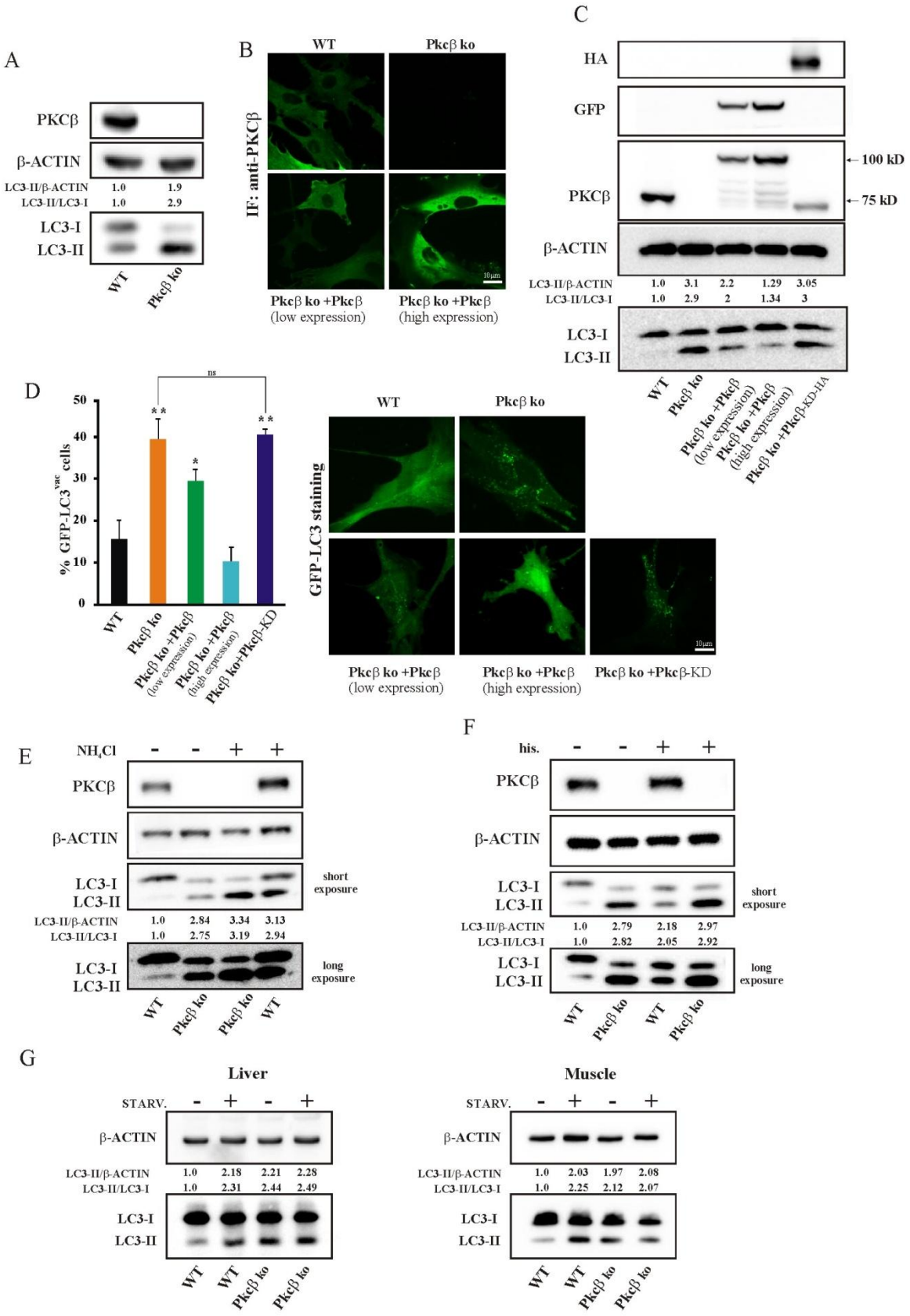

Figure 10 – Cell lacking PKCb display sustained levels of autophagy

PKCβ impairs mitochondrial homeostasis during autophagy

Mitochondria play central roles in cell survival by producing energy through oxidative phosphorylation and in cell death by regulating apoptosis. However, these organelles are also a main source of reactive oxygen species (ROS), which damage cellular components and often induce cell death.[144, 145] In healthy cells, complexes I–IV of the respiratory chain build up the proton gradient across the inner mitochondrial membrane that is required for oxidative phosphorylation and that forms the basis of the Ψ_m.[49] The maintenance of this Ψ_m is of vital importance for cellular bioenergetics, and although a transient loss of the Ψ_m can occur in physiological circumstances, a long-lasting or permanent Ψ_m dissipation is often associated with cell death.[146] Based on this understanding, we investigated the role of PKCβ in mitochondrial homeostasis. First, we analyzed the occurrence of Ψ_m changes in PKCβ-GFP-transfected cells compared to control cells (transfected with a GFP reporter), using the mitochondrial potential-sensitive dye tetramethyl-rhodamine methyl ester (TMRM). As shown in **Fig. 11A**, the Ψ_m in the PKCβ-expressing cells (identified by the GFP tag) was drastically smaller than that in the control cells, both when not starved (-21 ± 5.1 % from control levels, n=27, $p<0.01$) or starved for 1h (-18 ± 6.8 % from control levels, n=28, $p<0.01$). By contrast, the starvation treatment performed in the control cells resulted in a significant increase in the Ψ_m (14 ± 4.2 % from control levels, n=36, $p<0.05$).

It is generally accepted that the Ψ_m across the inner mitochondrial membrane provides a huge driving force for maintaining a correct amount of mitochondrial calcium (Ca^{2+}).[147] Thus, we performed detailed analyses of the Ca^{2+} homeostasis in HEK293 control cells and cells expressing PKCβ before and after starvation treatment to confirm an effective role of the kinase in mitochondrial physiology. First, using a mitochondrially targeted aequorin,[148] we measured the mitochondrial Ca^{2+} uptake in response to stimulation with ATP, an agonist that triggers IP3-sensitive Ca^{2+} release from the endoplasmic reticulum and the Golgi apparatus, which serve as IP3-sensitive intracellular calcium stores.[21]

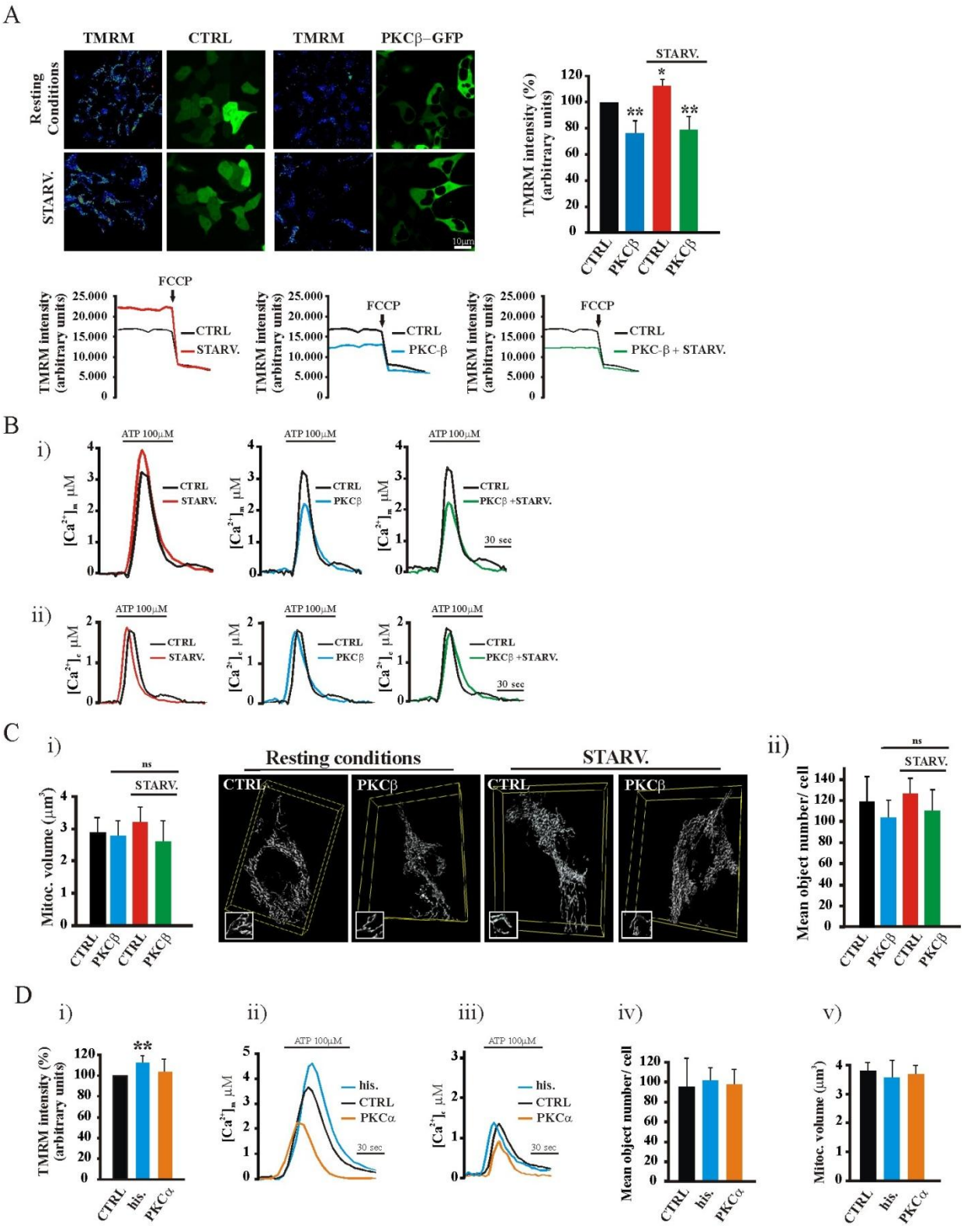

Figure 11 – PKCb attenuates mitochondrial fisiology

Interestingly, starvation treatment in control cells caused a significant increase in the Ca^{2+} uptake by mitochondria (peak amplitude: 3.89 ± 0.6 μM vs. 3.2 ± 0.89 μM [CTRL]; n=26; $p<0.05$) (**Fig. 11Bi**);

the effect of overexpressed PKC isoform β on this Ca^{2+} response was different. In fact, similarly to our previous work performed in HeLa cells,[149] in HEK293 cells overexpressing PKCβ, the ATP-dependent mitochondrial Ca^{2+} uptake was significantly reduced, both in untreated (peak amplitude: 2.23 ± 0.3 μM vs. 3.2 ± 0.89 μM [CTRL]; n=19; $p<0.01$) and starved cells (peak amplitude: 2.19 ± 0.5 μM vs. 3.2 ± 0.89 μM [CTRL]; n=20; $p<0.01$) (**Fig. 11Bi**). We investigated whether or not the changes in the mitochondrial Ca^{2+} concentration ($[Ca^{2+}]_m$) were paralleled by alterations in the cytosolic Ca^{2+} concentration ($[Ca^{2+}]_c$).

In the experiment shown in **Figure 11bii**, we monitored the cytosolic calcium levels in cells expressing either the PKCβ chimera and cytosolic aequorin or the control vector and cytosolic aequorin (control condition) in resting and starvation conditions.

No differences was assessed in the $[Ca^{2+}]_c$ between control and PKCβ-overexpressing cells, either not starved (peak amplitude: 1.75 ± 0.28 μM vs. 1.79 ± 0.29 μM [CTRL]; n=18) or starved for 1h (peak amplitude: 1.71 ± 0.4 μM vs. 1.79 ± 0.29 μM [CTRL]; n=18) (**Fig. 11Bii**). Similar results were obtained when HEK293 cells in control conditions were exposed to serum starvation for 1h (peak amplitude: 2.03 ± 0.76 μM vs. 1.79 ± 0.89 μM [CTRL]; n=16) (**Fig. 11Bii**).

Finally, we wished to rule out the possibility that the alteration of the Ψ_m and of the mitochondrial Ca^{2+} responses were consequences of a major structural perturbation of the organelle that could cause the loss of the ER–mitochondria contact sites, which are essential for the large and prompt Ca^{2+} uptake by mitochondria.

The mitochondrial structure was evaluated by confocal microscopy of HEK293 cells that were co-transfected with the PKCβ chimera or empty vector and a mitochondrially targeted red fluorescent protein (mtDsRed). After deconvolution and 3D reconstitution, the images were analyzed, evaluating two main aspects: the overall volume and the size distribution of individual mitochondrial objects. **Figure 11Ci** and **11Cii** illustrate that neither the starvation treatment, the overexpression of PKCβ, nor the combination of the overexpression of PKCβ and the starvation treatment affected either the total volume of the mitochondria (122 ± 12 μm^3 [STARV.], 102 ± 17 μm^3 [PKCβ], 110 ± 20 μm^3 [PKCβ+STARV.] vs. 118 ± 24 μm^3 [CTRL]) or the fragmentation of the mitochondrial network (3.18 ± 0.68 μm^3 [STARV.], 2.90 ± 0.72 μm^3 [PKCβ], 2.78 ± 0.91 μm^3 [PKCβ+STARV.] vs. 2.98 ± 0.7 μm^3 [CTRL]). Thus, we concluded that the overexpression of PKCβ (found to inhibit autophagy) negatively modulates mitochondrial activity, as demonstrated by a significant heterogeneity of the Ψ_m and of mitochondrial Ca^{2+} responses compared with control conditions (**Fig. 11A, B**). In contrast, serum starvation (a potent autophagy inducer) enhances mitochondrial bioenergetics, as demonstrated by a significant increase in the Ψ_m, which was

reflected in a major mitochondrial Ca^{2+} uptake, not affecting the mitochondrial morphology or the $[Ca^{2+}]_c$ levels (**Fig. 11A, B**).

Next, we aimed at confirming these observations in cells expressing only the endogenous kinase by administering the isoform-specific PKCβ inhibitor hispidin and by up-regulating PKCα to exclude a broad effect of the classic PKCs.

Therefore, we conducted mitochondrial parameter measurements in HEK293 cells that were transfected with PKCα or treated with hispidin. Treatment with hispidin resulted in an increase in the Ψ_m (+16 ± 4.1 % from control levels, n=16, p<0.05) (**Fig. 11Di**), which was reflected in a major change in the $[Ca^{2+}]_m$ (peak amplitude: 4.82 ± 0.74 μM [his.] vs. 3.76 ± 0.34 μM [CTRL] *n*=21, p<0.01) (**Fig. 11Dii**); in addition, we did not recognize any alteration in $[Ca^{2+}]_c$ or in the mitochondrial size and network (**Fig. 11Diii, 11Div**). Next, we assessed a possible change in the Ψ_m levels and the Ca^{2+} response in HEK293 cells expressing PKC isoform α. The results of the experiment are shown in **Figures 11Div** and **11Dv**. No difference was detected in the loading of the fluorescent dye TMRM (+4 ± 6 % from control levels, n=18) (**Fig. 11Di**) or in the mitochondrial number (98 ± 18 μm^3 [PKCα] vs. 95 ± 23 μm^3 [CTRL]) (**Fig. 11Div**) and volume (3.76 ± 0.73 μm^3 [PKCα] vs. 3.86 μm^3 ± 0.81 [CTRL]) (**Fig. 11Dv**) between the control and PKCα-overexpressing cells. However, this protein kinase C isoform promoted a significant reduction in the mitochondrial calcium uptake compared with the control (peak amplitude: 2.24 ± 0.44 μM [PKCα] vs. 3.76 ± 0.34 μM [CTRL] *n*=14, p<0.01) (**Fig. 11Dii**). Next, we investigated whether the $[Ca^{2+}]_m$ changes were paralleled by alterations in the cytosolic Ca^{2+} signals. In PKCα-transfected cells, the $[Ca^{2+}]_c$ increases evoked by stimulation with an agonist were significantly less than in control cells (peak amplitude: 0.89 ± 0.28 μM [PKCα] vs. 1.38 ± 0.32 μM [CTRL] *n*=22, p <0.01) (**Fig. 11Diii**), suggesting the possibility that ER loading (or its discharge properties) was modulated by the activity of PKCα.

Lack of PKCβ promotes a sustained mitochondrial physiology

We executed the same experiments in Pkcβ ko MEFs and compared the results with those obtained in MEFs derived from WT mice and in Pkcβ ko MEFs into which Pkcβ was reintroduced. As reported in **Figure 12A**, we found that Pkcβ ko MEFs exhibited higher Ψ_m levels compared with WT MEFs (+19.5 ± 5.8 % from WT levels, n=21). As expected, a loss of Pkcβ was reflected in an increase in the mitochondrial Ca^{2+} uptake (peak amplitude: 67.3 ± 3.2 μM [Pkcβ ko] vs. 49.4 ± 4.7 μM [WT] *n*=26, p <0.01) (**Fig. 12Bi**) that affected neither the total volume of the mitochondria nor the structure of the mitochondrial network (**Fig. 4Ci, ii**). Moreover, there were no differences in the $[Ca^{2+}]_c$ (peak amplitude: 1.6 ± 0.18 μM [Pkcβ ko] vs. 1.49 ± 0.23 μM [WT] *n*=18) (**Fig. 12Bii**).

Additionally, as reported in **Figures 12A** and **12B**, a low expression of the reintroduced Pkcβ-GFP chimera in ko cells restored the Ψ_m levels (TMRM intensity: +6.3 ± 3.8 % from WT levels, n=12) and $[Ca^{2+}]_m$ (peak amplitude: 54.5 ± 4.1 μM vs. 49.4 ± 4.7 μM [WT] *n*=13) to values comparable to those in WT MEFs; accordingly, higher level of expression of the kinase into Pkcβ ko MEFs resulted in a significant attenuation of mitochondrial parameters, such as Ψ_m (TMRM intensity: -16.2 ± 2.9 % from WT levels, n=8, p<0.05) and $[Ca^{2+}]_m$ (peak amplitude of $[Ca^{2+}]_m$ uptake: 36.4 ± 5.1 μM vs. 49.4 ± 4.7 μM [WT] *n*=11, p<0.05), without affecting the mitochondrial network (**Fig. 12A,B,C**).

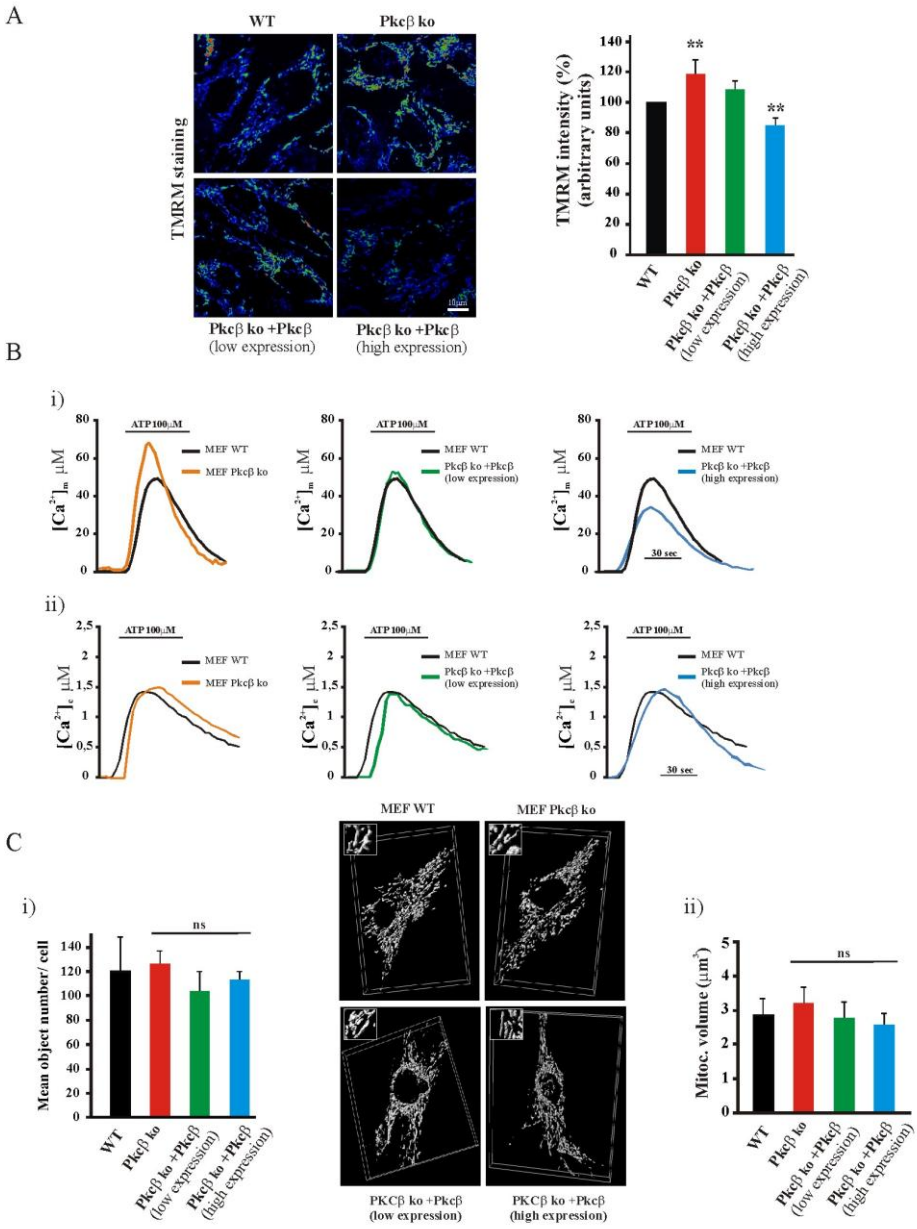

Figure 12 – Mitochondrial homeostasis in MEFs Pkcβ ko

Overall, these experiments indicate that PKCβ overexpression (a state in which autophagy is

attenuated) affects the mitochondrial physiology, inducing a reduction in the Ψ_m and in Ca^{2+} levels. In contrast, the lack of this PKC or the presence of a condition that activates autophagy (such as serum starvation) positively modulates mitochondrial bioenergetics.

Positive modulation of the Ψ_m contrasts the mitochondrial impairment mediated by PKCβ

As reported above, we have demonstrated that PKCβ selectively attenuates autophagy and impairs mitochondrial physiology without modifying mitochondrial morphology. Next, we asked whether a modulation in mitochondrial homeostasis could reverse the inhibitory effect induced by PKCβ against mitochondrial homeostasis and the autophagy machinery.

An important substrate for mitochondrial function is succinic acid (succinate). Succinate is a substrate for succinate dehydrogenase, which is also known as complex II of the mETC. In contrast to the other enzymes of the Krebs cycle, which are located in the mitochondrial matrix, succinate is bound to the inner mitochondrial membrane.[150]

Based on this information, we attempted to modulate mitochondrial physiology with an analogous succinic acid compound, the membrane-permeable methyl-succinate (MeS).[151] First, we tested the efficacy of MeS to modulate mitochondrial bioenergetics, measuring the Ψ_m in mock-transfected and PKCβ-transfected cells in the presence or absence of 5 mM MeS for different time periods (0.5h, 1h, 2h, 2.5h, 3h and 4h) (**Fig. 13A**). As expected, MeS treatment resulted in the hyperpolarization of mitochondria with a peak at approximately 1h. As reported in **Figure 13A,** this effect was maintained until the second hour and subsequently decreased to levels comparable to those of the control. Next, to determine whether MeS could recover the impaired mitochondrial homeostasis induced by the overexpression of PKCβ, we analyzed changes in the Ψ_m in mock-transfected and PKCβ-expressing cells.

The results of the experiment are shown in **Figure 13B**. As reported above, control cells treated with 5 mM of the mETC substrate MeS for 1h showed higher Ψ_m levels compared with the control. More interestingly, MeS was demonstrated to be able to mitigate the effect induced by PKCβ on the Ψ_m. In fact, PKCβ-expressing cells displayed a reduction in the Ψ_m value (-22 ± 3.2 % from control levels, n=19, $p<0.01$), but after MeS treatment, the Ψ_m was comparable to the levels found in control cells (-3.2 ± 1.9 % from control levels, n=17) (**Fig. 13B**).

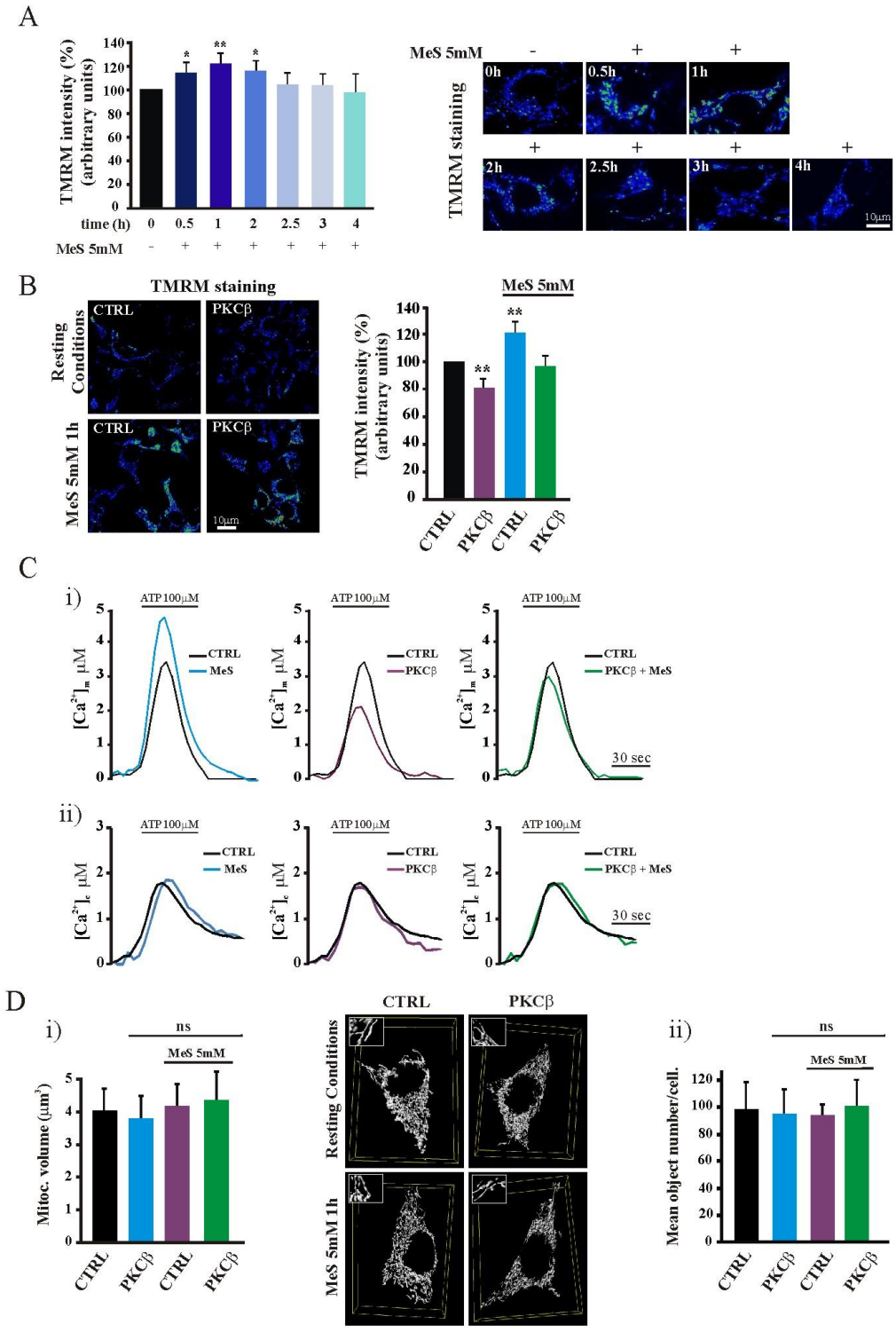

Figure 13 – MeS induce a boost in mitochondrial bioenergetic

Considering that the enhancement of the Ψ_m generally influences $[Ca^{2+}]_m$, we verified whether MeS could also modify this mitochondrial feature. Thus, we co-expressed the PKCβ chimera or empty vector (control) with aequorin probes, and before taking measurements, we incubated the transfected cells with 5 mM MeS for 1h.

In control cells pre-treated with MeS, the $[Ca^{2+}]_m$ increase evoked by ATP stimulation was 4.7 ± 0.87 μM, showing a greater mitochondrial response than the control cells (+34% from control levels, n=24, p<0.01) (**Fig. 13Ci**). In PKCβ-expressing cells, the mitochondrial Ca^{2+} accumulation was markedly reduced (peak amplitude: 2.04 ± 0.76 μM, n=23) (**Fig. 13Ci**), but after 1h of MeS treatment, the mitochondrial calcium uptake was significantly higher (+33.3%, n=20) (**Fig. 13Ci**) than that observed in PKCβ-expressing cells that were not treated with MeS.

Moreover, this marked increase induced by MeS was specific to mitochondria, as $[Ca^{2+}]_c$ levels were largely unaffected. In fact, as reported in Figure **13Cii**, a pre-treatment with 5 mM MeS for 1h in cells co-expressing the aequorin cytosolic Ca^{2+} probes and the PKCβ chimera (for PKCβ overexpression) or empty vector (control) did not affect the intracellular calcium concentrations (peak amplitude: 1.79 ± 0.34 μM [CTRL], 1.82 ± 0.29 μM [MeS], 1.74 ± 0.52 μM [PKCβ], 1.8 ± 0.44 μM [PKCβ+MeS]; n=16).

Next, to rule out a possible effect of MeS on mitochondrial morphology, we imaged mtDsRed in the presence of MeS. Either the mitochondrial structure and volume were not significantly altered by treatment with 5mM MeS for 1h (mitochondria structure: 4.1 ± 0.71 μm^3 [CTRL], 3.81 ± 0.76 μm^3 [MeS], 4.18 ± 0.53 μm^3 [PKCβ], 4.21 ± 0.98 μm^3 [PKCβ+MeS]; n=24; mitochondria volume: 99 ± 18.3 μm^3 [CTRL], 95 ± 15.8 μm^3 [MeS], 94 ± 7.23 μm^3 [PKCβ], 110 ± 20.2 μm^3 [PKCβ+MeS]; n=28) (**Fig. 13Di, ii**).

A sustained Ψ_m positively modulates autophagy and attenuates the inhibitory effects of PKCβ on autophagy

Finally, we sought to determine whether the effect of MeS on mitochondrial physiology could positively modulate autophagy and recover the ability of PKCβ to lower autophagy levels. To examine this possibility, we analyzed autophagy levels and dynamics in HEK293 cells that were exposed to 5 mM of the succinate dehydrogenase compound MeS for different time periods (0.5h, 1h, 2h, 2.5h, 3h and 4h). Interestingly, the presence of LC3 lipidation was maximal after the first and third hour after MeS treatment (**Fig. 14A**). The conversion of the autophagic marker LC3 that was observed via protein gel blotting was also confirmed by the quantification of GFP-LC3 puncta in cells transfected with the chimeric protein GFP-LC3 (**Fig. 14A**).

Having verified that treatment with MeS establishes a positive modulation of autophagy, we measured the level of autophagy by live microscopy, monitoring the formation of autophagosomes in HEK293 cells that were co-transfected with the PKCβ chimera or the empty vector and the GFP-LC3 reporter and then incubated with 5 mM MeS for 1h. As result, in control cells, treatment with MeS induced higher levels of autophagy, as evidenced by a punctate pattern of GFP-LC3 (40.9 ±

7.1 cells with GFP-LC3^{vac} vs. 16.2 ± 5.2 cells with GFP-LC3^{vac} [CTRL]; n=32) (**Fig. 14B**). Similar results were observed in PKCβ-expressing cells, where, as expected, GFP-LC3 staining was diffuse within the cytoplasm, with occasional puncta representing a low level of autophagy. Upon MeS treatment, we observed a marked increase in LC3-puncta, suggesting a clear role for MeS both in the modulation of autophagy and, partially, in recovering the ability of PKCβ to reduce autophagy (**Fig. 14B**).

Then, it was fundamental verify that the MeS treatment did not alter the normal rendering of the autophagic process. To reach this goal, we inferred LC3-II-PE turnover by western blot (**Fig. 14D**) in the presence and absence of the lysosomal inhibitor NH_4Cl. Comparing the LC3-II protein abundance during conditions with or without NH_4Cl treatment, we observed that the normal autophagic flux was maintained after MeS treatment. Furthermore, as reported in **Figure 14C**, western blots showing autophagy markers (the *LC3*-I/-II conversion) confirmed again that these changes were occurring in the whole population of cells. To confirm that the Ψ_m is a fundamental feature of the regulation of autophagy, we treated HEK293 cells with 200 nM staurosporine (STS) for different time periods (0.5h, 1h, 1.5h, 2h and 3h). STS is reported to positively modulate the Ψ_m, resulting in the hyperpolarization of mitochondria with a peak at approximately 1h and a subsequent decrease to nearly normal values.[152, 153] As expected, under our conditions, we observed a significant increase in the Ψ_m 30 minutes after STS treatment (**Fig. S5i**). This effect persisted until 1.5h and was reflected by an increase in the autophagy, as assessed by LC3-II protein gel blotting (**Fig. S5ii**).

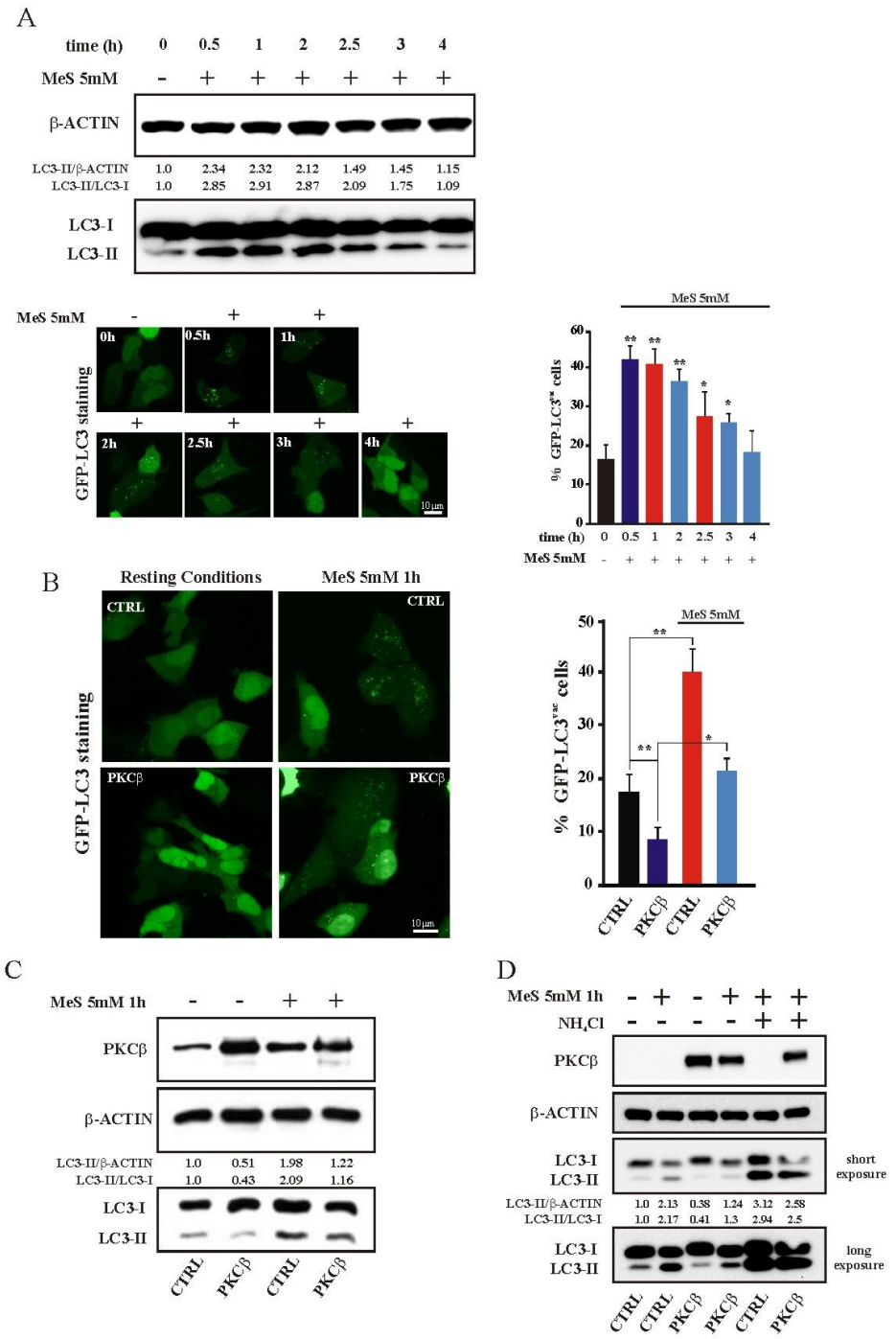

Figure 14 – MeS induce a strong promotion of autophagy

Together, these results suggest that the up-regulation of PKCβ leads to a negative modulation of autophagy, whereas the absence of PKCβ promotes an increase in autophagy. Moreover, treatment with MeS, which is capable of positively modulating mitochondrial homeostasis and particularly the mitochondrial membrane potential, leads to the induction of autophagy and contrasts the negative regulation of autophagy promoted by PKCβ.

Activation and modulation of the 66 kD isoform of Shc is a key event in PKCβ-mediated autophagy regulation

PKCβ is required for the phosphorylation/activation of $p66^{Shc}$ in Ser36 and for its translocation into mitochondria compartment, where is reported to be determinant for life span and apoptosis by perturbation of mitochondria functions. [115, 154]

Starting from these observations, we examined whether $p66^{Shc}$ might play a pivotal role in the modulation of autophagy by PKCβ.

As first, we investigated about the PKCβ-dependent phosphorylation of $p66^{Shc}$. The levels of phosphorylated $p66^{Shc}$ was detected in HEK293 cells, transfected with PKCβ chimera or with mock plasmid, and treated with the PKC activator PMA 10 nM for 30 minutes.

Both PKCβ overexpression and PMA treatment led to a significant increase in the levels of phosphorylated $p66^{Shc}$ in Ser36, compared with HEK293 cells transfected with empty vector under resting conditions (**Fig. 15Ai**). Then, to confirm the effective role of PKCβ in the regulation of $p66^{Shc}$ activity, we carried out the same experiments in MEFs Pkcβ ko and compared them with MEFs WT. As reported in **Figure 15Aii**, MEFs WT treated with PMA (10 nM 30 minutes) showed a strong increment of phosphorylated $p66^{Shc}$, whereas no significant increase in the levels of the phosphorylated protein has been detected in MEFs Pkcβ ko.

Because $p66^{Shc}$ phosphorylation takes place in the cytoplasm and it is a prior event to its translocation to mitochondria in the unphosphorylated form[61], we tested the hypothesis that PKCβ activation can modulate the mitochondrial entry of $p66^{Shc}$ protein. At this aim, we evaluated the mitochondrial pool of $p66^{Shc}$ in HEK293 cells that were transfected with the PKCβ chimera or the empty vector, and treated with PMA (10 nM 30 minutes).

Contemporarily, subcellular fractionations have been performed in MEFs Pkcβ ko and WT treated or not with the PKC activator. As result, the experiments showed that the localization of $p66^{Shc}$ appears to be highly dependent on PKC activity. In fact, the overexpression of PKCβ chimera and the pharmacological treatment suited for PKC activation enhanced the transfer of $p66^{Shc}$ to the organelle, whereas cells lacking PKCβ have no detectable effects on the recruitment of $p66^{Shc}$ to mitochondria (**Fig.15B and 15C**). Notably, the simple overexpression of PKCβ enhanced both phosphorylation and mitochondrial abundance of $p66^{Shc}$ protein. Next, to investigate whether regulation of $p66^{Shc}$ activity may be a mechanism for autophagy inhibition by PKCβ, we analyzed LC3-II lipidation in Pkcβ ko and WT MEFs, transfected with a $p66^{Shc}$-GFP chimera, in resting condition and after serum starvation.

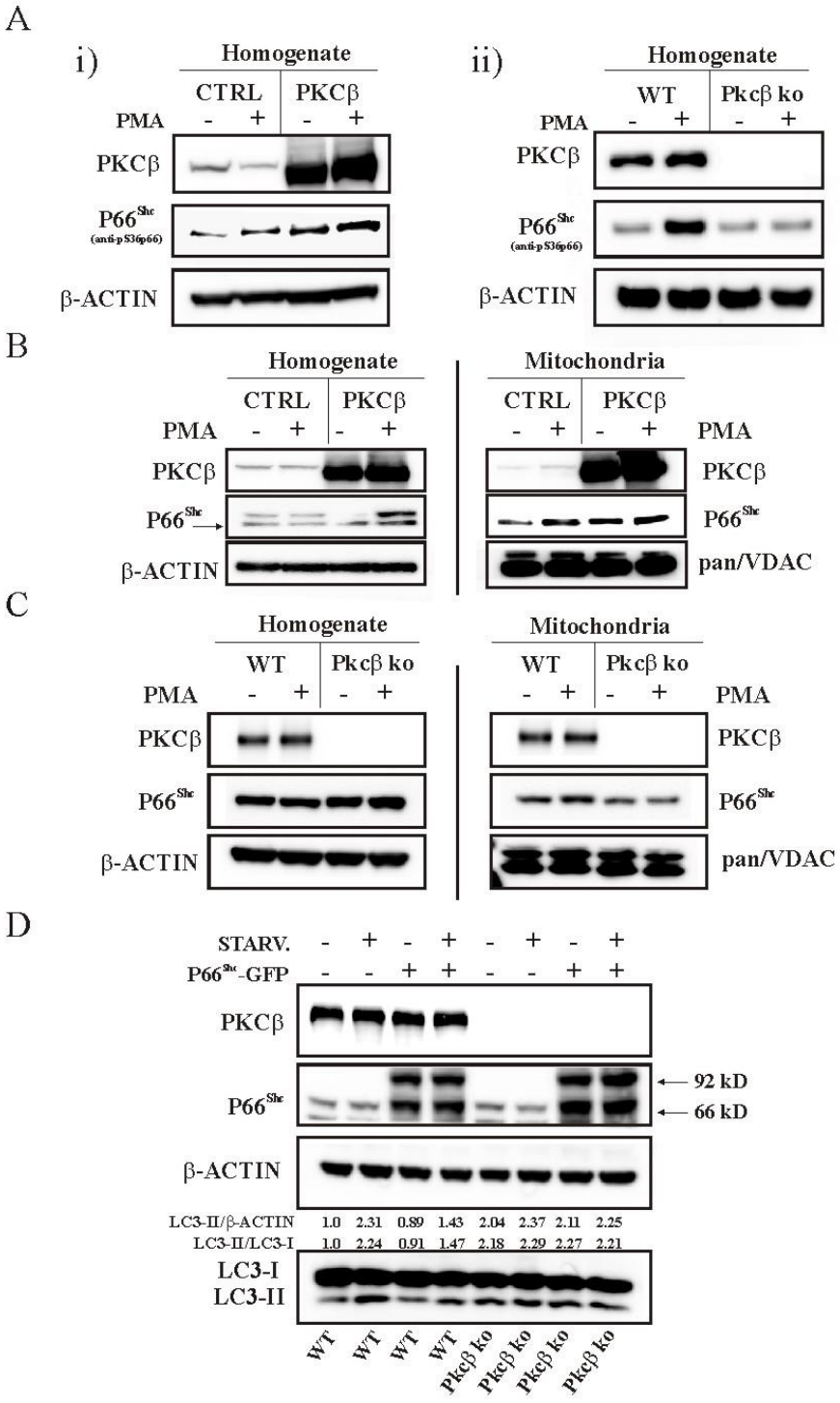

Figure 15 – PKCβ - and p66^{Shc}- dependent modulation of autophagy

As showed in **Figure 15D**, expression of p66^{Shc}-GFP in MEFs WT inhibits autophagy in response to serum starvation, whereas minor effects have been detected in PKCβ ko cells.

These findings highlight a possible molecular mechanism that links the negative regulation of the autophagic machinery promotes by PKCβ at the PKCβ–dependent mitochondrial translocation of p66^{Shc}.

Discussion

In this study, we demonstrated that PKCβ and the mitochondrial axis finely modulate the rate of autophagy. This conclusion is supported by the following observations: i) overexpression of PKCβ leads to an inhibition of autophagy and induces a decrease in the Ψ_m; ii) a lack of PKCβ stimulates autophagy and induces an increased Ψ_m; iii) nutrient deprivation induces autophagy and promotes a higher Ψ_m that is associated with a stronger mitochondrial Ca^{2+} response to agonist stimulation; iv) the pharmacological increase in the Ψ_m leads to an increase in the level of autophagy; v) this increase in the Ψ_m not only promotes autophagy but also contrasts with the down-regulation of autophagy that is mediated by PKCβ; and vi) $p66^{Shc}$ play a key role in PKCβ-dependent modulation of autophagy.

Autophagy in mammalian systems occurs under basal conditions and can be stimulated by stresses that include starvation, various pathologies, or treatment with pharmacological agents, such as rapamycin.[155]

The autophagy pathway can be an important therapeutic target for diseases such as neurodegeneration and cancer. It is a catabolic pathway that is characterized by the sequestration of cytoplasmic organelles and proteins in double-membrane vesicles (autophagosomes) that fuse with lysosomes, where proteins and organelles are digested by lysosomal hydrolases and are recycled to sustain cellular metabolism.[156]

PKCβ is a member of the protein kinase C (PKC) family, which consists of several serine/threonine kinases that are divided into three subfamilies on the basis of their general structure and activation requirements.[157]

PKCs play several roles in cell life and survival, especially in regulating cell survival and apoptosis.[61, 158, 159] Recently, it has been demonstrated that certain PKC isoforms are crucial for the modulation of autophagy, both in activating and in blocking the pathway [116-119, 160]. However, very little is known about the involvement of all PKC isoforms in autophagy. In the present study, we found that PKCβ significantly attenuates autophagy by modulating mitochondrial homeostasis.

When it was discovered, autophagy was believed to be a nonselective process that randomly recycled intracellular components to compensate for nutrient deprivation.[161] Later on, it was demonstrated that autophagy includes the selective elimination of different organelles, mitochondria in particular (in a process called mitophagy), to maintain quality control and a correct quantity of the organelle and to avoid an excessive accumulation of ROS.[162] In response to several stressors or damage, mitochondrial membrane permeabilization (MMP) occurs, and mitophagy may be initiated to remove these damaged and permeabilized organelles.[163]

To be engulfed by an autophagosome, a mitochondrion has to reach a major axis of approximately 1 μm, compared with the normal value of 5 μm. Thus, it has been suggested that the fragmentation of dysfunctional mitochondria is a crucial step that precedes mitophagy.[164, 165]

This phenomenon has been elegantly addressed to a specific ubiquitin ligase, PARKIN[166] and its interaction with the kinase PINK1 (PTEN-putative kinase 1).[167] Especially PINK1 undergoes to a voltage dependent cleavage in polarized mitochondria and, following Ψ_m collapse, an accumulation of PINK1 is observed, with consequent induction of PARKIN stabilization and initiation of mitochondrion engulfment. Such mechanism underlines an important Ψ_m selective role for mitochondrial destiny during mitophagy.

However, it has also been demonstrated that nutrient depletion induces the elongation of mitochondria and the maintenance of mitochondrial ATP production, which in turn acts as an escape from mitophagy.[43, 168]

This event was demonstrated to be dependent on PKA (Protein kinase A) activity, a well known nutrient sensing-mitochondrial kinase.[169,170] In agreement with these findings, our results indicate that autophagy induction by serum starvation preserves the mitochondrial network and generates an increase in the mitochondrial energy level, as demonstrated by higher Ψ_m and consequent major mitochondrial Ca^{2+} uptake.

Positive or negative regulation of the Ψ_m is described as a critical parameter of many human diseases, and several exogenous agents are reported to be capable of modulating it.[49] Among these agents, STS is reported to induce a significant increase in the Ψ_m within 0.5h-1h of treatment, which then remains elevated for approximately an hour [153, 171]. Having ascertained the effective STS-dependent modulation of the Ψ_m in our experimental conditions, we recognized a boost in the induction of autophagy that was directly correlated with the modulation of the Ψ_m promoted by STS. A similar effect has been shown on MCF7 cells, displaying increase on mitochondrial membrane potential after autophagy induction by exposure to Rapamycin 50 nM.[172] These observations suggest that, autophagy induction promotes mitochondrial network bioenergetic activity. Activation of PKCβ leads to a reduction in mitochondrial bioenergetics, which reflects a strong attenuation of autophagy without affecting mitochondrial morphology.

Accordingly, we demonstrated that cells lacking Pkcβ (Pkcβ ko MEFs) and cells treated with a pharmacological PKCβ inhibitor showed an increase in autophagy and a sustained mitochondrial physiology. Thus, it appears that the status of mitochondrial energy is deeply involved in the modulation of the autophagy machinery. Driven by these premises, we attempted to modulate the Ψ_m levels by treatment with MeS, a membrane-permeant methyl ester of succinate. As expected, MeS treatment generates a hyperpolarization of the Ψ_m, which is reflected in an increase in $[Ca^{2+}]_m$

without affecting the mitochondrial network and the global intracellular Ca^{2+} homeostasis, as revealed by the $[Ca^{2+}]_c$ measurements. Our observations that the fine modulation of the Ψ_m positively or negatively impacts the autophagy rate suggest an additional role for this modulator of the mitochondrial electron transport chain. In fact, we show that MeS treatment stimulates autophagy, partially restores the defective status of mitochondrial energy and the inhibition of autophagy that is induced by the activation of PKCβ. Considering that MeS treatment was not able to completely overcome PKCβ effect on Ψ_m and autophagy, we suppose that mitochondrial PKCβ-activity is not the only mechanism for autophagy regulation by such kinase, but, at least in this cellular model, a relevant one. Indeed, data obtained with MeS and STS confirmed the positive correlation between autophagy and Ψ_m. This evidence contrasts with other works describing the abolition of Ψ_m as general inducer of autophagy or mitophagy. Our results were obtained analyzing the whole energetic status of the mitochondrial network, without considering eventual single-mitochondrion selective mitophagic events. It could be then speculated that the observed prolonged elevation of Ψ_m might generate localized increased ROS production, mPTP opening and mitophagic events, therefore promoting organelle recycling events already addressed to mitophagy.[173]

Studies are underway to identify upstream regulators and downstream targets of PKCβ activation that occur during autophagy. Previously, we reported that PKCβ regulates mitochondrial physiology favoring phosphorylation and mitochondrial translocation of the adaptor protein $p66^{Shc}$, where it interacts with cytochrome c, a component of the electron transport chain, and increases ROS generation.[61] In the present work, we have showed as $p66^{Shc}$ expression attenuates autophagy in response to starvation, an aspect which has not been observed in Pkcβ ko MEFs. Thus, both PKCβ and $p66^{Shc}$ overexpression negatively regulate autophagy, and their activity on the process appears linked. In fact, Pkcβ ko cells display very low activity of $p66^{Shc}$, expressed as $p66^{Shc}$ phosphorylation and its abundance at mitochondrial level. We propose a novel role of PKCβ in the control of the autophagic process, through the attenuation of mitochondrial homeostasis and the regulation of mitochondrial $p66^{Shc}$ activity. It has been previously reported how

LC3 staining in neurons was enhanced on blocking $p66^{Shc}$ activation after preconditioning,[174, 175] and how PMA treatment, which induces PKCβ activation and $p66^{Shc}$ entry into mitochondria, strongly inhibits autophagy.[118] By this way, $p66^{Shc}$ ko cells should display higher levels of autophagy and this would correlate the increased lifespan observed in $p66^{Shc}$ ko mice with the proposed pro-survival role of autophagy. [106]

In conclusion, the identification of PKCβ as negative regulator of autophagy through the reduction of the Ψ_m and the regulation of the $p66^{Shc}$ translocation to mitochondria could shed light on the not yet completely understood relationship between autophagy and mitochondrial physiology.

Downregulation of the mitochondrial calcium uniporter (MCU) by cancer-related miR-25

Introduction

The main transporters involved in the uptake of Ca^{2+} into mitochondria is the MCU, characterized by a low affinity for Ca^{2+}; in fact, MCU takes up Ca^{2+} in the micromolar range and experiments in permeabilized cells report a K_d of the uniporter of 10 μM [26]. In addition, a biphasic effect of calcium on the MCU has been reported: beyond a certain level, cytosolic Ca^{2+} inactivates the uniporter, preventing further Ca^{2+} uptake and this process might avoid an excessive accumulation of the cation in mitochondria [27].

In spite of repeated efforts by different researchers, the molecular identity of the MCU has remained elusive. Recently, in 2011, two distinct laboratories have been identified a transmembrane protein (CCDC109A) that fulfilling the criteria for being the MCU [31, 32]. Indeed, in planar lipid bilayers CCDC109A showed channel activity with electrophysiological properties as those previously reported for the MCU [33]. The over-expression of CCDC109A (that now is called "MCU"), increases mitochondrial Ca^{2+} uptake and sensitizes cells to apoptotic stimuli, and the employment of short interfering RNA (siRNA) silencing of MCU strongly reduced mitochondrial Ca^{2+} uptake. This reduction is specific for mitochondria (Ca^{2+} cytosolic levels remain almost unaffected), does not induce impairment of the electrochemical gradient or change in mitochondrial morphology and the induction of specific mutations at the level of the putative pore-forming region reduce the mitochondrial calcium uptake and blocks the channel activity of the protein [31, 32].

MiRNAs are a class of small (19–25 nt), noncoding regulatory RNAs that regulate gene expression, causing target mRNA degradation or suppressing mRNA translation [176]. In human cancers, specific miRNAs are up- or down-regulated, with consequent alteration in the expression of target proteins [177, 178].

Thus, miRNAs may function as oncogenes or tumor suppressors. Among the oncogenic miRNAs, miR-25 is one of the most studied and well described. miR- 25 is 22 nucleotides in length, hosted by the minichromosome maintenance protein- 7 (MCM7) gene, and transcribed as part of the mir-106b~25 polycistron; it is overexpressed in several human cancers, including pediatric brain tumors, gastric adenocarcinoma, epidermal growth factor receptor-positive lung adenocarcinoma and prostate carcinoma and has been reported to target different regulators of the apoptotic pathway, such as BIM, PTEN and TRAIL.

Here we show that miR-25 decreases mitochondrial Ca^{2+} uptake through selective MCU downregulation, conferring resistance to apoptotic challenges. MCU appears to be downregulated in human colon cancer samples, and accordingly, miR-25 is aberrantly expressed, indicating the importance of mitochondrial Ca^{2+} regulation in cancer cell survival.

Results

Mir-25 down-regulates MCU and protects from Ca^{2+}-dependent apoptosis

By filtering the output of four target prediction algorithms [TargetScan [179], MicroT [180], MicroCosm [181], and miRanda [182] (Table 1)], we identified 5 cancer-related miRNA families (miR-15, miR-17, miR-21, miR-25, miR-137) that could be predicted to target MCU and/or MICU1.

		miRNA prediction					Cancer Link	
miRNA	Target	Tot.	Targetscan	microT	microCosm	Miranda		
miR-15/16/195/424/497	MCU/MICU1	2/4	X X	X X	X	X	Yes	Down
miR-17-5p/20/93.mr/106/519.d	MCU	1	X				Yes	Up
miR-21/590-5p	MCU	3	X		X	X	Yes	Up
miR-25/32/92/92ab/363/367	MCU/MICU1	3/3	X X	X	X	X X	Yes	Up
miR-137	MCU	4	X	X	X	X	Yes	Down

Table 1 – miRNA capable to modulate to target MCU and/or MICU1

We thus tested their effect on mitochondrial Ca^{2+} homeostasis by expressing them in HeLa cells and measuring mitochondrial [Ca^{2+}] with a targeted aequorin-based Ca^{2+} probe (mtAEQ) [148]. The data (Fig. 16A) showed that only miR-25 caused a marked reduction in the $[Ca^{2+}]_m$ rise evoked by cell stimulation with 100 μM histamine, an agonist coupled to the generation to $InsP_3$ and the release of Ca^{2+} from the ER.

The effects were predicted to depend on MCU downregulation. Indeed, the bioinformatics analysis of the 1896 nt 3'-UTR of MCU revealed a 100% match target seed sequence for miR-25 at nts 1075–1081, highly conserved across seven species (Fig. 16B), and insertion of the 759 nt 3'-UTR of MCU (but not of the 569 nt 3'-UTR of MICU1) downstream of the luciferase gene in a reporter plasmid led to significant miR-25-dependent decrease of reporter activity. We thus tested MCU expression by immunoblotting, and detected a marked reduction in the protein level upon miR-25 overexpression (Fig. 16C) and an increase in anti-miR-25 expressing cells. As expected, MCU mRNA abundance is significantly decreased by miR-25 (Fig. 16D).

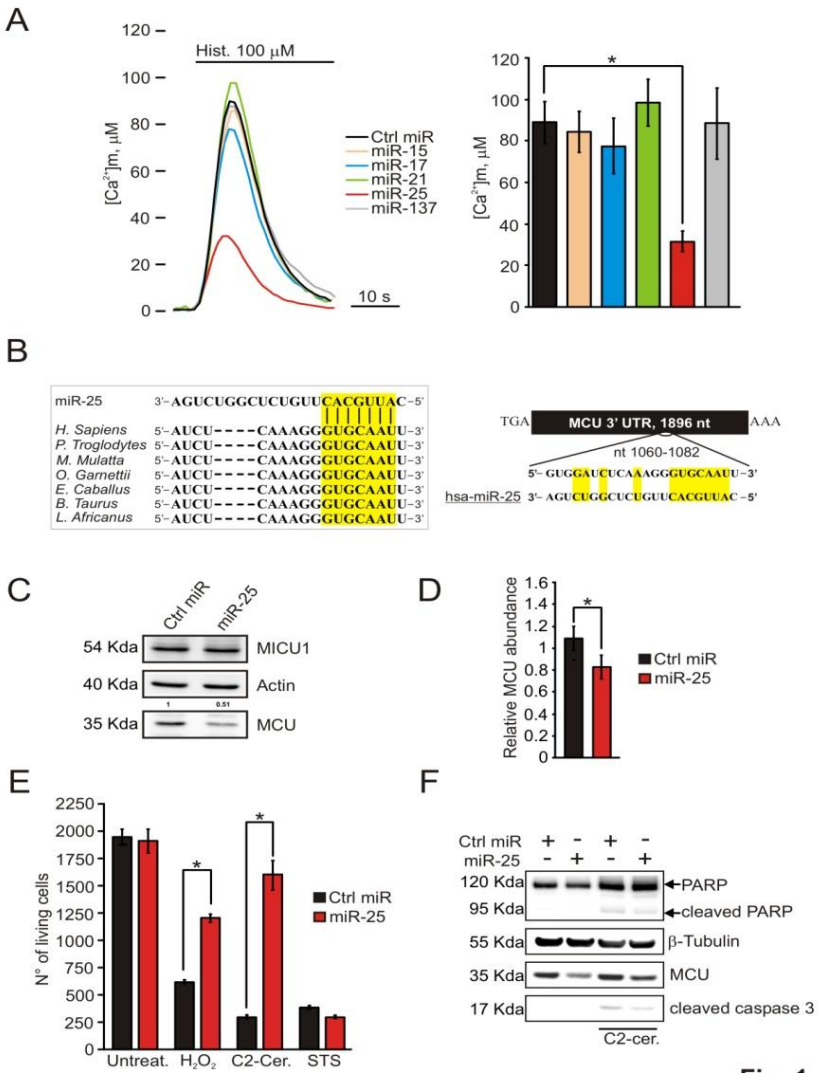

Figure 16 – miR-25 modulates the activity of MCU

The effect of miR-25 is shared by the other members of the miRNA family: miR-92a and miR-363 target MCU mRNA and reduce MCU protein levels and, accordingly, inhibit mitochondrial Ca^{2+} uptake, without affecting $[Ca^{2+}]_c$ and $[Ca^{2+}]_{er}$ (data not shown).

We investigated whether miR-25-dependent reduction in mitochondrial Ca^{2+} uptake correlates with increased resistance to apoptotic challenges. Microscopy counts of cell viability after treatment with H_2O_2, C2-ceramide or Staurosporine (STS) revealed that miR-25-expressing HeLa cells were strongly protected from death caused by C2-ceramide and H_2O_2 (Fig. 16E), apoptotic challenges for which mitochondrial Ca^{2+} loading acts as a sensitizing factor [50, 53, 183], whereas the sensitivity to STS was unaffected. Accordingly, PARP and caspase 3 cleavage upon C2-ceramide treatment were markedly reduced in miR-overexpressing cells (Fig. 16F).

Mir-25 induces reduction of mitochondrial Ca^{2+} uptake exclusively through MCU

We then proceeded to rule out that the effect on $[Ca^{2+}]_m$ was secondary to alterations of global Ca^{2+} signalling patterns or to morphological or functional dysregulation of mitochondria. On the former aspect, we investigated the cytosolic $[Ca^{2+}]$ changes and the state of filling and release kinetics of the ER. The results showed that miR-25, when expressed in HeLa cells, caused no difference in the amplitude of the $[Ca^{2+}]_c$ rise evoked by histamine (Fig. 17A), nor in the steady state $[Ca^{2+}]_{er}$ or in the release caused by the agonist (Fig. 17B). Thus, the effect of miR-25 on Ca^{2+} homeostasis is exclusively mitochondrial.

Then, we investigated the mitochondrial membrane potential (Ψ_m), the driving force for Ca^{2+} accumulation, and the morphology of mitochondria, i.e. both the contacts with the ER (that were shown to be a critical determinant of rapid Ca^{2+} transfer between the two organelle) [38, 184, 185] and the formation of largely interconnected tubules, that favours Ca^{2+} diffusion within mitochondria. On the former aspect, measurements with the Ψ_m-sensitive fluorescent dye tetramethyl rhodamine methyl ester (TMRM) revealed no difference between miR-overexpressing and control HeLa cells (Fig. 17C). As to morphology, mitochondrial labelling with the fluorescent probe Mt-Ds Red, showed that miR-25 overexpression causes no significant difference in mitochondrial volume or number (Fig. 17D). Similarly, co-transfection with Mt-Ds Red and an ER-targeted GFP showed no difference in the number of contact sites (Fig. 17D, contact sites in white).

Overall, the data reveal that the $[Ca^{2+}]_m$ reduction caused by miR-25 should be ascribed to reduction of mitochondrial Ca^{2+} uptake through MCU.

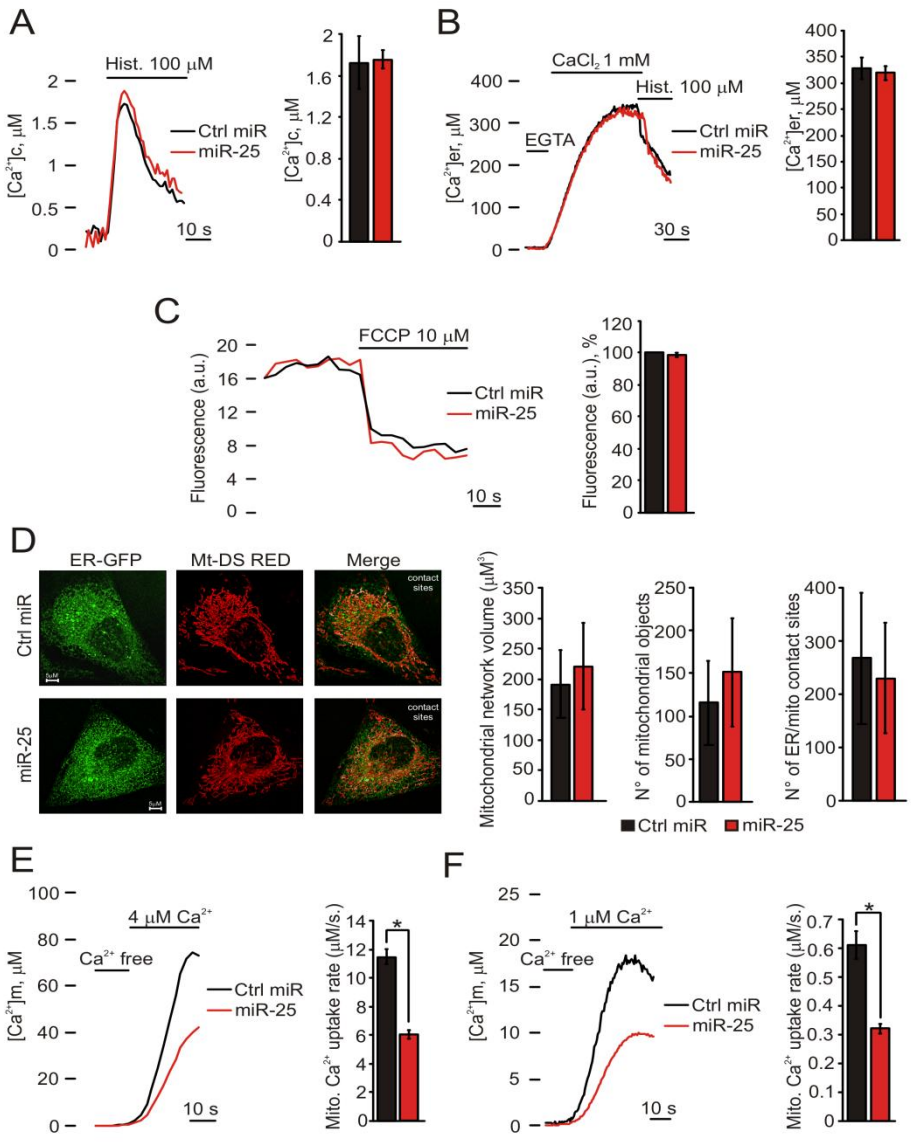

Figure 17 – miR-25 induces a reduction in mitochondrial Ca2+-uptake

To further confirm this notion, we measured mitochondrial Ca^{2+} accumulation in permeabilized cells. For this purpose, HeLa cells were perfused with a solution mimicking the intracellular milieu (IB), supplemented with 2 mM EGTA, and permeabilized with digitonin for 1 min. Then, the perfusion buffer was changed to IB with an EGTA-buffered [Ca^{2+}] of 4 µM (Fig. 17E) or 1 µM (Fig. 17F), eliciting a gradual rise in $[Ca^{2+}]_m$ that reached a plateau value of ~80 and ~20, respectively. At both buffered [Ca^{2+}], miR-25 overexpression causes a marked reduction in the rate of Ca^{2+} accumulation into mitochondria.

Mitochondrial Ca^{2+} alterations induced by miR-25 can be reverted by MCU re-expression in miR-25 expressing cells and, accordingly, this rescued Ca^{2+} affinity is mirrored in enhanced susceptibility to Ca^{2+}-dependent apoptosis. Moreover, 22Rv1 prostatic cells, which possess very

high levels of miR-25 (see figure 18), were strongly sensitized to apoptosis, after MCU overexpression. The increased ability of mitochondria to accumulate Ca^{2+} is a fundamental aspect in MCU-related promotion of cell death: indeed, apoptosis-induction observed in MCU over-expressing HeLa cells is almost abolished in the presence of intracellular Ca^{2+} buffer BAPTA.
Finally, although miR-25 has also been reported to exert anti-apoptotic effects via interference with the expression of pro-apoptotic proteins, such as Bim [186], TRAIL [187] and PTEN [188], these results show how MCU can be considered a fundamental target of miR-25-dependent apoptosis inhibition.

Inhibition of MCU levels by miR-25 is a key aspect in human colon cancer progression

We then extended the analysis to cancer cells and tissues. We first evaluated cell lines derived from human carcinomas, in which miR-25 was reported to be highly expressed [188-190]. Both in PC3, LnCaP and in the 22Rv1 (derived from prostate cancer) and in HCT116, RKO, SW80 and WiDr (derived from colon cancer) cell lines, we detected an inverse correlation between miR-25 levels and MCU mRNA expression, with high miR-25 levels and low MCU expression levels in cancer lines, compared to primary non-neoplastic cells (Fig. 18A). We then directly investigated human poorly differentiated colonic adenocarcinoma samples by immunohistochemistry and microarray. Also in this case, a significant difference in miR-25 expression levels was detected (Fig. 18B), which correlates with a downregulation of MCU expression. Indeed, in colonic adenocarcinoma samples with high miR-25 expression levels, MCU was virtually undetectable by immunohistochemistry in cancerous tissues, compared to relatively high protein abundance in the normal mucosa (Fig. 18C). To validate that miR-25 exerts its biological activity through its effect on MCU, we transfected cells with short hairpin RNA (ShRNA) targeting MCU: as for miR-25, ShRNA-MCU decreases MCU abundance and increases proliferation (Fig. 19A), indicating that MCU targeting is important for growth-promoting activity of miR-25.

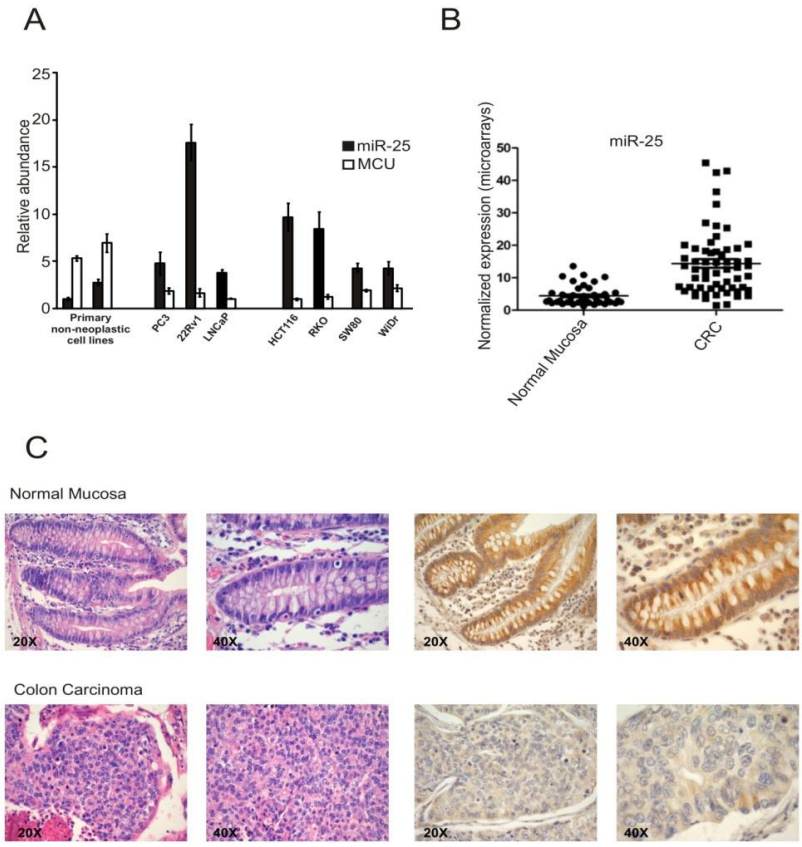

Figure 18 - Inhibition of MCU levels by miR-25 is a key aspect in cancer progression

We also tested the ability of MCU to inhibit the proliferation. We generated PC3 cells that stably expressed a MCU-flag tagged construct (MCU-flag), in which MCU level and activity was increased relative to that in empty vector (pcDNA3) stable clones (Fig. 19B-C), and found that they formed lower numbers of colonies in soft agar compared to control pcDNA3 stable clones (Fig. 19D). We then investigated whether miR-25-dependent inhibition of mitochondrial Ca^{2+} uptake, and the ensuing resistance to apoptosis, can be specifically reversed in cancer cells. For this purpose, we overexpressed anti-mir-25 in the PC3 and HCT116 cells lines investigated in Fig. 3. In both cell types, anti-miR-25 expression caused an ~40% increase in the $[Ca^{2+}]_m$ rise evoked by 100 μM ATP (Fig. 20A-B).

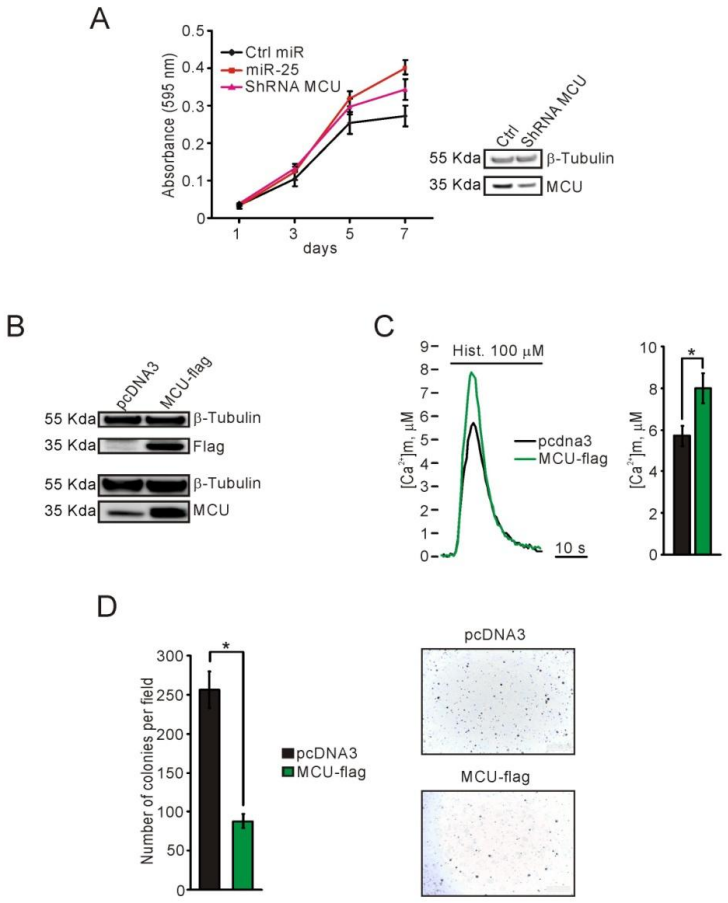

Figure 19 - Inhibition of MCU levels by miR-25 is a key aspect in cancer progression

Accordingly, sensitivity to C2-ceramide and H_2O_2 were enhanced, as revealed by the lower viability (Fig. 20C-D) and increased PARP and caspase 3 cleavage (Fig. 20E-F) detected in anti-miR-25 expressing cells.

Discussion

In the last two years, the discovery of the pore-forming subunit of the mitochondrial Ca2+ uptake channel (Mitochondrial Calcium Uniporter, MCU) and its regulatory subunits, termed MICU1 (mitochondrial calcium uptake 1) and MCUR1 (mitochondrial calcium uniporter regulator 1), opened a new era for the study of mitochondrial Ca^{2+} regulation and its key role in a variety of processes, including cell death. In the presence of an apoptotic stimulus, mitochondria receive Ca^{2+}-mediated inputs that induce the release of a number of pro-apoptotic factors from the mitochondria. Several oncogenes and tumor suppressors manipulate Ca^{2+} to exert their anti/pro-apoptotic activities. For example, Akt and Bcl-2 regulate ER Ca^{2+} flux to avoid mitochondrial Ca^{2+} overload and apoptosis; in contrast, pro-apoptotic genes, such as *Fhit* and *PML*, act at mitochondrial and ER

levels, respectively, to promote mitochondrial Ca^{2+} accumulation.

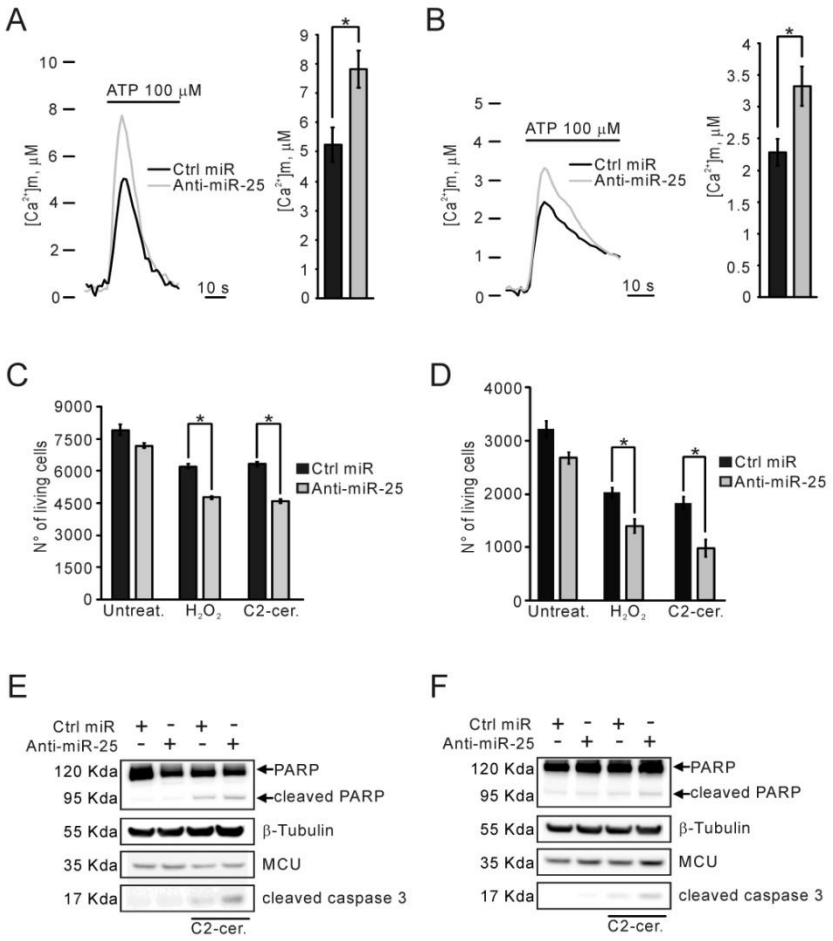

Figure 20 – anti-miR-25 enhances the sensitivity to apoptotic agents

Although the connection between mitochondrial Ca^{2+} increase and apoptosis is widely accepted, the mechanistic role of mitochondrial Ca^{2+} homeostasis in tumorigenesis is not fully understood.

MicroRNAs (miRNAs) are a class of naturally occurring small noncoding RNAs that are capable of regulating the expression of protein-coding genes at the posttranscriptional level, which consequently leads to a decrease in target protein abundance. Dysregulation of miRNA expression could lead to a variety of human disorders, including cancer.

Thus, miRNAs may function as oncogenes or tumor suppressors. Among the oncogenic miRNAs, miR-25 is one of the most studied and well described. miR- 25 is 22 nucleotides in length, hosted by the minichromosome maintenance protein- 7 (MCM7) gene, and transcribed as part of the mir-106b~25 polycistron; it is overexpressed in several human cancers, including pediatric brain tumors, gastric adenocarcinoma, epidermal growth factor receptor-positive lung adenocarcinoma

and prostate carcinoma and has been reported to target different regulators of the apoptotic pathway, such as BIM, PTEN and TRAIL. We found that Mir-25 also affects Ca^{2+} homeostasis through the specific downregulation of MCU, causing a strong decrease in mitochondrial Ca^{2+} uptake and, importantly, conferring resistance to Ca^{2+}-dependent apoptotic challenges. Prostate cancer cell lines, which exhibit high levels of miR-25, display very low amounts of MCU, and this inverse correlation (high miR-25/low MCU) is also maintained in colon cancer cell lines. Expression of miR-25 inhibitor in HCT116 cells increases mitochondrial Ca^{2+} levels and re-sensitizes cells to apoptosis.

A cancer link has been established through the detection of high miR-25 levels in stage II and III colonic adenocarcinoma samples, whereas MCU is virtually undetectable by immunohistochemistry.

Other members of the miR-25 family, such as miR-92a and miR-363, have the same effect on MCU expression and Ca^{2+} signaling as miR-25. These observations not only highlight the deep involvement of the whole family in the regulation of Ca^{2+} homeostasis, but also suggest how cancer cell survival, which is favored by MCU downregulation, might be ascribed to the upregulation of all miR-25 family members or strong expression of a singular miR, different from miR-25. Thus, both miR-25-5p, which is the different mature miR that originates from the opposite arm of the same pre-miRNA, and members of the same miRNA cluster, i.e., miR-106b, were predicted to target MCU mRNA, although their activity has not yet been tested. Therefore, the miR-106b~25 cluster might also play an important role in the control of MCU levels. Regulation of intracellular Ca^{2+} levels by miRNAs might be considered a fundamental aspect in several physio-pathological conditions. In the Ca^{2+}-dependent apoptosis context, which is characterized by sustained Ca^{2+} release from the ER and consequent accumulation at the mitochondrial level, the specific expression of miR-targeting mitochondrial Ca^{2+} effectors, such as miR-25, may be considered one of the most rapid intracellular mechanisms to prevent mitochondrial Ca^{2+} overload and avoid cell death. This process appears to be aberrantly overexpressed in tumors, especially in colon and prostate cancer cells.

Interplay between the modulation of Ca^{2+} levels and miRNAs has also been highlighted in other pathological scenarios.

For example, in cardiomyocytes, loss of miR-133a-mediated IP3R II (inositol 1,4,5 trisphosphate receptor, the calcium channel within the membranes of sarco/ endoplasmic Ca^{2+} stores) repression generates a positive feedback loop to drive the hypertrophic response, a process that is primarily Ca^{2+} dependent. In the same cellular setting, miR-214 protects the mouse heart from ischemic injury by controlling Ca^{2+} overload and cell death through the repression of the miRNA

encoding sodium/calcium exchanger 1 (Ncx1), a key regulator of Ca^{2+} influx. Moreover, miR-708, which is transcriptionally repressed in metastatic breast cancer, targets the ER protein neuronatin to decrease intracellular calcium levels, resulting in decreased cell migration and impaired metastases.

In conclusion, the interplay between intracellular Ca^{2+} and miRNAs might be a key aspect in several pathological conditions. Specifically, the suppression of mitochondrial Ca^{2+} entry by cancerrelated miR-25 represents the first study of the control of the mitochondrial uniporter by miRNA19 and offers initial clues to the relevance of this pathway in human cancers.

Overall, the data identify a microRNA (miR-25), highly expressed in cancer cells, that by targeting the newly discovered calcium channel of mitochondria reduces the sensitivity of cancer cells to apoptotic agents. This not only represents conclusive evidence of the key role of organelle Ca^{2+} accumulation in the mitochondria-dependent apoptotic routes, but also highlights a novel, unexpected target in cancer therapy. Now, the exciting task of unveiling the structural and functional properties of this long awaited component of the calcium signaling machinery of the cell finds an immediate translational application in a disease area of paramount importance.

Tumour necrosis factor alpha inhibits oligodendrocytes differentiation by inhibiting mitochondrial functions

Introduction

Multiple sclerosis (MS) is a neurological disorder of the central nervous system characterized by demyelination and neurodegeneration. MS is characterized by its relapsing-remitting course and neuro-pathologically manifests with multifocal areas of perivascular leukocyte infiltration associated with demyelination of the CNS. Early clinical symptoms result from oligodendrocytic damage and/or demyelination. The regression of symptoms is attributed to resolution of immunebased attack, associated edema and to partial remyelination or redistribution of sodium channels along demyelinated segments of axons. Although the pathogenesis of MS is not completely understood, various studies suggest that immune-mediated losses of myelin and mitochondrial dysfunction are associated with the disease [191]. In particular, mitochondrial functions might be required for proper oligodendrocyte differentiation and myelination. Specifically, it has been demonstrated that i) mitochondrial transcripts and copy number are induced by oligodendroglia differentiation, ii) slight mitochondrial inhibition inhibits differentiation, and iii) stronger mitochondrial inhibition selectively decreases viability of differentiating oligodendroglia but not undifferentiated cells [192].

Recent reports have documented impaired activity of several mitochondrial respiratory complexes in MS plaques [193].

Oligodendrocytes are particularly susceptible to oxidative injury. Having a low concentration of the antioxidant glutathione predisposes these cells to the accumulation of intracellular hydrogen peroxide. Contributing factors include their high metabolic rate and ATP requirement for the synthesis of large amounts of myelin membrane, the high production of hydrogen peroxide in peroxisomes, and the large intracellular stores of iron. Whereas iron is critical for myelin production, this metal can also trigger free radical formation and lipid peroxidation, via conversion of hydrogen peroxide into hydroxyl radicals [194]. Microglia present at the sites of injury play an important role in triggering or potentiating oligodendrocyte injury by several mechanisms. Both resting and activated microglia may release glutamate via a cystine-glutamate antiporter.

They can also release proinflammatory cytokines, such as tumour necrosis factor (TNFα), which impair expression or function of glutamate transporters in astrocytes and oligodendrocytes. TNFα can also trigger oligodendrocyte apoptosis both via death receptors and by activation of sphingomyelinase, with consequent release of ceramide [195]. There is in vitro evidence that cytokine-

induced oligodendrocyte injury may be mediated by iron and involves mitochondrial dysfunction [194].

Evidence that implicates TNFα in the underlying pathology of MS includes: i) the observation that, at autopsy, MS patients have elevated TNFα levels at the site of active MS lesions; ii) reports that CSF and serum TNFα levels in individuals with MS are elevated compared to unaffected individuals and TNFα levels correlate to the severity of the lesions; and iii) evidence that peripheral blood mononuclear cells from MS patients just prior to symptom exacerbation have increased TNFα secretion after stimulation compared to cells from the same patients during remission [196, 197]. Based on these strong clinical parameters implicating TNFα signalling in contributing to MS disease severity, the effects of manipulation of the TNFα pathway were investigated in mouse models of MS. Specifically, overexpression of TNFα leads to demyelinating disease and neutralization of TNFα with anti- TNFα antibodies or receptor fusion proteins is protective in experimental autoimmune encephalomyelitis (EAE) transgenic mouse models [198].

To date it is widely reported how TNFα is able to impair oligodendrocytes differentiation. At low concentration TNFα has been shown to induce retardation in appearance of adult oligodendrocytes in vitro, while at higher concentration it appear to be able to induce also cell death.

Moreover, in leukemic cell lines, TNFα induced cell death requires the impaired activity of Complex I of the mitochondrial respiratory chain, NADH dehydrogenase, strategic for the regulation of ATP synthesis, as well as being one of the most important sources of ROS within cells.

In this study we address the possibility that TNFα induces a blocking in oligodendrocytes differentiation by impairing mitochondrial physiology. This finding may open the opportunity to reveal novel molecular mechanisms at the basis of MS, and test a series of chemical compounds targeting selected feature of mitochondria to try to revert effect of TNFa on OPCs differentiation and thus, to detect a new pharmacological target and for develop a specific therapeutic approach against MS.

Results

TNFα at distinct concentrations impair oligodendrocyte differentiation or cell death

The first point considered was the ability of TNFα to impair oligodendrocytes differentiation in our in vitro system, set up following the protocol published by Chen et al. [199].

Oligodendrocyte progenitor cells (OPCs) were obtained by overnight shaking of mixed glial cultures generated from rat cortex. Isolated OPCs were then cultured for 7 days in presence of a

selective chemically defined DMEM (OPC medium). Immunostaining with marker for total oligodendrocytes population (OSP), oligodendrocyte precursors (NG2), marker of fully differentiated oligodendrocytes (MBP) and marker of astrocytes (GFAP) were performed to verify the purity of the culture, assessed at about 95% of OPCs (data not shown). After 7 days of culture OPCs where treated for 24h with sublethal concentration of TNFα, 10ng/ml, as suggested by literature [200]. Subsequently the growth factors present within the medium (fundamentals for OPCs replication) were substituted with T3 thyroid hormone to stimulate cell differentiation. After 5 days cells where fixed and immunostained for antigens able to mark different stages of oligodendrocytes maturation.

According to the literature three different antigens were selected for three stages of differentiation: NG2 chondroitin sulphate proteoglycan for precursor, O4 for immature oligodendrocytes and MBP for fully differentiated [201].

All the cells were contemporary stained for the oligodendrocytes specific antigen OSP to restrict the analysis only to the oligodendrocytes population and avoid artefacts coming from any contaminants. Cells were then acquired through an image based high content throughput system and classified by antigen positivity and nuclear features. Further we tested the ability of TNFα to induce cell death.

Cells were growth, exposed to TNFα and induced to differentiate as described previously. After fixation, cells were stained for a TUNEL assay. This technique is based on an enzymatical incorporation of fluorescence labeled deoxynucleotide in DNA breaks in nuclei making it very sensitive for identification of apoptotic nuclei.

TUNEL assay reveal that only at high concentration TNFα was able to promote apoptosis, moreover the effect appear generalized in all the populations, explaining why no relative enrichment of some populations were observed (Fig 21). (control 6.28% ± 3.69; TNFα 10ng/ml 7.43%±1.85, TNFα 50ng/ml 11.14%±3.89, $p<0.1$; TNFα 100ng 13.51±3.36, $p<0.05$ $n>6$).

Taken together these data support the hypothesis that at low concentrations TNFα is more able to affect oligodendrocytes differentiation, causing a block in very early stages with a consequent accumulation mostly of NG2+ oligodendrocytes. On opposite, higher TNFα concentration cause an increase of apoptosis induction.

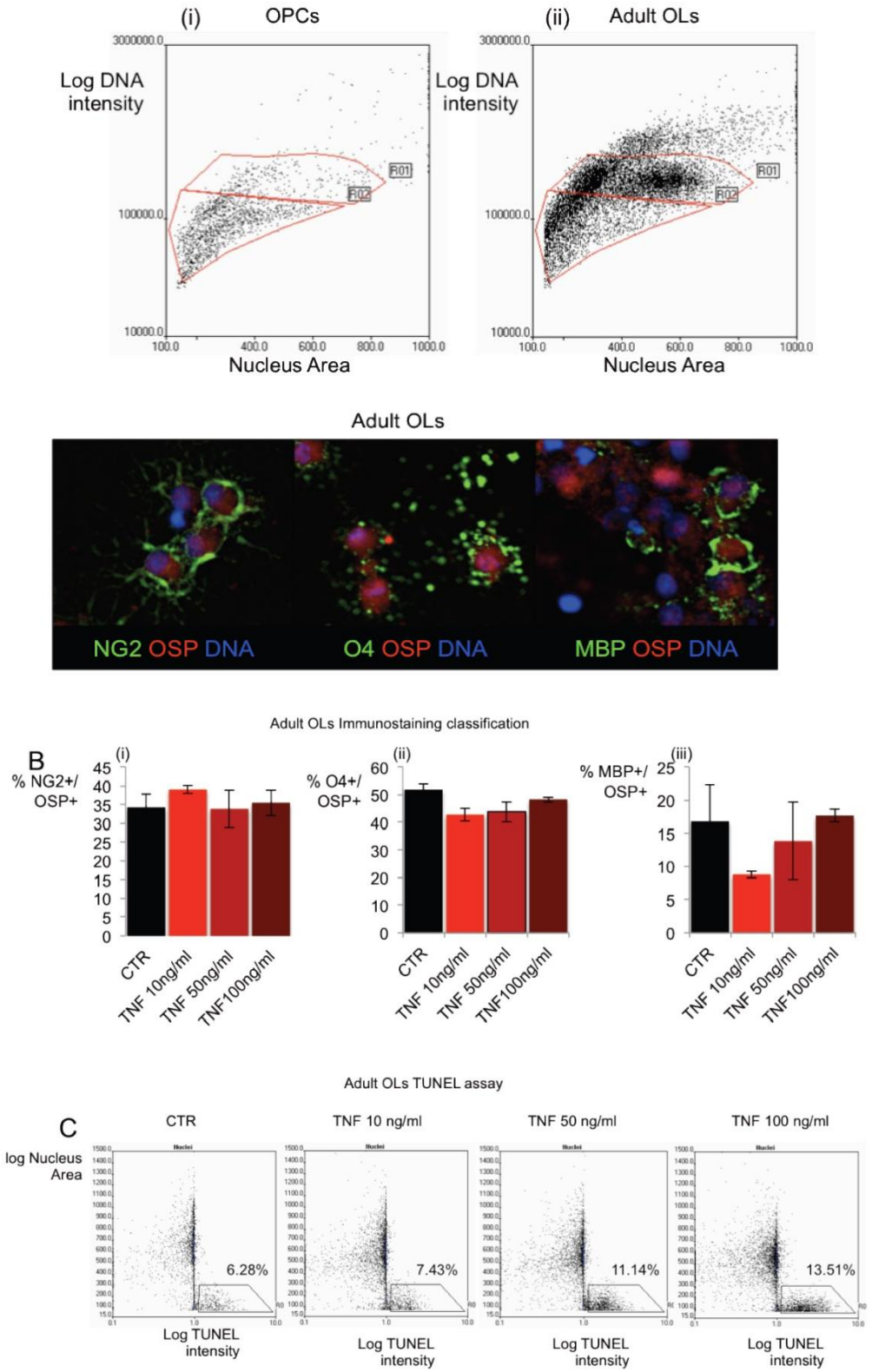

Figure 21. Distinct cell response initiated by TNFα. Nuclear pattern for scoring OPCs **(Ai)** or Adult Oligodendrocytes **(Aii)** and typical immunostaining for antigens used to score oligodendrocytes populations. (B) Oligodendrocytes enrichment for precursor (i), immature (ii) and adult cells (iii) during different concentration of TNFα. **(C)** Tunel assay in Oligodendrocytes populations during exposure to TNFα

Low concentration of TNFα selectively impair mitochondrial Ca^{2+} uptake

During differentiation process in fact oligodendrocytes undergoes through deep rearrangement of cell and nuclear shape, especially nuclei increase their volume while reaching adulthood.

Second part was to consider mitochondrial physiology under TNFα exposure. As previously discussed mitochondrial Ca^{2+} uptake could be considered as an affordable readout for monitor mitochondrial physiology. It is true that Ca^{2+} is up-taken by mitochondria through the driving force provided by Ψ_m at the site in which mitochondria take contact with the ER. Once entered into mitochondria, Ca^{2+} flow within the entire network because of the high amount of dynamic interconnections existing between mitochondria into the same cell. Noteworthy both Ψ_m and mitochondrial interconnectivity (or fragmentation) could be considered readout of mitochondria energy status, as well as exposure to stress or apoptosis induction.

Thus to monitor mitochondrial physiology under TNFα exposure we tested their ability to uptake Ca^{2+} following agonist exposure. To this attempt OPCs where infected with an adenoviral vector carrying cDNA for mitochondrial targeted mutant aequorin, 24h post infection cells were exposed to different TNFα concentrations (as previously described) and at 24h of TNFα exposure aequorin measurements were performed.

We elicited Ca^{2+} waves by stimulation with Carbachol (CCH) that after binding on its muscarinic receptor expressed on OPCs surface was able to induce IP3 generation and Ca^{2+} release from ER stores.

CCH stimulation induce a rapid increase in $[Ca^{2+}]_m$ in OPC, measured at 53.64 μM (n:6, ± 6.73) that recover to basal levels within one minute (Fig.22A). On opposite TNFα exposure was able to reduce mitochondrial Ca^{2+} accumulation showing stronger effect at low concentration, $[Ca^{2+}]_m$ values are reported as follow:

[TNFα] (ng/ml)	**Measured $[Ca^{2+}]_m$ (μM)**	**SD**	**P value**	**% variation VS control**
10	**29.35**	**10.35**	**0.00035**	**-45.27**
50	**37.53**	**11.39**	**0.00904**	**-30.03**
100	**48,62**	**13.30**	**0.07449**	**-9.46**

The most interesting observation is linked to the complete absence of a proportional dose response dependency.

Nonetheless what has been considered more interesting for prosecution of investigation is the observation that when TNFα is already able to impair differentiation without sensibly affecting

apoptosis, is also able to induce a strong effect on mitochondrial physiology, while with instauration of clear apoptosis induction the effect on mitochondrial physiology become progressively attenuated. Based on this observation is the choice to further investigate only the effects elicited by TNFα 10ng/ml.

To further address the events linking altered mitochondrial physiology to Ca^{2+} uptake we investigated whether TNFα was able to affect global Ca^{2+} signalling homeostasis. We tested this hypothesis by performing the previous experiments but measuring cytosolic Ca^{2+} responses using aequorin located in the cytosol (cytAEQ).

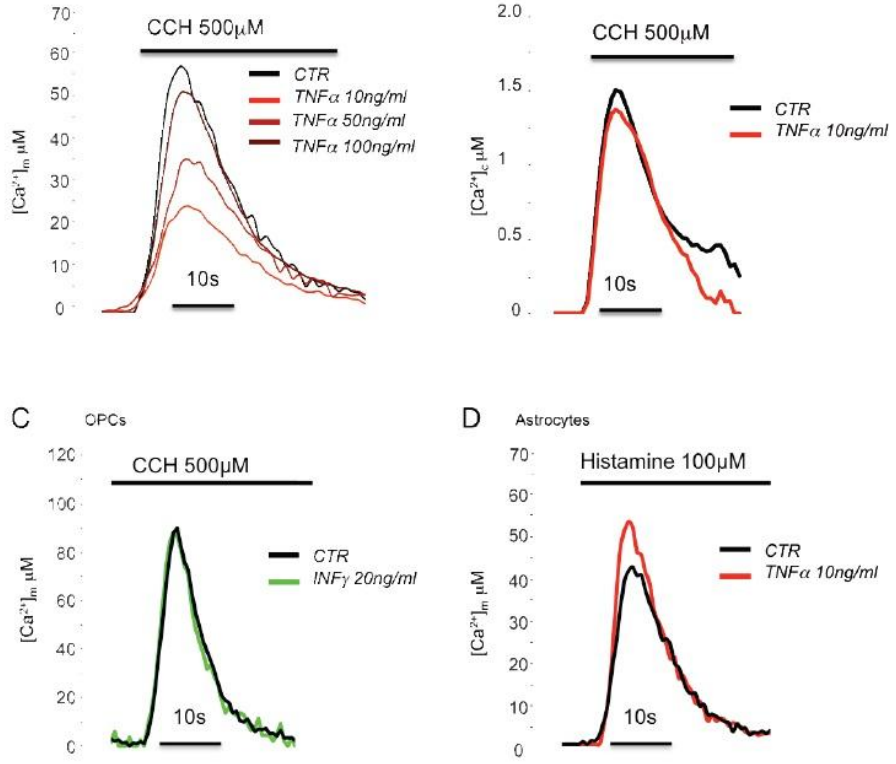

Figure 22 - TNFα selectively impair mitochondrial physiology in oligodendrocytes progenitors. Mitochondrial Ca^{2+} measurement in OPCs during agonist stimulation at different TNFα exposure **(A)** or INFγ **(C)**. Cytoplasmic waves in OPCs during low concentration TNFα exposure. Effect of TNFα on Mitochondrial Ca^{2+} response in astrocytes.

As shown in Fig.21B, in control cells carbachol rapidly and transiently increases cytosolic Ca^{2+} concentration ($[Ca^{2+}]c$) reaching maximum values (1.82 ± 0.08 µM, n=25) similar to those detected in OPC pretreated with 10 ng/ml for 24h (1.72 ± 0.09 µM, n=25, p>0.05), indicating that the observed effects were restricted to mitochondrial physiology.

We then investigated the effects of IFN-gamma (INFγ) on mitochondrial Ca^{2+} homeostasis. It is in fact well known how this cytokine, as for TNFα, is able to mediate inflammation execution during Multiple Sclerosis and other demyelinating disorders. OPC were treated with IFNγ 20 ng/ml for

24h, then mitochondrial Ca^{2+} variations elicited by agonist stimulation were investigated. As show in Fig.21C, no significant difference in $[Ca^{2+}]_m$ was observed between IFNγ treated and control cells (peak amplitude 79.7 ± 5.14 µM vs 89.4 ± 5.74 µM, n = 16; p >0.05).

In summary we observed that TNFα is able to perturb $[Ca^{2+}]_m$ in OPCs only at concentration nonpermissive for efficient apoptosis initiation. Contemporary these variations were not reproducible neither by INFγ, suggesting a selective and fine regulated link between mitochondria and TNFα in OPCs.

TNFα impairs mitochondrial bioenergetics and promote Superoxide production

To clearly define how TNFα was able to promote mitochondrial impairments observed measuring $[Ca^{2+}]_m$ we monitored Ψ_m and network integrity.

Electric potential is generated across inner mitochondrial membrane due to the activity of respiratory chain that consumes oxygen to pump protons to the intermembrane space. This proton gradient will be used by ATP synthase to drive ATP synthesis. Ψ_m could be easily monitored by fluorescence microscopy trough the use of different selective dyes. In our case we performed the measurement through the use of the potential sensitive dye TMRM and laser scanning confocal microscopy. Cells were treated with TNFα 10ng/ml or vehicle for 24h, loaded with TMRM 10nM then acquired before and after FCCP depolarization. The delta value induced by mitochondrial depolarization were considered as index of Ψ_m and compared between TNFα exposed cells and controls. The results evidentiate a strong Ψ_m reduction, of 30.5% (S.E. ±9.76, $p<0.05$), in cells treated with TNFα, suggesting an important decrease of respiratory chain activity (Fig.23A).

Subsequently we measured alterations of mitochondrial structure through digital deconvolution microscopy. OPCs were infected by adenoviral vector carrying cDNA for mitochondria targeted GFP, then acquired by fluorescence microscopy at high magnification, deconvolved and reconstructed in 3D images. Number and mean volume of mitochondria per cells were obtained and compared between TNFα exposed and control oligodendrocyte. Total network volume per cells is about 40837,4 voxels (S.D. ±12213,18) in control and 43501 voxels (S.D. ±6463,33) in TNFα treated cells (Fig.22Bi), while volume for single mitochondrion was 121,35voxel/object (S.D. ±382,88) in control and 922,69voxel/object (S.E. ±183,17) in TNFα (Fig.23Bii). Nor total network volume neither single particle volume result significantly different between conditions.

These results addressed the previous observed reduced $[Ca^{2+}]_m$ as a consequence of impaired Ψ_m .

It has been reported how impairment of respiratory chain could alter ROS metabolism leading to different ROS generation, nonetheless TNFα itself has been shown to stimulate the same effect.

Electron leak from respiratory chain has been reported mostly to promote generation of superoxide anion, that is mainly reversed to mitochondrial matrix and partly into the inter membrane space.

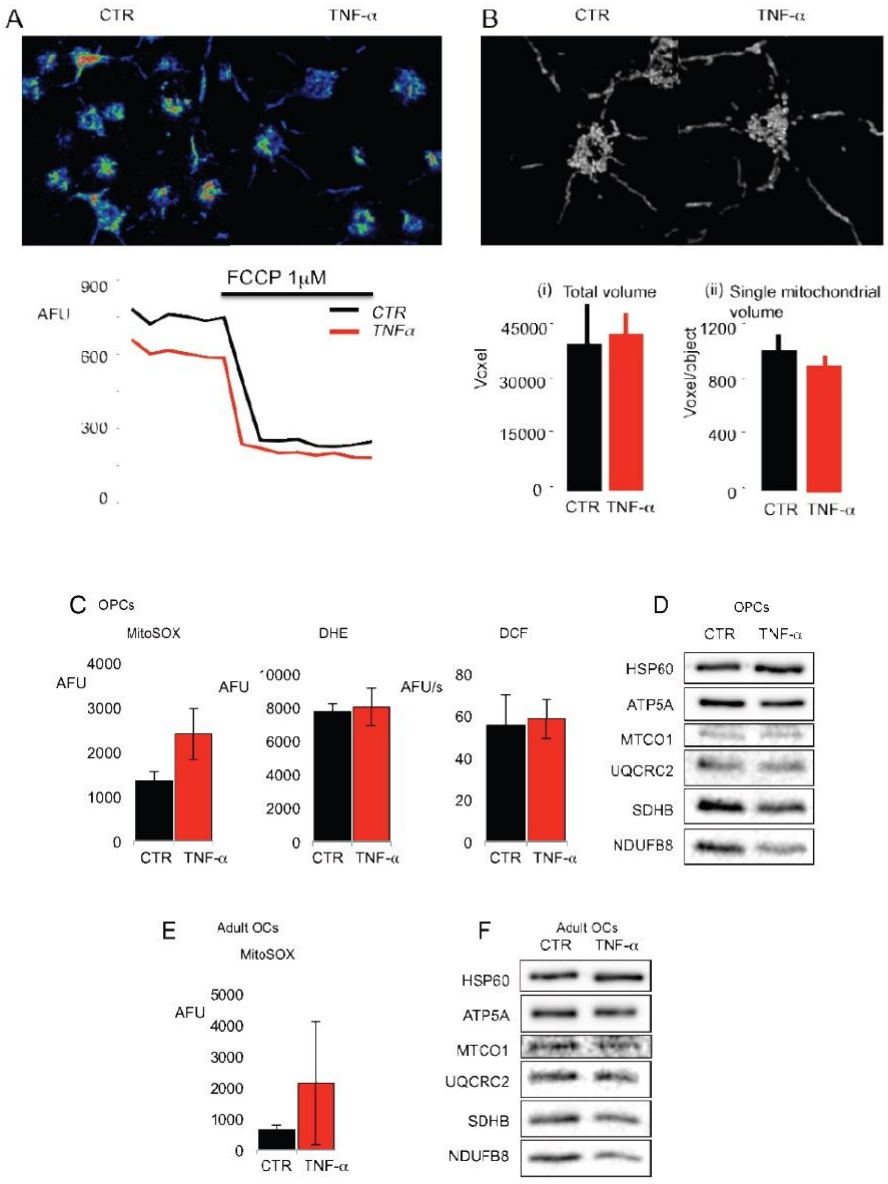

Figure 23- Perturbation of mitochondrial physiology mediated by TNFα in OPCs. (A) Measurements of Ψ_m with potentiometric dye TMRM. **(B)** Representative volume rendering of control OPCs and TNFα treated cells, (i) voxel quantification of total mitochondrial volume and (ii) single mitochondrial volume. Measurement of Superoxide in OPCs mitochondria (i) cytoplasm (ii) and measurement of H2O2 levels (iii). Expression of respiratory complex subunit in OPCs **(D)** and Adult **(F)**, NDUF8B for complex I, SDHB, for complex II, UQCRC2 for complex III, MTCO1 for Complex IV and ATP5A for Complex V. HSP60 has been used as loading marker. Analisis of mitochondrial superoxide in adult cells **(E).**

Due to effect of Super Oxide Dismutase, O_2 -. is rapidly converted to H_2O_2 then detoxified to H_2O by catalase. Was in turn considered fundamental to monitor ROS production, three different

fluorimetric approaches were used to obtain an overview of general ROS metabolism, based on three different ROS sensitive dyes: dichlorodihydrofluorescein (DCF), Dihydroethidium (DHE) and MitoSOX.

DHE and MitoSOX are well known ethidium based O_2 -. Sensitive dyes, with the peculiar difference that could be selectively localized to cytoplasm and mitochondria respectively, while

DCF is generally used as sensor for H_2O_2. To perform this measurments cells where growth for 7 days in multiwells, then exposed to TNFα 10ng/ml for 24h, after treatment cells were stained and measured as further described (see materials and methods). Interestingly within all these three parameters only MitoSOX display significant variations (MitoSOX control 1336.64AFU± 255.06; TNF 10ng/ml: 2397.71AFU± 560.73, n: 3 $p<0.05$; DHE control 7725.72AFU± 543.87; TNF 10ng/ml: 7987.0AFU± 896.15, n: 3; DCF control 55.37AFU/s± 15.41; TNF 10ng/ml: 58.40AFU/s± 9.82, n: 3). Considering that MitoSOX has high selectivity for mitochondrial O_2 -. we found this result linear with what previously observed (Fig 23C).

In order to obtain a further comprehension the mechanism by which TNFα was able to produce this effect on ROS production we monitor expression of respiratory complexes by immunoblotting.

Immunoreaction was performed with the OxPhos antibody cocktail that allow contemporary to monitor subunits in all the five respiratory complexes, specially the detectable targets are: NDUFB8 for complex I, SDHB for complex II, UQCRC2 for complex III, MTCO1 for complex IV and ATP5A for complex V. As loading marker was chosen mitochondrial HSP60.

The blot display a strong and almost selective reduction in marker for Complex I, even if weak alterations has been displayed for Complex II (Fig.23D).

We consider the alteration of respiratory complex I level as the very basic effect able to induce all the other alterations observed ($[Ca^{2+}]_m$, Ψ_m , and O_2 -. production). Considering that mitochondria undergoes to continuous processes of degradation and biogenesis, allowing old and damaged organelles recycling, as well as several mitochondrial features are transcriptionally regulated during stress conditions, we tested if alterations in Complexes expression and ROS metabolism were maintained during differentiation or if oligodendrocytes undergoes trough adaption.

Experiment were performed as for antigen recognition, briefly cells after 7 days of colture were exposed to TNFα 10ng/ml for 24h then placed in presence of T3 thyroid hormone and let differentiate for 5 days. At the end of this period cells were alternatively used for ROS measurements or immunoblotting. MitoSOX staining resulted yet higher in treated cells compared to control (Fig.23E), but higher variability was measured reducing the significativity of the result (MitoSOX control 644.71AFU± 107.81; TNFα 10ng/ml: 2132.15AFU± 2085.7, n: 3).

Interestingly immunoblot result obtained in the same conditions reveal that variations in expression levels of Respiratory Complex I still exist in adult oligodendrocytes as observed in OPCs (Fig.23F).

Tumour necrosis factor alpha modulates oligodendrocytes differentiation and mitochondrial functions also in mixed-glia coltures.

Now, we wished to confirm the presence of a critical regulation of mitochondrial homeostasis in a more physiological system. To reach this, we started to assess experiments in organotypic slides obtained from rat brain, following the protocol of Gogolla et al. [202], according that, the cultures can be easy to execute and can be maintained for several weeks. This last peculiarity was essential for our experiment of live calcium measurements. We demonstrated to be able performing these cultures. In fact, our organotypic slides reflected the criteria reported in the published protocol (the slices were transparent, firmly attached to the membrane and without a significant cell death when labelled with propidium iodide). Unfortunately, even if we tried to obtain an appropriate efficiency of transfection by the employment of different techniques of transfection (lipofectamine technology and recombinant virus mediated expression), we recognized invaluable transfection, with a consequent series of unreliable and not significant results. Thus, we decided to assess our experiments in an alternative physiological system, represented by mixed-glia (MG) culture, where OPCs are been grown on top of bed layers of astrocytes. Verified the purity of the cultures (assessing the presence of OSP, NG2, MBP and GFAP), we started to measure the principal mitochondrial parameters (Figure 24).

We performed single cell calcium measurements by the employment of the GFP-based Ca^{2+} probe Cameleon selectively targeted to the mitochondrial matrix (mtCameleon) using live fast microscopy. Cells expressing fluorescent probes were observed 36h after transfection on an inverted fluorescence microscope (Zeiss Axiovert 200M), with an oil immersion objective (63x, N.A. 1.40). Excitation light was setting at appropriate wavelengths: 440 nm for CFP-CaM, 500 nm for M13-YFP. Dichroic beam splitter was 455DRLP. Emission filters were 480DF30 (for CFP) and 545DF35 (for YFP) in the case of cameleon and were alternated using a filter wheel.

MG coltures were transfected with the calcium indicator mtCameleon and treated with treated with 10 ng/ml TNFα, and after 24h we measured $[Ca^{2+}]_m$. The results evidenziated a strong reduction in mitochondrial calcium uptake in OPCs grown on the bed layers of astrocytes and treated with TNFα of 23.4% (S.E. ± 2.12). Next, to rule out the possibility that the effect observed was not only circumscribed to the OPCs cells, the same experiment was also performed in astrocytes cells. As expected, treatment with 10 ng/ml of TNFα does not affect the mitochondrial calcium uptake in astrocytes.

As reported above, Ca^{2+} influx into mitochondria is highly driven by the electronegative potential within mitochondria. Thus, we evaluated the mitochondrial bioenergetic by laser scanning confocal imaging of the fluorescent dye TMRM. The results evidentiate a strong reduction of Ψ_m in OPCs grown on the bed of astrocytes and treated with TNFα of 15% (S.E. ±0.76) indicating an important reduction of activity of respiratory chain. Afterwards, we investigated if the cytokine TNFα could also affect the electronegative potential within mitochondria of astrocytes cells. As result, we checked any change in Ψ_m of this cell type, at demonstration that the inflammatory cytokine TNFα seems to modulate negatively only the mitochondrial energetic of OPCs.

Experiments were then carried out to exclude that the observed effects were secondary to changes in mitochondrial morphology (fragmentation or swelling). On the former aspect, mitochondria was labelled in living cells by adenoviral infection with expressing green fluorescent protein specifically targeted to the mitochondria compartments (mtGFP). As result, we have not noticed different for total volume cells and volume for single mitochondrion between astrocytes and oligodendrocytes cell in control condition and after TNFα treatment.

By these result, we can assert that the cell types (OPCs and astrocytes) showed the typical three-dimensional interconnected network, with no difference in mitochondrial number and volume between control and TNFα treated cells, suggesting that TNFα induced reduction in MMP and mitochondrial Ca^{2+} uptake is not a consequence thereinafter mitochondrial fragmentation. We have observed that an alteration of mitochondrial homeostasis following treatment with TNFα at sub-toxic doses determinates a significantly lower amount of MBP. Thus, we asked if we could observe the same effect also in MG cultures performing immunoblot and immunostaining analysis of the total amount of MBP.

As result, we found that mixed-glia cultures treated with TNF reveal a significant reduction in MBP expression (by WB) and in presence of MBP+/Oligo-1+ compared to control cells (by immunostaining).

Therefore, we have demonstrated (before performing experiment in cultured OPCs, and then in a more physiological system, as like MG coltures) that TNFα induce a reduction in mitochondrial activity and physiology, an alteration that seems to be responsible for the lacking of OPCs differentiation in mature oligodendrocyte.

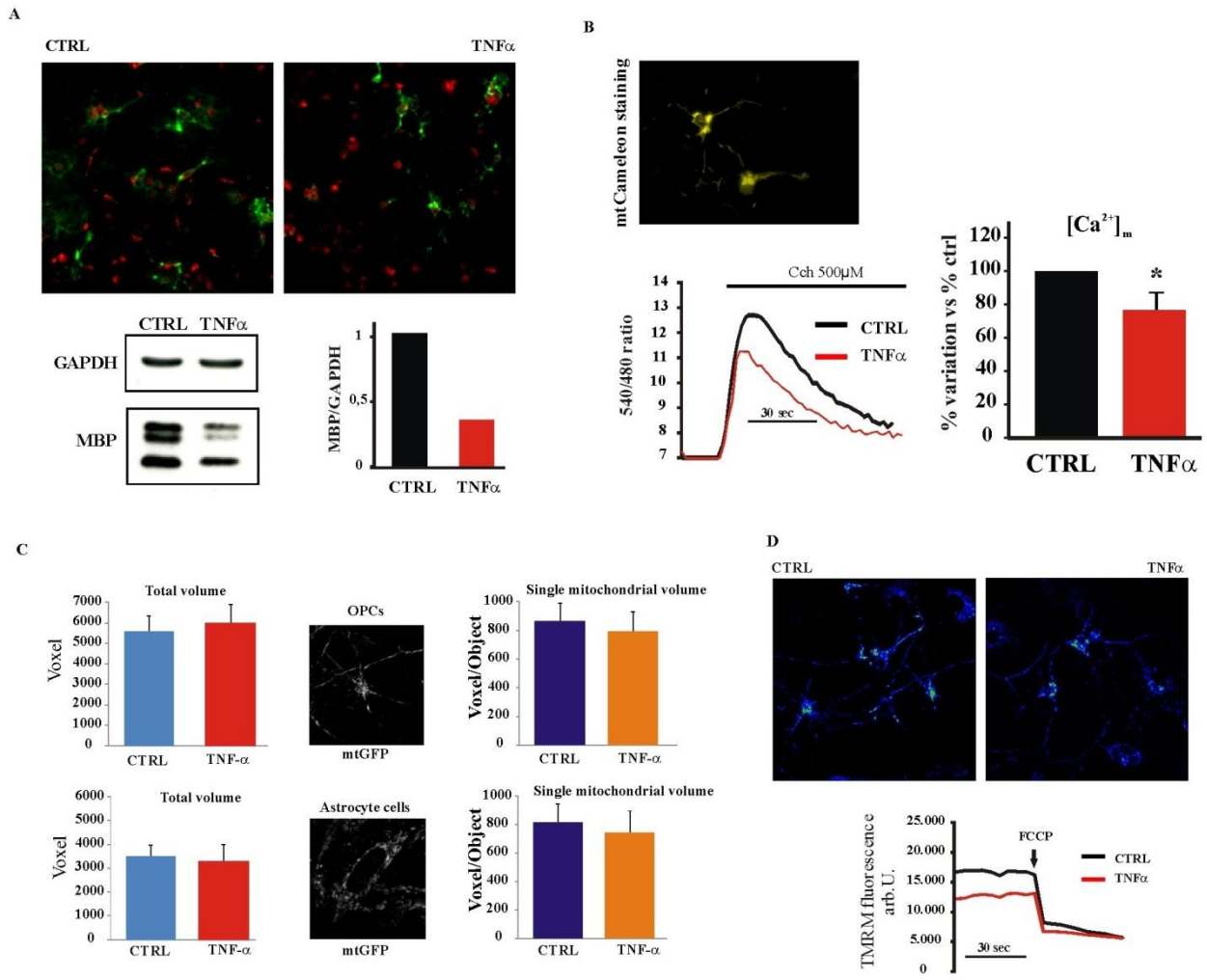

Figure 24 – mitochondrial physiology in mixed-glia coltures

Tumour necrosis factor alpha reduce the total amount of MBP around the axon.

Meantime, we performed a series of myelinization assays following the protocol reported in Brain Research Protocol [203], where OPCs were co-cultured with primary neurons from rat cerebrum on a feeder layer of rat cerebrum astrocytes. The final intent will be to verify that an oligodendroglial precursor cell with a lower mitochondrial functioning (due to TNFα exposure) is not more capable to differentiate in a mature oligodendrocyte, the cell responsible for MBP production.

Briefly, OPCs were cultured and maintained undifferentiated in OPC-medium supplemented with PDGF and bFGF. Neurons were co-cultured on a feed layer of cultured astrocytes for 4-7 days.

Before experiments OPCs were treated with 10 ng/ml TNFα, and after 24h plated on these neurons/astrocytes co-coltures. After 4-6 days, we were ready to estimate myelin formation by WB and immunostaining (Figure 25 and26).

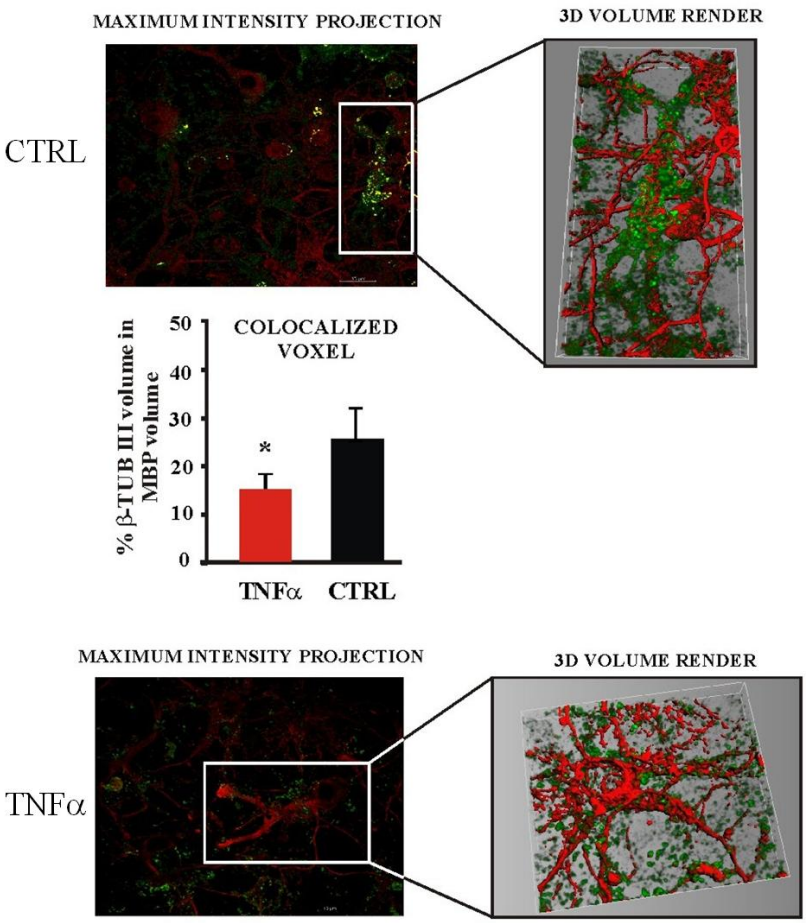

Figure 25 - Myelinization in vitro. OPCs were treated with TNFa 10ng/ml (TNFα) or vehicle (CTRL) for 24h, plated on then feed layer of cultured astrocytes/neurons and finally harvested for immunochemistry analyses. Immunostaining for β-TUB III (red, neurons) and MBP (green, for fully differentiated oligodendrocytes).

We have monitored the various differentiative stages, which occur during our myelinization assays. Such as described, we have plated on then feed layer of cultured astrocytes/neurons, the OPCs treated with TNFα 10ng/ml or vehicle for 24h and performed WB with marker of precursors oligodendrocytes (NG2), marker of precursors and fully differentiated oligodendrocytes (Oligo-1), marker of premyelinating/ immature oligodendrocytes (GalC), marker of fully differentiated oligodendrocytes (MBP) and a marker of neurons (b-tubulin III) for verify that in all conditions the neurons total number remained was the same.

In addition, to avoid an involvement of apoptotic pathway, and thus a possible reduction in cell number, we also performed detection of cleaved-PARP.

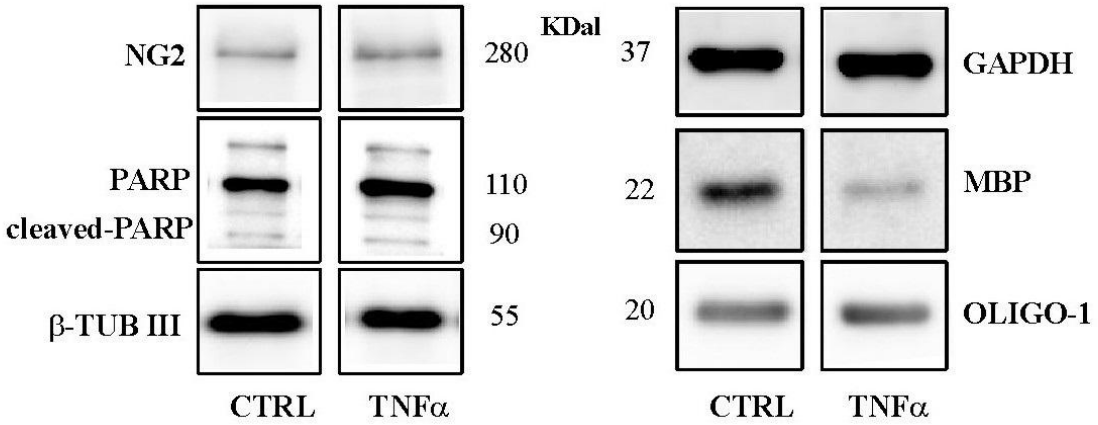

Figure 26 – Myelinization assays. Immunoblot analysis with marker of precursors oligodendrocyte (NG2), marker of precursors and fully differentiated oligodendrocyte (Oligo-1), marker of fully differentiated oligodendrocyte (MBP), marker of neurons (b-tub III), apoptosis marker (PARP/cleaved-PARP) and loading marker (GAPDH).

As first, the results corresponded with our previous remark: a sub-toxic treatment with TNF does not mediate apoptotic cell death in OPCs, but determinates a significantly lower amount of MBP (and thus the number of mature oligodendrocytes.

In addition, we found that: the total amount of neurons in presence/absence of TNFα remained the same; NG2 levels were unchanged in both conditions; we did not recognize alteration in Oligo-1 levels; finally, we checked a significant augment in total amount of GalC in the cultures treated with TNFα, compared to the control.

Thanks to these remarks, we can suppose that TNFα lower mitochondria bioenergetic (without affect apoptosis level), which induce a reduction in MBP-expressing cells. This lacking, can be induced by a blocking in a specific stage of OPCs differentiation: how is reported in our results, it seems that during the differentiation, OPCs are blocking in the premyelinating/immature state.

At demonstration of this hypothesis, we have confirmed the results obtained by immunostaining assays by the employment of the markers reported above.

Discussion

It has been well established that the Tumour Necrosis Factor alpha is one of the most relevant cytokines involved in the pathogenesis of Multiple Sclerosis. In fact, it has been widely reported how the levels of this cytokine correlate with the exacerbation of the pathology as well as how it could affect the physiology of Oligodendrocytes (the principal target of degeneration during aetiology of MS) *in vitro*. This impairment is principaly manifested by the induction of cell death (at high concentrations) as also by blockage of their differentiation process.

In this study we address the hypothesis that impairment of differentiation due to TNFα exposure is linked to affected mitochondrial physiology.

Initially, we confirmed that exposure to low concentrations of TNFα (10ng/ml) is able to impair OPCs differentiation. We observed an accumulation of NG2+ cells (early progenitors) while reducing the relative amount of O4+ and MBP+ (immature oligodendrocytes and adult oligodendrocytes respectively). This phenomenon was not accompanied by a significant induction of apoptosis. On the other hand, exposure to higher concentrations of TNFα induced a strong increase in cell death, with no significant accumulation any specific oligodendrocytes population.

This led to the hypothesis that TNFα is able to induce an immediate effect in the progenitor population that could generate two distinct outcomes: blockade of differentiation or induction of cell death. These data were in agreement with previously reported results.

Basing on this hypothesis we tested whether at this early stage, TNFα was able to affect mitochondrial physiology. As an initial readout we chose to monitor mitochondrial Ca2+ uptake as it is often an initial reporter of alterations of mitochondrial physiology.

We took advantage of the Ca^{2+} sensitive luminescent protein Aequorin, (targeted to mitochondria) to measure mitochondrial Ca^{2+} homeostasis in OPCs at an early stage of TNFα exposure.

Interestingly we observed a significant reduction in $[Ca^{2+}]_m$ only at a low TNFα concentration. This was in accordance with the "two destinies" hypothesis, suggesting that mitochondrial impairment was a specific event during the differentiation impairment process. The effect on mitochondrial homeostasis was confirmed by measuring cytoplasmic Ca^{2+} waves, with the use of a cytoplasmic aequorin.

Cells treated with TNFα [10ng/ml] did not display any differences in cytoplasmic Ca^{2+} compared to controls, indicating that alterations in $[Ca^{2+}]_m$ were not due to a general perturbation of the whole intracellular Ca^{2+} homeostasis.

Next to TNFα, another cytokine, INFγ is well known to participate in the pathogenesis of MS. We have also addressed this cytokine to verify the cytotoxic effects on oligodendrocytes since no relations with the differentiation process have not yet been reported. We used subtoxic concentrations of IFNγ [20ng/ml] to verify if perturbations of mitochondrial physiology could be considered a general activity of proinflammatory cytokines and we reported no significant variation in $[Ca^{2+}]_m$.

But in order to properly be able to identify a selective relationship between TNFα and OPCs there is a need to test the $[Ca^{2+}]_m$ also in other cell types, known to be sensitive to this cytokine. We found it interesting to monitor $[Ca^{2+}]_m$ in astrocytes cultures, due to the huge amount of reports indicating how astrocytes sense TNFα and also participate to its metabolism.

We found that $[Ca^{2+}]_m$ was strongly modified in TNFα-exposed astrocytes. However, instead of being reduced, as measured in OPCs, it was significantly increased. This suggests that a perturbation on mitochondrial physiology was occurring, but in an opposite direction and, presumably, involving different pathways.

It appears clear that a selective cytokine-dependent and cell-dependent relationship exists between mitochondrial physiology and OPCs during TNFα exposure.

To obtain a deeper comprehension about what this mitochondrial perturbation consists of, we measured the Ψ_m and mitochondrial fragmentation during early TNFα exposure, considering them principal features linked to $[Ca^{2+}]_m$. Mitochondrial Ca^{2+}uptake is driven by the mitochondrial membrane potential, and is it's direct function. Moreover, once in mitochondria, Ca^{2+} flows from the ingress sites (contact sites with endoplasmic reticulum) to the entire network. Due to these features, both, variations of Ψ_m as well as of the mitochondrial network interconnections are reflected in alterations in average Ca^{2+} uptake. Interestingly, while mitochondria in treated cells did not significantly change in neither size nor number, they displayed a significantly lower Ψ_m.

Variations of the Ψ_m are often linked to impaired energy production as also to alterations of ROS metabolism. In particular, a strong elevation of Ψ_m have been reported to lead to accumulation of different reactive species of oxygen. Moreover TNFα itself is a known ROS inducer in different cellular systems.

To obtain a general overview of ROS metabolism we monitored production of both O_2 .- and H_2O_2 with fluorimetric dyes. We were also able to distinguish between mitochondrial and cytoplasmic O_2 .- through the use of two different dyes (MitoSOX and DHE respectively), proper recognition of the two different amount of O_2 .- was fundamental to properly address the real source. It is well known that mitochondria are the site for the synthesis of a significant amount of O_2 .-, but it is also generated in large amounts in other organelles. What is more, O_2 .- has a very short half-life and is usually rapidly dysmutated to H_2O_2 by SODs, making the measurement of O_2 .- difficult. Thus, to more precisely assess the overall contribution of ROS, it is crucial to also use other probes, such as DCF (to monitor H_2O_2). Interestingly, we found that only MitoSOX gave a significantly higher staining in treated cells compared to control, suggesting that mitochondria were stimulated in O_2 .- production by TNFα.

To date, the two most important mitochondrial sources for O_2 .- are both within the respiratory chain. They are respiratory complexes I and III. Impairment of their activity leads to rapid and robust O_2.- production, with a peculiar difference. Complex I leave the O_2 .- produced within the mitochondrial matrix only, whereas complex III is able to generate it both in the matrix and the IMS. Since DHE is not able to distinguish between the cytoplasm and the IMS (due to high

permeability of the OMM) and due to the different behaviour between MitoSOX and DHE we suggest an impairment of Complex I. Similar suggestions do arrive from the literature. In leukemic cells, TNFα was able to induce death by selectively promoting ROS by complex I, while in rat left ventricle TNFα led to a O_2 .--dependent reduction in Complex I expression.

Through immunoblot we verified that OPCs treated with TNFα for 24h display a strong reduction in respiratory complex I subunit NDUFB8 and even more interestingly, the altered levels were maintained in adult cells during differentiation.

Impairment of the transcript level of this complex could lead to the reduction of Ψ_m measured in OPCs and gained our particular interest in light of the observed differentiation impairment. It was in fact reported that during differentiation, OPCs undergo to a deep rearrangement of expression of genes involved in metabolism, and that respiratory complex inhibitors like rotenone (for complex I) or azide (for complex IV) strongly impair oligodendrocytes differentiation.

To further link mitochondrial impairment with oligodendrocytes differentiation we observed that exposure to a low concentration of a generic mitochondrial uncoupler, FCCP, was able to reproduce the reduction in Ψ_m observed for TNFα, as also to reduce the amount of MBP+ and O4+ cells with concomitant accumulation of NG2+ positive cells. This gave strength to the hypothesis that the mitochondrial impairment exerted by TNFα is able to generate a block at an early stage of OPCs differentiation.

To extend these observations in a more physiological system, we assessed experiments in a mixed-glia culture, where OPCs grow on top of a bed layers of astrocytes. As result, we observed that also in this environment, TNFα led to a reduction in mitochondrial activity and physiology, an alteration that seems to be responsible for the lacking of OPCs differentiation in mature oligodendrocyte. Moreover, performing a series of myelinization assays (where OPCs were co-cultured with primary neurons from rat cerebrum on a feeder layer of rat cerebrum astrocytes), we observed that sub-toxic treatment with TNFα determinate a significantly lower amount of MBP around the axon (and thus the number of mature oligodendrocytes).

The results proposed to now shows a correlation between TNFα induced differentiation blockade and mitochondrial conditioning. Starting from observation reported in literature, we believe mitochondria cover a crucial role during MS pathogenesis; thus, we would able to identify novel molecular mechanism at the basis of MS and a consequent therapeutical approaches. To achieve this, our intention is to test chemical compounds targeting selected feature of mitochondria to try to revert effect of TNFα on OPCs differentiation. At the moment, we are screening a series of mitochondrial active compounds: succinate (substrate for II mitochondrial respiratory complex), ciclosporin-A (inhibitor of the mitochondrial permeability transition pore), cgp37157 (inhibitor of

mitochondrial Na^+/Ca^{2+} exchanger), tempol (a synthetic antioxidant), metformin (regulator of mitochondrial respiration), to name but a few.

Contemporarily, our purpose is also to modulate the mitochondrial Ca^{2+} buffering by means of the expression of the recently discovered Mitochondrial Calcium Uniporter and its principal regulators MICU1 and MCUR1. Thus, we could verify if it is possible to revert the negative effect of the cytokine on OPCs differentiation, through the modulation of the levels of $[Ca^{2+}]_m$. Thus, we strongly believe that our studies and our goals will be important for addressing novel therapeutic approaches.

MATERIALS AND METHODS

Cell culture and transfection.

HEK293 cells were maintained in a humidified 5% CO_2, 37°C incubator in Dulbecco's modified Eagle's medium (DMEM) supplemented with 10% fetal bovine serum (FBS; Life technologies, 10270) 100 U/ml penicillin (EuroClone, 3001D), 100 mg/ml streptomycin (EuroClone, 3000D). HEK293 were transfected with a standard calcium-phosphate procedure.

HeLa, HCT116 and RKO cells were cultured in Dulbecco's modified Eagle's medium (DMEM) supplemented with 10% fetal calf serum (FCS), L-glutamine and penicillin/streptomycin in 75-cm^2 Falcon flasks. PC3, 22Rv1 and LnCaP cells were cultured in RPMI 1640, supplemented with 10% FCS, 2 mM L-glutamine, and penicillin/streptomycin, in 75-cm^2 Falcon flasks. HeLa, HCT116, RKO, PC3, 22Rv1 and LnCaP cells were transfected using Lipofectamine 2000 procedure. For aequorin measurements, we used mtAEQmut for HeLa cells and mtAEQ for PC3 and HCT116 cells. All measurements were performed 24 h after transfection. All miR and anti-miR molecules (hsa-miRNA precursor and hsa-miRNA inhibitor) were purchased from Ambion®. Short hairpin RNA (ShRNA) targeting MCU (TRCN0000133861) was purchased from Sigma-Aldrich.

Mouse embryonic fibroblast (MEFs) were maintained in a humidified 5% CO_2, 37°C incubator in Dulbecco's modified Eagle's medium (DMEM) supplemented with 10% fetal bovine serum (FBS; Life technologies, 10270) 100 U/ml penicillin (EuroClone, 3001D), 100 mg/ml streptomycin (EuroClone, 3000D) were transfected using JetPEI (Polyplus transfection™, 101-10) or infected by recombinant adenovirus expressing mitochondrially and cytosolic targeted aequorin, PKCβ-GFP and GFP-LC3. For aequorin measurements, the cells were seeded before transfection onto 13mm glass coverslips and allowed to grow to 50% confluence. For immunostaining, mitochondrial morphology analysis, PKCs localization, autophagy measurements by fluorescence microscopy and single cells $[Ca^{2+}]_m$ measurements, cells were seeded on 24mm glass coverslip. For immunoblotting analysis, cells were seeded on 6 well plates in the same conditions of growth.

Primary oligodendrocytes (OPCs) were prepared following the protocol of Chen et al., 2007. This method contemplates the generation of a population of oligodendrocytes precursor cell on a layer of astrocytes, originated by mixed glia cultures of P1-P2 pup rats. For the separating of the two kind of primary cell cultures, after 10 days of growth in DMEM 20% FBS, the whole preparation is exposed to sheer forces generated by its shaking on an orbital shaker at 190rpm. Collected oligodendrocytes progenitors are separated by residual microglia and astrocytes by incubation of 1h on uncoated petri dish, and then filtered in cell strainers with 40μM holes. Cell where then seeded

on coverslip of different dimension, according with the planned experiment and kept in culture for 7 days in chemically defined medium composed by DMEM, 4 mM L-glutamine, 1 mM sodium pyruvate, 0.1% BSA, 50 mg/ml Apo-transferrin, 5 mg/ml insulin, 30 nM sodium selenite, 10 nM Dbiotin and 10 nM hydrocortisone, 10 ng/ml PDGF-AA and 10 ng/ml bFGF.

Aequorin measurements. Probes used are chimeric aequorins targeted to the cytosol (cytAEQ) and mitochondria (mtAEQmut). For the experiments with cytAEQ and mtAEQmut, cells were incubated with 5 mM coelenterazine (Fluka, 7372) for 1–2h in DMEM supplemented with 1% FBS. A coverslip with transfected cells was placed in a perfused thermostated chamber located in close proximity to a low-noise photomultiplier with a built-in amplifier/ discriminator.
All aequorin measurements were carried out in KRB supplemented with 1mM $CaCl_2$. Agonist was added to the same medium as specified in figure legends. The experiments were terminated by lysing cells with 100 mM digitonin in a hypotonic Ca^{2+}-containing solution (10mM $CaCl_2$ in H_2O), thus discharging the remaining aequorin pool. The output of the discriminator was captured by a Thorn EMI photon-counting board and stored in an IBM-compatible computer for further analyses. The aequorin luminescence data were calibrated offline into [Ca^{2+}] values using a computer algorithm based on the Ca^{2+} response curve of wild-type and mutant aequorins.

Immunoblotting. For immunoblotting cells were scraped into ice-cold phosphate –buffered saline and lysed in a modified 10mM Tris buffer pH 7.4 containing 150mM NaCl, 1% Triton X-100, 10% glycerol, 10mM EDTA and protease inhibitor cocktail. After 30 minutes of incubation on ice, the lysates were cleared via centrifugation centrifuged at 12,000g at 4°C for 10 minutes. Protein concentration were determined by the Bio-Rad procedure. Protein extracts, 25µg, were separated on 4-12% and 4-20% Bis-Tris acrylamide (Life technologies, NP0323 and EC6026) and electron-transferred to PVDF or Nitrocellulose membrane according to standard procedures. Unspecific binding sites were saturated by incubating membranes with TBS- Tween 20 (0.05%) supplemented with 5% non fat powdered milk for 1h. Next, the membranes were incubated over-night with primary antibodies and the revelation was assessed by the employment of appropriate HRP-labeled secondary antibodies [SantaCruz, sc-2004 (goat anti-rabbit) and sc-2005 (goat anti-mouse)] plus a chemiluminescent substrate (Thermo Scientific, 34080).

Immunofluorescence. Cells were washed with PBS, fixed in 4% formaldehyde for 10 minutes and washed with PBS. Then, cells were permeabilized for 10 minutes with 0.1% Triton X-100 in PBS and blocked in PBS containing 2% BSA and 0.05% Triton X-100 for 1h. Cells were then incubate

with primary antibody for 3h at room temperature and washed three times with PBS. The appropriate isotype-matched, AlexaFluor-conjugated secondary antibodies [Life Technologies, A11008 (488 goat anti-rabbit) and A11001 (488 goat anti-mouse)] were used. Images were taken with a Nikon Swept Field Confocal equipped with CFI Plan Apo VC60XH objective (numerical aperture, 1.4) (Nikon Instruments) and an Andor DU885 electron multiplying charge-coupled device (EM-CCD) camera (Andor Technology Ltd).

Isolation of mitochondria

Cells were washed twice with PBS, resuspended and homogenized in a buffer containing 250 mM sucrose, 1 mM EGTA, 50 mM Tris-HCl, 1mM DTT, protease inhibitor cocktail, pH 7.4 with 40 μg of digitonin per ml in a glass homogenizer. Homogenate was centrifuged at 1,500 x g for 5 min twice. The final supernatant was collected and centrifuged at 10,000 x g for 10 min, the mitochondrial pellets were resuspended with homogenization buffer (without digitonin) and centrifuged again at 10,000 x g for 10 min. Mitochondrial pellets were disrupted in 100μl lysis buffer at 4°C, incubated 30 min on ice and then centrifuged at 17,000 x g for 30 min. Protein concentration in the supernatant was determined by the Bio-Rad protein estimation kit. To control the equal loading of lanes, it was used an anti-β-ACTIN antibody (for homogenate) and an anti-pan/VDAC antibody (for mitochondria).

Mouse experiments and tissue processing. Pkcβ WT and Pkcβ ko mice [204] were bred and maintained according to both the Federation for Laboratory Animal Science Associations and the Animal Experimental Ethics Committee guidelines. They were housed in a temperature-controlled environment with 12h light dark cycles and received food and water ad libitum. For studies of effects of starvation, mice were deprived of food for 24h. These mice had free access to drinking water. After killing, mice tissues were homogenized in a 20mM Tris buffer, pH 7.4, containing 150mM NaCl, 1% Triton X-100, 10mM EDTA and protease inhibitor cocktail. Tissue extract were then centrifuged at 12,000g at 4°C for 10 minutes. Protein extracts, 15μg, were subjected to SDS-PAGE and immunoblotting. Quantification of intensities of the immunoreactive bands was carried out using ImageQuant™ LAS-4000 chemiluminescence imaging system (GE Healthcare).

Measurements of mitochondrial Ψ_m. Mitochondrial Ψ_m was measured by loading cells with 20nM tetramethyl rhodamine methyl ester (TMRM; Life Technologies, T-668) for 30 minutes at 37°C. Images were taken on an inverted microscope (*Nikon* LiveScan Swept Field Confocal Microscope (*SFC*) Eclipse Ti equipped of NIS-Elements microscope imaging software). TMRM excitation was

performed at 560nm and emission was collected through a 590–650nm band-pass filter. Images were taken every 5s with a fixed 20ms exposure time. FCCP (carbonyl cyanide p-trifluoromethoxyphenylhydrazone, 10 µM), an uncoupler of oxidative phosphorylation, was added after 12 acquisitions to completely collapse the electrical gradient established by the respiratory chain.

Fluorescence microscopy and quantitative analysis of GFP-LC3 dots. HEK293 cells were cultured in a 24-mm glass coverslips and transfected at 50% confluence with 6µg of plasmid DNA (control cells: 4µg pcDNA3 + 2µg GFP-LC3; PKC-overexpressing cells: 4µg PKC + 2µg GFP-LC3). MEFs WT, MEFs Pkcβ ko and MEFs Pkcβ ko expressing PKCβ, were cultured in a 24mm glass coverslips and transfected at 50% confluence: MEF WT and MEFs Pkcβ ko: 4µg pcDNA3 + 2µg GFP-LC3; MEFs Pkcβ ko expressing Pkcβ: 4µg Pkcβ + 2µg GFP-LC3 (for high expression); 2µg Pkcβ + 2µg GFP-LC3 (for low expression); MEFs Pkcβ ko expressing Pkcβ-KD: 4µg Pkcβ-KD + 2µg GFP-LC3. After 36h, images were taken on a *Nikon* LiveScan Swept Field Confocal Microscope (*SFC*) Eclipse Ti equipped of NIS-Elements microscope imaging software. For each condition, the number of GFP-LC3 dots was counted in at least 25 independent visual fields.

Mitochondrial morphology analysis. The cells were seeded before transfection onto 24-mm glass coverslips, allowed to grow to 50% confluence and then transfected with a mitochondrially fluorescent protein (mtDsRed) or ErGFP. At 24 hours after transfection, cells were imaged with a laser scanning confocal Zeiss LSM 510, illuminating GFP at 488 nm and dsRed at 543 nm. Z stack of 51 planes were obtained with an objective Plan-Apo 63x/1.4 Oil Ph3 with a voxel size of 105 x 105 x 200 nm (X x Y x Z). To obtain the best object reality, images were next deconvolved using the open source software Fiji (http://fiji.sc/wiki/index.php/Fiji, last accessed June 20, 2011), and especially through the 3D iterative deconvolution plugin (http://www.optinav.com/Iterative-Deconvolve-3D.htm). A theoretical PSF were build using the "PSF generator" plugin available at http://bigwww.epfl.ch/algorithms/psfgenerator/.

Once reconstructed a mitochondrial and endoplasmic reticulum mask were manually chosen to obtain a binarized image of overlapping areas. The resulting areas were described in number and volume, using the 3D object counter, available in Fiji.

FRET- based measurements of mitochondrial Ca^{2+}. Single-cell measurements of mitochondrial Ca^{2+} were performed in HEK293 cells transfected with 4mtD3cpv. After 36h, cells were imaged on a Zeiss Axiovert 200M microscope with a cooled CCD camera (Photometrics), equipped of a C-

apochromat 40x/1.2 W CORR objective and controlled by METAFLUOR 7.0 Software (Universal Imaging). Emission ratio imaging of the *cameleon* was accomplished by using a 436DF20 excitation filter, a 450 nm dichroic mirror, and two emission filters (475/40 for ECFP and 535/25 for citrine) controlled by a Lambda 10-2 filter changer (Sutter Instruments). Fluorescence images were background corrected. Exposure times were typically 100–200ms, and images were collected every 5–15s.

Quantitative analysis of the Autophagic-Flux. HEK293 cultured on 24-mm glass coverslips were transfected with 6µg of plasmid DNA (control cells: 4µg pcDNA3 + 2µg mCherry-eGFP-LC3; PKCβ-overexpressing cells: 4µg PKCβ + 2µg mCherry-eGFP-LC3). After 36h expression cells were treated as described and then imaged on a *Nikon* LiveScan Swept Field Confocal Microscope (*SFC*) Eclipse *Ti* with a 60x magnification and equipped of NIS-Elements microscope imaging software. Obtained puncta image were merge to compare the RFP signals with GFP signals using ImageJ software. For each condition, the colocalization of these two signals was determined by manual counting of fluorescent puncta in at least 20 independent visual fields.

Vectors and luciferase assay

Portions of 3'UTR of human MCU and MICU1 genes, containing miR-25 putative target regions, were amplified through PCR, using the following primers:

MCU_3UTR_F: 5'-CACTCGAGACACTGCATGAGGTTGTTGG-3'

MCU_3UTR_R: 5'-CAGTTTAAACCACCTGGAGTCTGGGTTTGT-3' (760 bp);

MICU1_3UTR_F: 5'-CACTCGAGAGAATTCAGGGAACCATCCA-3'

MICU1_3UTR_R: 5'-CAGTTTAAACACAGGGAACTTTGGGGATGT-3' (570 bp).

Growth in semisolid medium

The bottom layer was obtained by covering six-well dishes with 3 ml of 0.6% agar in RPMI. The following day, 5×10^4 stable clone PC3 cells were plated on this bottom layer in triplicate, in 2 ml of 0.3% agar in RPMI + 10% FBS. After 4 weeks, colonies were stained with 0.005% crystal violet and counted at 4x magnification. Five fields for each well were counted. A Leica DM IL LED microscope was used. Colonies were counted automatically using a custom made macro in the Fiji software. Briefly, dark objects were thresholded using the Yen algorithm and counted through the analyze particles tool; objects smaller than 70 pixels were excluded.

Real Time RT-PCR to evaluate microRNA and mRNA expression

Total RNA was extracted from cells with Trizol reagent (Invitrogen), according to the manufacturer's instructions.

Immunohistochemistry

Four-micrometer thick sections were cut from formalin-fixed paraffin-embedded blocks. One section for each block was routinely stained with hematoxylin and eosin for histological examination.

For immunodetection of MCU, tissue sections were deparaffinized with xilene and rehydrated by sequential ethanol (from 100% to 80%) and rinsed in distilled water. Before immunostaining, sections were processed by microwave-oven for antigen retrival in Tris-EDTA-Citrate buffer (pH 7.8) for 30 minutes. After rinse with distilled water and rehydratation with PBS buffer, sections were incubated in a buffer solution with 3% of H_2O_2 for 15 minutes at room temperature to block endogenous peroxidase activity.

Tissue sections were then incubated with the primary rabbit anti-MCU antibody (Sigma-Aldrich), diluted 1:100 for 1h at room temperature. We then used the Ultravision Detection System (Large Volume Polyvalent-HRP) (Thermo Scientific) and the Dab Detection Kit (Cell Marque) according to manufacturers' instructions. Counterstaining was conducted with Mayer's hematoxylin.

ROS measurements

Total release of ROS from mitochondria was estimated fluorimetrically by oxidation of Dihydroethidium, MitoSOX or DCF. Fluorescence was measured in multiwell plate reader (Infinite M200, Tecan, Austria) using 510 ± 10 nm excitation and 595 ± 35 nm emission wavelengths for MitoSOX and DHE while 513 ± 10 nm excitation and 530 ± 25 nm emission.

Statistical analysis. The results were expressed as the mean ± SD and the *n* refers to the number of independent experiments. The probability of statistical differences between experimental groups was determined by the Student's *t* test.

REFERENCES:

1. Dyall, S.D., Brown, M.T. & Johnson, P.J. Ancient invasions: from endosymbionts to organelles. *Science* **304**, 253-257 (2004).
2. Frey, T.G. & Mannella, C.A. The internal structure of mitochondria. *Trends Biochem Sci* **25**, 319-324 (2000).
3. Vogel, F., Bornhovd, C., Neupert, W. & Reichert, A.S. Dynamic subcompartmentalization of the mitochondrial inner membrane. *J Cell Biol* **175**, 237-247 (2006).
4. Benard, G. & Rossignol, R. Ultrastructure of the mitochondrion and its bearing on function and bioenergetics. *Antioxid Redox Signal* **10**, 1313-1342 (2008).
5. Cereghetti, G.M. & Scorrano, L. The many shapes of mitochondrial death. *Oncogene* **25**, 4717-4724 (2006).
6. Santel, A. & Fuller, M.T. Control of mitochondrial morphology by a human mitofusin. *J Cell Sci* **114**, 867-874 (2001).
7. James, D.I., Parone, P.A., Mattenberger, Y. & Martinou, J.C. hFis1, a novel component of the mammalian mitochondrial fission machinery. *J Biol Chem* **278**, 36373-36379 (2003).
8. Smirnova, E., Griparic, L., Shurland, D.L. & van der Bliek, A.M. Dynamin-related protein Drp1 is required for mitochondrial division in mammalian cells. *Mol Biol Cell* **12**, 2245-2256 (2001).
9. Yoon, Y., Krueger, E.W., Oswald, B.J. & McNiven, M.A. The mitochondrial protein hFis1 regulates mitochondrial fission in mammalian cells through an interaction with the dynamin-like protein DLP1. *Mol Cell Biol* **23**, 5409-5420 (2003).
10. Yu, T., Robotham, J.L. & Yoon, Y. Increased production of reactive oxygen species in hyperglycemic conditions requires dynamic change of mitochondrial morphology. *Proc Natl Acad Sci U S A* **103**, 2653-2658 (2006).
11. Csordas, G. & Hajnoczky, G. SR/ER-mitochondrial local communication: calcium and ROS. *Biochim Biophys Acta* **1787**, 1352-1362 (2009).
12. Krebs, H.A. & Eggleston, L.V. The oxidation of pyruvate in pigeon breast muscle. *Biochem J* **34**, 442-459 (1940).
13. Kennedy, E.P. & Lehninger, A.L. Oxidation of fatty acids and tricarboxylic acid cycle intermediates by isolated rat liver mitochondria. *J Biol Chem* **179**, 957-972 (1949).
14. Lambeth, D.O., Tews, K.N., Adkins, S., Frohlich, D. & Milavetz, B.I. Expression of two succinyl-CoA synthetases with different nucleotide specificities in mammalian tissues. *J Biol Chem* **279**, 36621-36624 (2004).

15. Amemori, S. *et al.* Oral dimethyl sulfoxide for systemic amyloid A amyloidosis complication in chronic inflammatory disease: a retrospective patient chart review. *J Gastroenterol* **41**, 444-449 (2006).
16. Quinn, P.J. & Dawson, R.M. Interactions of cytochrome c and [14C]. *Biochem J* **115**, 65-75 (1969).
17. Lenaz, G. & Genova, M.L. Structure and organization of mitochondrial respiratory complexes: a new understanding of an old subject. *Antioxid Redox Signal* **12**, 961-1008 (2010).
18. Boyer, P.D. Catalytic site forms and controls in ATP synthase catalysis. *Biochim Biophys Acta* **1458**, 252-262 (2000).
19. Berridge, M.J., Lipp, P. & Bootman, M.D. The versatility and universality of calcium signalling. *Nat Rev Mol Cell Biol* **1**, 11-21 (2000).
20. de Brito, O.M. & Scorrano, L. Mitofusin 2 tethers endoplasmic reticulum to mitochondria. *Nature* **456**, 605-610 (2008).
21. Patergnani, S. *et al.* Calcium signaling around Mitochondria Associated Membranes (MAMs). *Cell Commun Signal* **9**, 19 (2011).
22. Rossi, C.S. & Lehninger, A.L. Stoichiometric relationships between mitochondrialion accumulation and oxidative phosphorylation. *Biochem Biophys Res Commun* **11**, 441-446 (1963).
23. Scarpa, A. & Graziotti, P. Mechanisms for intracellular calcium regulation in heart. I. Stopped-flow measurements of Ca++ uptake by cardiac mitochondria. *J Gen Physiol* **62**, 756-772 (1973).
24. Lehninger, A.L. Mitochondria and calcium ion transport. *Biochem J* **119**, 129-138 (1970).
25. Giorgi, C., Romagnoli, A., Pinton, P. & Rizzuto, R. Ca2+ signaling, mitochondria and cell death. *Curr Mol Med* **8**, 119-130 (2008).
26. Bragadin, M., Pozzan, T. & Azzone, G.F. Kinetics of Ca2+ carrier in rat liver mitochondria. *Biochemistry* **18**, 5972-5978 (1979).
27. Moreau, B., Nelson, C. & Parekh, A.B. Biphasic regulation of mitochondrial Ca2+ uptake by cytosolic Ca2+ concentration. *Curr Biol* **16**, 1672-1677 (2006).
28. Trenker, M., Malli, R., Fertschai, I., Levak-Frank, S. & Graier, W.F. Uncoupling proteins 2 and 3 are fundamental for mitochondrial Ca2+ uniport. *Nat Cell Biol* **9**, 445-452 (2007).
29. Brookes, P.S. *et al.* UCPs--unlikely calcium porters. *Nat Cell Biol* **10**, 1235-1237; author reply 1237-1240 (2008).

30. Perocchi, F. *et al.* MICU1 encodes a mitochondrial EF hand protein required for Ca(2+) uptake. *Nature* **467**, 291-296 (2010).
31. De Stefani, D., Raffaello, A., Teardo, E., Szabo, I. & Rizzuto, R. A forty-kilodalton protein of the inner membrane is the mitochondrial calcium uniporter. *Nature* (2011).
32. Baughman, J.M. *et al.* Integrative genomics identifies MCU as an essential component of the mitochondrial calcium uniporter. *Nature* (2011).
33. Kirichok, Y., Krapivinsky, G. & Clapham, D.E. The mitochondrial calcium uniporter is a highly selective ion channel. *Nature* **427**, 360-364 (2004).
34. Mallilankaraman, K. *et al.* MCUR1 is an essential component of mitochondrial Ca2+ uptake that regulates cellular metabolism. *Nat Cell Biol* **14**, 1336-1343 (2012).
35. Jiang, D., Zhao, L. & Clapham, D.E. Genome-wide RNAi screen identifies Letm1 as a mitochondrial Ca2+/H+ antiporter. *Science* **326**, 144-147 (2009).
36. Nowikovsky, K. *et al.* The LETM1/YOL027 gene family encodes a factor of the mitochondrial K+ homeostasis with a potential role in the Wolf-Hirschhorn syndrome. *J Biol Chem* **279**, 30307-30315 (2004).
37. Palty, R. *et al.* NCLX is an essential component of mitochondrial Na+/Ca2+ exchange. *Proc Natl Acad Sci U S A* **107**, 436-441 (2010).
38. Giorgi, C., De Stefani, D., Bononi, A., Rizzuto, R. & Pinton, P. Structural and functional link between the mitochondrial network and the endoplasmic reticulum. *The international journal of biochemistry & cell biology* **41**, 1817-1827 (2009).
39. De Giorgi, F., Lartigue, L. & Ichas, F. Electrical coupling and plasticity of the mitochondrial network. *Cell Calcium* **28**, 365-370 (2000).
40. Rizzuto, R. *et al.* Close contacts with the endoplasmic reticulum as determinants of mitochondrial Ca2+ responses. *Science* **280**, 1763-1766 (1998).
41. Lombardi, A., Damon, M., Vincent, A., Goglia, F. & Herpin, P. Characterisation of oxidative phosphorylation in skeletal muscle mitochondria subpopulations in pig: a study using top-down elasticity analysis. *FEBS Lett* **475**, 84-88 (2000).
42. Collins, T.J., Berridge, M.J., Lipp, P. & Bootman, M.D. Mitochondria are morphologically and functionally heterogeneous within cells. *EMBO J* **21**, 1616-1627 (2002).
43. Gomes, L.C., Di Benedetto, G. & Scorrano, L. During autophagy mitochondria elongate, are spared from degradation and sustain cell viability. *Nat Cell Biol* **13**, 589-598 (2011).
44. Pinton, P., Giorgi, C., Siviero, R., Zecchini, E. & Rizzuto, R. Calcium and apoptosis: ER-mitochondria Ca2+ transfer in the control of apoptosis. *Oncogene* **27**, 6407-6418 (2008).

45. Rimessi, A., Giorgi, C., Pinton, P. & Rizzuto, R. The versatility of mitochondrial calcium signals: from stimulation of cell metabolism to induction of cell death. *Biochim Biophys Acta* **1777**, 808-816 (2008).
46. Rizzuto, R., Brini, M., Murgia, M. & Pozzan, T. Microdomains with high Ca2+ close to IP3-sensitive channels that are sensed by neighboring mitochondria. *Science* **262**, 744-747 (1993).
47. Szabadkai, G. *et al.* Chaperone-mediated coupling of endoplasmic reticulum and mitochondrial Ca2+ channels. *J Cell Biol* **175**, 901-911 (2006).
48. Hayashi, T. & Su, T.P. Sigma-1 receptor chaperones at the ER-mitochondrion interface regulate Ca(2+) signaling and cell survival. *Cell* **131**, 596-610 (2007).
49. Kroemer, G., Galluzzi, L. & Brenner, C. Mitochondrial membrane permeabilization in cell death. *Physiol Rev* **87**, 99-163 (2007).
50. Garrido, C. *et al.* Mechanisms of cytochrome c release from mitochondria. *Cell death and differentiation* **13**, 1423-1433 (2006).
51. Hill, M.M., Adrain, C. & Martin, S.J. Portrait of a killer: the mitochondrial apoptosome emerges from the shadows. *Mol Interv* **3**, 19-26 (2003).
52. Ravagnan, L., Roumier, T. & Kroemer, G. Mitochondria, the killer organelles and their weapons. *J Cell Physiol* **192**, 131-137 (2002).
53. Pinton, P. *et al.* The Ca2+ concentration of the endoplasmic reticulum is a key determinant of ceramide-induced apoptosis: significance for the molecular mechanism of Bcl-2 action. *The EMBO journal* **20**, 2690-2701 (2001).
54. Szalai, G., Krishnamurthy, R. & Hajnoczky, G. Apoptosis driven by IP(3)-linked mitochondrial calcium signals. *EMBO J* **18**, 6349-6361 (1999).
55. Danial, N.N. & Korsmeyer, S.J. Cell death: critical control points. *Cell* **116**, 205-219 (2004).
56. Youle, R.J. & Karbowski, M. Mitochondrial fission in apoptosis. *Nat Rev Mol Cell Biol* **6**, 657-663 (2005).
57. Ricchelli, F. *et al.* Disaccharide modulation of the mitochondrial membrane fluidity changes induced by the membrane potential. *IUBMB Life* **51**, 111-116 (2001).
58. Rapizzi, E. *et al.* Recombinant expression of the voltage-dependent anion channel enhances the transfer of Ca2+ microdomains to mitochondria. *J Cell Biol* **159**, 613-624 (2002).
59. Wieckowski, M.R. *et al.* Overexpression of adenine nucleotide translocase reduces Ca2+ signal transmission between the ER and mitochondria. *Biochem Biophys Res Commun* **348**, 393-399 (2006).

60. Turrens, J.F. Mitochondrial formation of reactive oxygen species. *J Physiol* **552**, 335-344 (2003).
61. Pinton, P. *et al.* Protein kinase C beta and prolyl isomerase 1 regulate mitochondrial effects of the life-span determinant p66Shc. *Science* **315**, 659-663 (2007).
62. Giorgio, M. *et al.* Electron transfer between cytochrome c and p66Shc generates reactive oxygen species that trigger mitochondrial apoptosis. *Cell* **122**, 221-233 (2005).
63. Wang, C.W. & Klionsky, D.J. The molecular mechanism of autophagy. *Mol Med* **9**, 65-76 (2003).
64. Seglen, P.O. & Bohley, P. Autophagy and other vacuolar protein degradation mechanisms. *Experientia* **48**, 158-172 (1992).
65. Deter, R.L. & De Duve, C. Influence of glucagon, an inducer of cellular autophagy, on some physical properties of rat liver lysosomes. *J Cell Biol* **33**, 437-449 (1967).
66. Deter, R.L., Baudhuin, P. & De Duve, C. Participation of lysosomes in cellular autophagy induced in rat liver by glucagon. *J Cell Biol* **35**, C11-16 (1967).
67. Tsukada, M. & Ohsumi, Y. Isolation and characterization of autophagy-defective mutants of Saccharomyces cerevisiae. *FEBS Lett* **333**, 169-174 (1993).
68. Klionsky, D.J. *et al.* A unified nomenclature for yeast autophagy-related genes. *Dev Cell* **5**, 539-545 (2003).
69. Farre, J.C. & Subramani, S. Peroxisome turnover by micropexophagy: an autophagy-related process. *Trends Cell Biol* **14**, 515-523 (2004).
70. Massey, A., Kiffin, R. & Cuervo, A.M. Pathophysiology of chaperone-mediated autophagy. *Int J Biochem Cell Biol* **36**, 2420-2434 (2004).
71. Martinez-Vicente, M., Sovak, G. & Cuervo, A.M. Protein degradation and aging. *Exp Gerontol* **40**, 622-633 (2005).
72. Sengupta, S., Peterson, T.R. & Sabatini, D.M. Regulation of the mTOR complex 1 pathway by nutrients, growth factors, and stress. *Mol Cell* **40**, 310-322 (2010).
73. Mizushima, N. The role of the Atg1/ULK1 complex in autophagy regulation. *Curr Opin Cell Biol* **22**, 132-139 (2010).
74. Kang, R., Zeh, H.J., Lotze, M.T. & Tang, D. The Beclin 1 network regulates autophagy and apoptosis. *Cell Death Differ* **18**, 571-580 (2011).
75. Tanida, I., Ueno, T. & Kominami, E. LC3 conjugation system in mammalian autophagy. *Int J Biochem Cell Biol* **36**, 2503-2518 (2004).
76. Ravikumar, B. *et al.* Regulation of mammalian autophagy in physiology and pathophysiology. *Physiol Rev* **90**, 1383-1435 (2010).

77. Gottlieb, R.A. & Carreira, R.S. Autophagy in health and disease. 5. Mitophagy as a way of life. *Am J Physiol Cell Physiol* **299**, C203-210 (2010).
78. Koh, H. & Chung, J. PINK1 as a molecular checkpoint in the maintenance of mitochondrial function and integrity. *Mol Cells* **34**, 7-13 (2012).
79. Narendra, D., Kane, L.A., Hauser, D.N., Fearnley, I.M. & Youle, R.J. p62/SQSTM1 is required for Parkin-induced mitochondrial clustering but not mitophagy; VDAC1 is dispensable for both. *Autophagy* **6**, 1090-1106 (2010).
80. Ashrafi, G. & Schwarz, T.L. The pathways of mitophagy for quality control and clearance of mitochondria. *Cell Death Differ* **20**, 31-42 (2013).
81. Zhang, J. & Ney, P.A. Role of BNIP3 and NIX in cell death, autophagy, and mitophagy. *Cell Death Differ* **16**, 939-946 (2009).
82. Zhang, J. *et al.* Mitochondrial clearance is regulated by Atg7-dependent and -independent mechanisms during reticulocyte maturation. *Blood* **114**, 157-164 (2009).
83. Gomes, L.C. & Scorrano, L. Mitochondrial morphology in mitophagy and macroautophagy. *Biochim Biophys Acta* **1833**, 205-212 (2013).
84. Radoshevich, L. *et al.* ATG12 conjugation to ATG3 regulates mitochondrial homeostasis and cell death. *Cell* **142**, 590-600 (2010).
85. Cedarbaum, J.M. & Blass, J.P. Mitochondrial dysfunction and spinocerebellar degenerations. *Neurochem Pathol* **4**, 43-63 (1986).
86. Tatsuta, T. & Langer, T. Quality control of mitochondria: protection against neurodegeneration and ageing. *EMBO J* **27**, 306-314 (2008).
87. Otera, H. & Mihara, K. Molecular mechanisms and physiologic functions of mitochondrial dynamics. *J Biochem* **149**, 241-251 (2011).
88. Lassmann, H., Bruck, W. & Lucchinetti, C.F. The immunopathology of multiple sclerosis: an overview. *Brain Pathol* **17**, 210-218 (2007).
89. Bush, W.S. *et al.* Evidence for polygenic susceptibility to multiple sclerosis--the shape of things to come. *Am J Hum Genet* **86**, 621-625 (2010).
90. Gold, R., Linington, C. & Lassmann, H. Understanding pathogenesis and therapy of multiple sclerosis via animal models: 70 years of merits and culprits in experimental autoimmune encephalomyelitis research. *Brain* **129**, 1953-1971 (2006).
91. Wiendl, H. & Hohlfeld, R. Multiple sclerosis therapeutics: unexpected outcomes clouding undisputed successes. *Neurology* **72**, 1008-1015 (2009).
92. Taoufik, E. *et al.* Positive and negative implications of tumor necrosis factor neutralization for the pathogenesis of multiple sclerosis. *Neurodegener Dis* **5**, 32-37 (2008).

93. Panitch, H.S., Hirsch, R.L., Schindler, J. & Johnson, K.P. Treatment of multiple sclerosis with gamma interferon: exacerbations associated with activation of the immune system. *Neurology* **37**, 1097-1102 (1987).
94. Segal, B.M. *et al.* Repeated subcutaneous injections of IL12/23 p40 neutralising antibody, ustekinumab, in patients with relapsing-remitting multiple sclerosis: a phase II, double-blind, placebo-controlled, randomised, dose-ranging study. *Lancet Neurol* **7**, 796-804 (2008).
95. Lassmann, H. Multiple sclerosis pathology: evolution of pathogenetic concepts. *Brain Pathol* **15**, 217-222 (2005).
96. Kutzelnigg, A. *et al.* Cortical demyelination and diffuse white matter injury in multiple sclerosis. *Brain* **128**, 2705-2712 (2005).
97. Lassmann, H. & van Horssen, J. The molecular basis of neurodegeneration in multiple sclerosis. *FEBS Lett* **585**, 3715-3723 (2011).
98. Lucchinetti, C. *et al.* Heterogeneity of multiple sclerosis lesions: implications for the pathogenesis of demyelination. *Ann Neurol* **47**, 707-717 (2000).
99. Aboul-Enein, F. *et al.* Preferential loss of myelin-associated glycoprotein reflects hypoxia-like white matter damage in stroke and inflammatory brain diseases. *J Neuropathol Exp Neurol* **62**, 25-33 (2003).
100. Witte, M.E. *et al.* Enhanced number and activity of mitochondria in multiple sclerosis lesions. *J Pathol* **219**, 193-204 (2009).
101. Dutta, R. *et al.* Mitochondrial dysfunction as a cause of axonal degeneration in multiple sclerosis patients. *Ann Neurol* **59**, 478-489 (2006).
102. Mahad, D., Lassmann, H. & Turnbull, D. Review: Mitochondria and disease progression in multiple sclerosis. *Neuropathol Appl Neurobiol* **34**, 577-589 (2008).
103. Stys, P.K. General mechanisms of axonal damage and its prevention. *J Neurol Sci* **233**, 3-13 (2005).
104. Kremer, D., Aktas, O., Hartung, H.P. & Kury, P. The complex world of oligodendroglial differentiation inhibitors. *Ann Neurol* **69**, 602-618 (2011).
105. Mizushima, N. & Komatsu, M. Autophagy: renovation of cells and tissues. *Cell* **147**, 728-741 (2011).
106. Levine, B. & Kroemer, G. Autophagy in the pathogenesis of disease. *Cell* **132**, 27-42 (2008).
107. Bernales, S., Schuck, S. & Walter, P. ER-phagy: selective autophagy of the endoplasmic reticulum. *Autophagy* **3**, 285-287 (2007).

108. Wang, K. & Klionsky, D.J. Mitochondria removal by autophagy. *Autophagy* **7**, 297-300 (2011).
109. Kondo, Y. & Kondo, S. Autophagy and cancer therapy. *Autophagy* **2**, 85-90 (2006).
110. Sinha, S. & Levine, B. The autophagy effector Beclin 1: a novel BH3-only protein. *Oncogene* **27 Suppl 1**, S137-148 (2008).
111. Ogier-Denis, E. & Codogno, P. Autophagy: a barrier or an adaptive response to cancer. *Biochim Biophys Acta* **1603**, 113-128 (2003).
112. Arico, S. *et al.* The tumor suppressor PTEN positively regulates macroautophagy by inhibiting the phosphatidylinositol 3-kinase/protein kinase B pathway. *J Biol Chem* **276**, 35243-35246 (2001).
113. Maiuri, M.C. *et al.* BH3-only proteins and BH3 mimetics induce autophagy by competitively disrupting the interaction between Beclin 1 and Bcl-2/Bcl-X(L). *Autophagy* **3**, 374-376 (2007).
114. Martiny-Baron, G. & Fabbro, D. Classical PKC isoforms in cancer. *Pharmacol Res* **55**, 477-486 (2007).
115. Pinton, P. & Rizzuto, R. p66Shc, oxidative stress and aging: importing a lifespan determinant into mitochondria. *Cell Cycle* **7**, 304-308 (2008).
116. Chen, J.L. *et al.* Novel roles for protein kinase Cdelta-dependent signaling pathways in acute hypoxic stress-induced autophagy. *J Biol Chem* **283**, 34432-34444 (2008).
117. Sakaki, K., Wu, J. & Kaufman, R.J. Protein kinase Ctheta is required for autophagy in response to stress in the endoplasmic reticulum. *J Biol Chem* **283**, 15370-15380 (2008).
118. Jiang, H., Cheng, D., Liu, W., Peng, J. & Feng, J. Protein kinase C inhibits autophagy and phosphorylates LC3. *Biochem Biophys Res Commun* **395**, 471-476 (2010).
119. Silva, R.D., Manon, S., Goncalves, J., Saraiva, L. & Corte-Real, M. Modulation of Bax mitochondrial insertion and induced cell death in yeast by mammalian protein kinase Calpha. *Exp Cell Res* **317**, 781-790 (2011).
120. Chen, J.L. *et al.* PKC delta signaling: a dual role in regulating hypoxic stress-induced autophagy and apoptosis. *Autophagy* **5**, 244-246 (2009).
121. Mellor, H. & Parker, P.J. The extended protein kinase C superfamily. *Biochem J* **332 (Pt 2)**, 281-292 (1998).
122. Steinberg, S.F. Structural basis of protein kinase C isoform function. *Physiol Rev* **88**, 1341-1378 (2008).
123. Rosse, C. *et al.* PKC and the control of localized signal dynamics. *Nat Rev Mol Cell Biol* **11**, 103-112 (2010).

124. Giorgi, C. *et al.* Redox control of protein kinase C: cell- and disease-specific aspects. *Antioxid Redox Signal* **13**, 1051-1085 (2010).
125. Kowalczyk, J.E. *et al.* Protein kinase C beta in postischemic brain mitochondria. *Mitochondrion* **12**, 138-143 (2012).
126. Lin, G., Brownsey, R.W. & MacLeod, K.M. Regulation of mitochondrial aconitase by phosphorylation in diabetic rat heart. *Cell Mol Life Sci* **66**, 919-932 (2009).
127. Nunnari, J. & Suomalainen, A. Mitochondria: in sickness and in health. *Cell* **148**, 1145-1159 (2012).
128. Giorgi, C. *et al.* Mitochondrial calcium homeostasis as potential target for mitochondrial medicine. *Mitochondrion* **12**, 77-85 (2012).
129. Schapira, A.H. Mitochondrial diseases. *Lancet* **379**, 1825-1834 (2012).
130. Wallace, D.C., Fan, W. & Procaccio, V. Mitochondrial energetics and therapeutics. *Annu Rev Pathol* **5**, 297-348 (2010).
131. Vives-Bauza, C. *et al.* PINK1-dependent recruitment of Parkin to mitochondria in mitophagy. *Proc Natl Acad Sci U S A* **107**, 378-383 (2010).
132. Mizushima, N., Yoshimori, T. & Levine, B. Methods in mammalian autophagy research. *Cell* **140**, 313-326 (2010).
133. Kabeya, Y. *et al.* LC3, a mammalian homologue of yeast Apg8p, is localized in autophagosome membranes after processing. *EMBO J* **19**, 5720-5728 (2000).
134. Mizushima, N. & Yoshimori, T. How to interpret LC3 immunoblotting. *Autophagy* **3**, 542-545 (2007).
135. Klionsky, D.J. *et al.* Guidelines for the use and interpretation of assays for monitoring autophagy in higher eukaryotes. *Autophagy* **4**, 151-175 (2008).
136. Komatsu, M. *et al.* Homeostatic levels of p62 control cytoplasmic inclusion body formation in autophagy-deficient mice. *Cell* **131**, 1149-1163 (2007).
137. Komatsu, M. Potential role of p62 in tumor development. *Autophagy* **7**, 1088-1090 (2011).
138. Mizushima, N. Methods for monitoring autophagy. *Int J Biochem Cell Biol* **36**, 2491-2502 (2004).
139. Kimura, S., Noda, T. & Yoshimori, T. Dissection of the autophagosome maturation process by a novel reporter protein, tandem fluorescent-tagged LC3. *Autophagy* **3**, 452-460 (2007).
140. Gonindard, C. *et al.* Synthetic hispidin, a PKC inhibitor, is more cytotoxic toward cancer cells than normal cells in vitro. *Cell Biol Toxicol* **13**, 141-153 (1997).
141. Rimessi, A., Rizzuto, R. & Pinton, P. Differential recruitment of PKC isoforms in HeLa cells during redox stress. *Cell Stress Chaperones* **12**, 291-298 (2007).

142. Takahashi, H. & Namiki, H. Mechanism of membrane redistribution of protein kinase C by its ATP-competitive inhibitors. *Biochem J* **405**, 331-340 (2007).
143. Soh, J.W. & Weinstein, I.B. Roles of specific isoforms of protein kinase C in the transcriptional control of cyclin D1 and related genes. *J Biol Chem* **278**, 34709-34716 (2003).
144. Fleury, C., Mignotte, B. & Vayssiere, J.L. Mitochondrial reactive oxygen species in cell death signaling. *Biochimie* **84**, 131-141 (2002).
145. Marchi, S. *et al.* Mitochondria-ros crosstalk in the control of cell death and aging. *J Signal Transduct* **2012**, 329635 (2012).
146. Gottlieb, E., Armour, S.M., Harris, M.H. & Thompson, C.B. Mitochondrial membrane potential regulates matrix configuration and cytochrome c release during apoptosis. *Cell Death Differ* **10**, 709-717 (2003).
147. Drago, I., Pizzo, P. & Pozzan, T. After half a century mitochondrial calcium in- and efflux machineries reveal themselves. *EMBO J* **30**, 4119-4125 (2011).
148. Pinton, P., Rimessi, A., Romagnoli, A., Prandini, A. & Rizzuto, R. Biosensors for the detection of calcium and pH. *Methods in cell biology* **80**, 297-325 (2007).
149. Pinton, P., Leo, S., Wieckowski, M.R., Di Benedetto, G. & Rizzuto, R. Long-term modulation of mitochondrial Ca2+ signals by protein kinase C isozymes. *J Cell Biol* **165**, 223-232 (2004).
150. Heart, E. *et al.* Ca2+, NAD(P)H and membrane potential changes in pancreatic beta-cells by methyl succinate: comparison with glucose. *Biochem J* **403**, 197-205 (2007).
151. Akhmedov, D. *et al.* Mitochondrial matrix pH controls oxidative phosphorylation and metabolism-secretion coupling in INS-1E clonal beta cells. *FASEB J* **24**, 4613-4626 (2010).
152. Poppe, M. *et al.* Dissipation of potassium and proton gradients inhibits mitochondrial hyperpolarization and cytochrome c release during neural apoptosis. *J Neurosci* **21**, 4551-4563 (2001).
153. Mookherjee, P. *et al.* Mitochondrial-targeted active Akt protects SH-SY5Y neuroblastoma cells from staurosporine-induced apoptotic cell death. *J Cell Biochem* **102**, 196-210 (2007).
154. Xiao, D. & Singh, S.V. p66Shc is indispensable for phenethyl isothiocyanate-induced apoptosis in human prostate cancer cells. *Cancer Res* **70**, 3150-3158 (2010).
155. Codogno, P. & Meijer, A.J. Autophagy and signaling: their role in cell survival and cell death. *Cell Death Differ* **12 Suppl 2**, 1509-1518 (2005).
156. Cecconi, F. & Levine, B. The role of autophagy in mammalian development: cell makeover rather than cell death. *Dev Cell* **15**, 344-357 (2008).

157. Roffey, J. *et al.* Protein kinase C intervention: the state of play. *Curr Opin Cell Biol* **21**, 268-279 (2009).
158. Bononi, A. *et al.* Protein kinases and phosphatases in the control of cell fate. *Enzyme Res* **2011**, 329098 (2011).
159. Reyland, M.E. Protein kinase C isoforms: Multi-functional regulators of cell life and death. *Front Biosci* **14**, 2386-2399 (2009).
160. Akar, U. *et al.* Tissue transglutaminase inhibits autophagy in pancreatic cancer cells. *Mol Cancer Res* **5**, 241-249 (2007).
161. He, C. & Klionsky, D.J. Regulation mechanisms and signaling pathways of autophagy. *Annu Rev Genet* **43**, 67-93 (2009).
162. Youle, R.J. & Narendra, D.P. Mechanisms of mitophagy. *Nat Rev Mol Cell Biol* **12**, 9-14 (2011).
163. Kim, I., Rodriguez-Enriquez, S. & Lemasters, J.J. Selective degradation of mitochondria by mitophagy. *Arch Biochem Biophys* **462**, 245-253 (2007).
164. Gomes, L.C. & Scorrano, L. Mitochondrial morphology in mitophagy and macroautophagy. *Biochim Biophys Acta* (2012).
165. Twig, G. *et al.* Fission and selective fusion govern mitochondrial segregation and elimination by autophagy. *EMBO J* **27**, 433-446 (2008).
166. Narendra, D., Tanaka, A., Suen, D.F. & Youle, R.J. Parkin is recruited selectively to impaired mitochondria and promotes their autophagy. *J Cell Biol* **183**, 795-803 (2008).
167. Narendra, D.P. *et al.* PINK1 is selectively stabilized on impaired mitochondria to activate Parkin. *PLoS Biol* **8**, e1000298 (2010).
168. Rambold, A.S., Kostelecky, B., Elia, N. & Lippincott-Schwartz, J. Tubular network formation protects mitochondria from autophagosomal degradation during nutrient starvation. *Proc Natl Acad Sci U S A* **108**, 10190-10195 (2011).
169. Feliciello, A., Gottesman, M.E. & Avvedimento, E.V. cAMP-PKA signaling to the mitochondria: protein scaffolds, mRNA and phosphatases. *Cell Signal* **17**, 279-287 (2005).
170. Antico Arciuch, V.G., Alippe, Y., Carreras, M.C. & Poderoso, J.J. Mitochondrial kinases in cell signaling: Facts and perspectives. *Adv Drug Deliv Rev* **61**, 1234-1249 (2009).
171. Scarlett, J.L. *et al.* Changes in mitochondrial membrane potential during staurosporine-induced apoptosis in Jurkat cells. *FEBS Lett* **475**, 267-272 (2000).
172. Paglin, S. *et al.* Rapamycin-sensitive pathway regulates mitochondrial membrane potential, autophagy, and survival in irradiated MCF-7 cells. *Cancer Res* **65**, 11061-11070 (2005).

173. Chu, C.T. A pivotal role for PINK1 and autophagy in mitochondrial quality control: implications for Parkinson disease. *Hum Mol Genet* **19**, R28-37 (2010).
174. Brown, J.E. *et al.* Essential role of the redox-sensitive kinase p66shc in determining energetic and oxidative status and cell fate in neuronal preconditioning. *J Neurosci* **30**, 5242-5252 (2010).
175. Kleman, A.M. *et al.* p66(shc)'s role as an essential mitophagic molecule in controlling neuronal redox and energetic tone. *Autophagy* **6**, 948-949 (2010).
176. Filipowicz, W., Bhattacharyya, S.N. & Sonenberg, N. Mechanisms of post-transcriptional regulation by microRNAs: are the answers in sight? *Nature reviews* **9**, 102-114 (2008).
177. Bartel, D.P. MicroRNAs: target recognition and regulatory functions. *Cell* **136**, 215-233 (2009).
178. Lovat, F., Valeri, N. & Croce, C.M. MicroRNAs in the pathogenesis of cancer. *Seminars in oncology* **38**, 724-733 (2011).
179. Lewis, B.P., Burge, C.B. & Bartel, D.P. Conserved seed pairing, often flanked by adenosines, indicates that thousands of human genes are microRNA targets. *Cell* **120**, 15-20 (2005).
180. Maragkakis, M. *et al.* DIANA-microT web server: elucidating microRNA functions through target prediction. *Nucleic acids research* **37**, W273-276 (2009).
181. Dong, H. *et al.* Thyroid hormone may regulate mRNA abundance in liver by acting on microRNAs. *PloS one* **5**, e12136 (2010).
182. John, B. *et al.* Human MicroRNA targets. *PLoS biology* **2**, e363 (2004).
183. Scorrano, L. *et al.* BAX and BAK regulation of endoplasmic reticulum Ca2+: a control point for apoptosis. *Science (New York, N.Y* **300**, 135-139 (2003).
184. Grimm, S. The ER-mitochondria interface: the social network of cell death. *Biochimica et biophysica acta* **1823**, 327-334 (2012).
185. Simmen, T., Lynes, E.M., Gesson, K. & Thomas, G. Oxidative protein folding in the endoplasmic reticulum: tight links to the mitochondria-associated membrane (MAM). *Biochimica et biophysica acta* **1798**, 1465-1473 (2010).
186. Zhang, H. *et al.* MiR-25 regulates apoptosis by targeting Bim in human ovarian cancer. *Oncology reports* **27**, 594-598 (2012).
187. Razumilava, N. *et al.* miR-25 targets TNF-related apoptosis inducing ligand (TRAIL) death receptor-4 and promotes apoptosis resistance in cholangiocarcinoma. *Hepatology (Baltimore, Md* **55**, 465-475 (2012).

188. Poliseno, L. *et al.* Identification of the miR-106b~25 microRNA cluster as a proto-oncogenic PTEN-targeting intron that cooperates with its host gene MCM7 in transformation. *Science signaling* **3**, ra29 (2010).
189. Lanza, G. *et al.* mRNA/microRNA gene expression profile in microsatellite unstable colorectal cancer. *Molecular cancer* **6**, 54 (2007).
190. Nishida, N. *et al.* Microarray Analysis of Colorectal Cancer Stromal Tissue Reveals Upregulation of Two Oncogenic miRNA Clusters. *Clin Cancer Res* **18**, 3054-3070 (2012).
191. Brandt-Rauf, P.W., Monaco, R. & Pincus, M.R. Conformational effects of environmentally induced, cancer-related mutations in the p53 protein. *Proc Natl Acad Sci U S A* **91**, 9262-9266 (1994).
192. Schoenfeld, R. *et al.* Oligodendroglial differentiation induces mitochondrial genes and inhibition of mitochondrial function represses oligodendroglial differentiation. *Mitochondrion* **10**, 143-150 (2010).
193. Stadelmann, C. Multiple sclerosis as a neurodegenerative disease: pathology, mechanisms and therapeutic implications. *Curr Opin Neurol* **24**, 224-229 (2011).
194. Benarroch, E.E. Oligodendrocytes: Susceptibility to injury and involvement in neurologic disease. *Neurology* **72**, 1779-1785 (2009).
195. Tong, W. *et al.* Involvement of lipid mediators on cytokine signaling and induction of secretory phospholipase A2 in immortalized astrocytes (DITNC). *J Mol Neurosci* **12**, 89-99 (1999).
196. Selmaj, K., Raine, C.S., Cannella, B. & Brosnan, C.F. Identification of lymphotoxin and tumor necrosis factor in multiple sclerosis lesions. *J Clin Invest* **87**, 949-954 (1991).
197. Musabak, U., Demirkaya, S., Genc, G., Ilikci, R.S. & Odabasi, Z. Serum adiponectin, TNF-alpha, IL-12p70, and IL-13 levels in multiple sclerosis and the effects of different therapy regimens. *Neuroimmunomodulation* **18**, 57-66 (2011).
198. McCoy, M.K. & Tansey, M.G. TNF signaling inhibition in the CNS: implications for normal brain function and neurodegenerative disease. *J Neuroinflammation* **5**, 45 (2008).
199. Chen, Y. *et al.* Isolation and culture of rat and mouse oligodendrocyte precursor cells. *Nat Protoc* **2**, 1044-1051 (2007).
200. Ben-Hur, T. *et al.* Effects of proinflammatory cytokines on the growth, fate, and motility of multipotential neural precursor cells. *Mol Cell Neurosci* **24**, 623-631 (2003).
201. Agresti, C. *et al.* ATP regulates oligodendrocyte progenitor migration, proliferation, and differentiation: involvement of metabotropic P2 receptors. *Brain Res Brain Res Rev* **48**, 157-165 (2005).

202. Gogolla, N., Galimberti, I., DePaola, V. & Caroni, P. Preparation of organotypic hippocampal slice cultures for long-term live imaging. *Nat Protoc* **1**, 1165-1171 (2006).
203. Itoh, K. Culture of oligodendrocyte precursor cells (NG2(+)/O1(-)) and oligodendrocytes (NG2(-)/O1(+)) from embryonic rat cerebrum. *Brain Res Brain Res Protoc* **10**, 23-30 (2002).
204. Bansode, R.R., Huang, W., Roy, S.K., Mehta, M. & Mehta, K.D. Protein kinase C deficiency increases fatty acid oxidation and reduces fat storage. *J Biol Chem* **283**, 231-236 (2008).